UCSF
UC San Francisco Electronic Theses and Dissertations

Title
Multiple Signal Integration by the Glucocorticoid Receptor

Permalink
https://escholarship.org/uc/item/6nn1s222

Author
Pantoja, Carlos J.

Publication Date
2009

Peer reviewed|Thesis/dissertation

eScholarship.org Powered by the California Digital Library
University of California

Multiple Signal Integration by the Glucocorticoid Receptor

by

Carlos José Albuquerque Brasiliense Pantoja

DISSERTATION

Submitted in partial satisfaction of the requirements for the degree of

DOCTOR OF PHILOSOPHY

in

Biochemistry and Molecular Biology

in the

GRADUATE DIVISION

of the

UNIVERSITY OF CALIFORNIA, SAN FRANCISCO

[redacted]

Dedicated to:

My mother (Virgínia Brasiliense Pantoja) and my father (Roberto Silva Pantoja) for their unconditional support and love through all my life.

My grandmother (Raimunda Lins Brasiliense) for being generous and graceful at all moments.

Acknowledgments

This thesis would not have been possible without the constant support and love of my parents, siblings, and extended family. They are the origin and inspiration for the work described here.

I thank my friends in Brazil and in the USA. None of this would have been worth it without your presence.

Thank you Betsy Madden for bringing joy to my life and being a friend, companion and role model.

Branka Kovacic, Francisco Neves and Ralff Ribeiro were my first scientific mentors. I will be forever grateful for their attention, generosity, and patience.

I wish to thank Peter Walter, Rik Derynck, Cynthia Kenyon, Dan Minor and Tom Scanlan for mentoring and thinking critically about my work. Without their help I would not have been able to complete this work and feel confident to continue a career in science.

David Gardner, Prescott Woodruff, Brian Feldman and Tony Gerber showed me how to think of my work in relation to Medicine and the impact that Science has in human health.

I thank the members of the Yamamoto lab for creating a scientific environment that was productive and exciting. I learned my scientific skills and grew as a person because of them.

I will be always indebted for my relationship with my mentor and friend Keith Yamamoto. He is the model for the person and scientist I aspire to be.

Multiple Signal Integration by the Glucocorticoid Receptor

Carlos José Albuquerque Brasiliense Pantoja

Abstract

Glucocorticoids are steroid hormones that control multiple aspects of mammalian physiology. Glucocorticoids act through the glucocorticoid receptor (GR), a ligand-regulated transcriptional regulatory factor that is ubiquitously expressed. It is still unknown how the structurally simple glucocorticoid hormones generate diverse physiological outputs across multiple target tissues. To examine this question we characterized the activities of synthetic glucocorticoid ligands across a panel of GR-induced biological activity profiles. Our studies demonstrated that ligand structure is an important determinant of GR function. We found that arylpyrazole glucocorticoid compounds supported GR activities related to adipogenesis, inhibition of cell proliferation, inhibition of asthma marker gene expression and anti-inflammation, but did not inhibit osteoblast differentiation in cell culture. Additionally, arylpyrazole GR ligands displayed gene-specific transcriptional effects.

To investigate the therapeutic effects of glucocorticoids in lung epithelial cells during asthma treatment we developed a cell culture-based model for gene regulation. We found that dexamethasone and budesonide repressed the IL-13-induced asthma marker genes

POSTN, SERPINB2 and CLCA1 in primary human bronchoepithelial cells. We found that the kinetics of regulation of asthma marker genes was slower when compared than that of other IL-13 regulated genes. In addition, the gene SERPINB2 was regulated by dexamethasone as part of a cluster of SERPINB genes that were all also induced by IL-13 treatment.

Finally, we discovered that glucocorticoids induce a novel state during adipogenesis in cell culture. Dex-primed preadipocytes are an intermediate cellular state between preadipocytes and adipocytes that differentiate into adipocytes when exposed to cAMP signaling. Importantly, we found that the mode of differentiation influences the metabolic properties of adipocytes. In summary, our results suggest that the diversity of glucocorticoid activities is generated by the combined actions of signals induced by the ligand itself, the cellular context and additional signaling pathways that affect glucocorticoid activity and the associated phenotypes.

Table of Contents

List of Tables and Figures

Chapter 1

Chapter 2

Chapter 3

Introduction

The maintenance of homeostasis in complex multicellular organisms depends on the control of physiological functions at varied structural and temporal scales. Single cells respond to external signals and have internal feedback mechanisms that maintain metabolic homeostasis and precisely control decisions to enter or leave the cell cycle, to apoptosis, to senesce, to differentiate, etc. At higher order organizational levels, tissues or even the whole organism can also respond to changes in internal and external states by orchestrating complex and coordinated responses. To solve the problem of information integration at the whole organism scale animals have evolved interrelated and highly sophisticated nervous and endocrine systems.

Neuronal circuits collect, process, store and relay information to control physiological and behavioral states. Signaling occurs at relatively short time scales and is mediated by neurotransmitters acting locally at synapses on target cells and organs. Endocrine glands employ hormones as signals for long-range control of tissues. Hormones signal at varied time scales and induce physiological programs associated with development, normal adult life and disease states. The mechanisms through which the nervous and endocrine systems integrate signals and initiate complex responses remain for the most part unclear. To explore this and related issues the work described in this thesis examined the glucocorticoid endocrine control system.

Glucocorticoids are steroid hormones produced in the cortex of the adrenal gland. Glucocorticoid secretion in the circulation occurs in pulses and is controlled by a combination of negative feedback loops and external inputs. Importantly, hormone-

induced outputs seem to depend on the molecular structure of the glucocorticoid ligand, magnitude and duration of stimulus, interactions with additional signaling pathways and the identity of the affected tissue. How structurally simple hormones convey such wealth of information remains an unresolved puzzle.

The active glucocorticoids in humans and rodents are cortisol and corticosterone, respectively. Glucocorticoid activity is mediated by GR, a transcriptional regulatory factor of the nuclear hormone family that is widely expressed in mammalian tissues. Hormone production follows a circadian rhythm with a circulating peak coincident with the beginning of daily awake activity. Control of glucocorticoid synthesis is the major regulatory step for hormone release and is mediated by the hypothalamus-pituitary-adrenal (HPA) axis. Pituitary secretion of the peptide hormone adrenocorticotropic hormone (ACTH) induces steroidogenesis in the adrenal cortex and glucocorticoid production. The release of ACTH is in turn regulated by the hypothalamic release of corticotropin-releasing hormone (CRH). In addition to CRH, vasopressin and inflammatory cytokines are also known to regulate ACTH secretion. CRH secretion is regulated by circadian stimuli and by general bodily stressors, e.g., injury, fever, or hypoglycemia. Finally, glucocorticoids inhibit the transcription of CRH, ACTH and vasopressin, introducing negative feedback to the HPA axis[1].

Circulating glucocorticoids are present in two states, an inactive form bound to the corticoid binding globulin and a free active form that is competent for cellular uptake. In peripheral tissues the enzyme 11β-hydroxysteroid dehydrogenase (11β-HSD) regulates hormone activity[2,3]. 11β-HSD is present in two isoforms that differentially regulate glucocorticoid activity. 11β-HSD1 is expressed in the liver, fat, gonads and central

nervous system to convert the inactive glucocorticoid cortisone to the active form cortisol. 11β-HSD2 is expressed in the kidneys, colon, placenta, salivary glands, the nucleus of the solitary tract, the subcomissural organ, and the ventromedial nucleus of the hypothalamus to inactivate cortisol and convert it to cortisone[4].

Glucocorticoids act in various target tissues to modulate immune responses, promote apoptosis, induce differentiation and to dramatically affect organ and cellular function. Notably, patients and animals deficient for glucocorticoid production display decreased survival when subjected to the stress associated with large surgical procedures or generalized injury. Glucocorticoids are also very potent anti-inflammatory agents and have been used therapeutically since their isolation in the late forties. They are routinely used in the treatment of a wide range of conditions, including inflammatory diseases (e.g., asthma, rheumatoid arthritis), blood malignancies and the pulmonary complications associated with pre-term birth. However, chronic use of glucocorticoids induces severe side effects, such as diabetes, osteoporosis, fat redistribution, myopathy, hypertension and increased susceptibility to infections. Interestingly, there is a substantial clinical overlap between conditions of excess glucocorticoids (e.g. Cushing's syndrome) and the constellation of risk factors present in approximately 47 million U.S. adults known as the metabolic syndrome[5]. Both classes of patients are characterized by insulin resistance, central obesity, hypertension, dyslipidemia and an increased risk of cardiovascular disease and stroke. Despite major advances in the past three decades the molecular mechanisms through which GR induces such complex physiological programs remain for the most part unknown.

Analysis of GR structure has identified three subdomains. The N-terminal region contains the transcriptional activation function 1 (AF-1) and interacts with co-regulatory factors. The DNA binding domain (DBD) contains two zinc fingers that mediate sequence-specific interactions with DNA, a homodimerization surface, and additional surfaces for interaction with co-factors. The ligand binding domain (LBD) of GR is composed of a three-layer helical sandwich that contains a hydrophobic pocket that binds ligand. Additional surfaces on the LBD mediate nuclear import, receptor dimerization and interaction with cofactors. GR also receives regulatory input from phosphorylation, acetylation, ubiquitylation and sumoylation signals[6].

In the absence of hormone GR is located in the cytoplasm in a complex with chaperones and co-chaperones. Hormone binding to the LBD leads to conformational changes that allow nuclear import and shift the equilibrium of receptor localization towards nuclear accumulation. Structural studies have shown that the ligand binding pocket of GR is very plastic and accommodates structurally diverse ligands, that include non-steroidal compounds[7-10]. This fact led to the hypothesis that the LBD does not act as a simple ligand-controlled binary switch that turns the receptor on or off. In fact, it seems that ligands may act as allosteric effectors of receptor function. According to this model ligand structure is read by the LBD and ultimately affects transcriptional outputs. Kian Tee et al.[11] tested this model in the estrogen receptor (ER) by studying the effects of selective ER modulators on transcriptional responses. They used microarrays to determine the transcriptional effects of estradiol, tamoxifen or raloxifene treatment in U2OS cells stably expressing ERα. Strikingly, only a 20-40% overlap was observed in comparisons of the genes regulated by each pair of ligands. This result is a clear

demonstration of how different ligands can induce profound changes in the regulatory properties of a given transcription factor[11].

Once in the nucleus GR is recruited to thousands of sites of in the genome[12,13]. Transcriptional regulation is mediated by glucocorticoid response elements (GREs). GREs are genomic regions to which GR and associated transcriptional regulatory factors are recruited to regulate transcription. The cellular context and the sequence of a given GRE appear to determine if recruitment of GR to a GRE will affect target gene transcription[14]. Additionally, the specific sequence to which GR binds acts as a signal that modifies receptor activity[15]. GR nucleated complexes are capable of activation or repression of associated genes. Transcriptional regulation appears to be highly gene-specific, but some general commonalities have been observed. GR-dependent transcriptional activation involves recruitment of protein complexes that modify and remodel chromatin to promote its open state. Additionally, cofactors also interact with the transcription machinery to promote preinitiation complex assembly and increase transcription rates. Repression by GR is less well understood. GR inhibits transcriptional activators through tethering mechanisms, interacts with complexes that exhibit corepressor activity and in some cases appears to squelch coactivators that would otherwise be used by transcriptional activators.

Genome-wide studies have demonstrated that glucocorticoid treatment affects transcript levels of hundreds to thousands of genes. An unmet challenge is the establishment of causality chains that connect GR binding to genomic sites, regulatory complex formation, transcriptional regulation of relevant target genes and physiological output. This knowledge will greatly contribute to the rational development of more specific

glucocorticoid-based therapies. Indeed, a major challenge is the development of synthetic glucocorticoids that are able to dissociate the beneficial effects of glucocorticoid treatment from the serious adverse effects associated with long-term treatment. Currently, advances in glucocorticoid therapy aimed to avoid side effects have mainly come from changes in the pharmacokinetic profiles and routes of administration of these drugs.

Until recently, the prevailing view was that the activities of GR related to transcriptional repression were responsible for the beneficial effects associated with glucocorticoid anti-inflammatory actions. Conversely, transcriptional activation was thought to regulate genes responsible for GR-induced adverse effects[16]. This paradigm guided research programs at pharmaceutical and biotech companies. Thus, screens have been developed to seek ligands that repress but fail to activate from simple synthetic response elements in transfected reporter genes. Commonly used "GR repression" reporter genes contain nuclear factor kappa B (NFκB) or activator protein-1 (AP-1) response elements. Inflammatory cytokines activate reporter transcription, which is inhibited by glucocorticoid treatment. GR activation reporter genes employ simple GREs containing multimerized GR binding sites (GBSs) to drive reporter gene activation.

Data from our lab and others suggest that this model is oversimplified, and indeed incorrect[17]. Ligand-dependent dissociation of reporter gene repression from activation in a single cell type does not appear to predict ligand dissociation in animal models of disease. The failure of reporter gene-based approaches invalidated the previous paradigm and implies that reporter assays do not capture the complexity of GR transcriptional programs. There is a clear need for cell-based assays that may model accurately the responses of natural response elements and genes in their normal chromosomal contexts –

genes that participate in anti-inflammatory effects, as well as those that contribute to adverse effects in the course of corticosteroid therapies. Importantly, for most tissues where GR is known to perform pharmacological activities the relevant target genes have not been identified.

This thesis describes a strategy to study GR signaling that uses intermediate complexity assays and phenotypes to navigate between GR ligand structure and tissue physiology. We applied this strategy to characterize GR arylpyrazole ligands and study the regulation of adipogenesis and asthma target genes by GR. Our approach identified selective GR modulators that were able to regulate human asthma genes, but that did not inhibit bone differentiation. In addition, we discovered that glucocorticoids define a novel commitment stage during adipogenesis *in vitro*. These studies advanced our understanding of glucocorticoid signaling and increased our knowledge of signal integration by biological systems. One of our primary goals was to generate knowledge that might advance GR ligand development and positively impact human health.

Chapter 1: Novel arylpyrazole compounds selectively modulate glucocorticoid receptor regulatory activity

Chapter 1 Introduction

Glucocorticoids are steroid hormones that exert their biological functions through the intracellular glucocorticoid receptor (GR). GR is a transcriptional regulator that, upon binding to cognate ligands, occupies specific genomic glucocorticoid response elements (GREs) and modulates the transcription of nearby genes[18,14].

Based on conventional views, physiological ligands such as cortisol and corticosterone, and synthetic compounds such as dexamethasone and prednisolone, are agonists that promote the biological functions of GR, whereas ligands such as RU486 are antagonists that bind to GR but inhibit its functions. It is now apparent, however, that ligand activities are strongly context dependent. For example, selective estrogen receptor modulators (SERMs), such as tamoxifen and raloxifene, are agonist-like or antagonist-like in different tissues, and modulate distinct subsets of ER target genes in a given cell type[19,20,11]; selective ligands for FXR have also been reported[21]. Accordingly, the definitions of agonist and antagonist are relative to particular phenotypes or specific subsets of target genes, and therefore it is likely that any ligand could act as either agonist or antagonist depending on the context.

Glucocorticoids are among the most effective agents for treating asthma, arthritis, and autoimmune diseases because of their potent anti-inflammatory and immunosuppressive effects. However, chronic systemic glucocorticoid therapy also produces deleterious side effects, including diabetes mellitus, onset of hypertension, weight gain, muscle atrophy, and osteoporosis[16]. Therefore, one of the main challenges in glucocorticoid pharmacology is to develop agents that can dissociate anti-inflammatory and

immunosuppressive effects from these side effects. One approach was suggested by the notion that GR confers anti-inflammatory effects by transcriptional repression, whereas the side effects reflect transcriptional activation by GR[22]. However, it has been shown that some glucocorticoid-activated genes, such as annexin I, are important in the anti-inflammatory effect, whereas some glucocorticoid-repressed genes, such as endothelial nitric oxide synthase (eNOS)[23-25], are associated with deleterious side effects. Therefore, the ideal compounds would display a more complex profile: They would selectively regulate anti-inflammatory genes, leaving the "side-effect" genes unaffected. Unfortunately, the genes that are responsible for the unwanted side effects have not been identified. Moreover, the selectivity by which GR ligands modulate the transcriptional activities of genomic target genes has not been investigated.

Shah and Scanlan[26] described methods to synthesize novel arylpyrazole compounds that are ligands for GR. They studied 15 of these compounds, each carrying a different adduct at only a single position on the arylpyrazole backbone. The binding affinities of these compounds are similar to those of dexamethasone, prednisolone, and the physiological glucocorticoid, cortisol. All but one of the compounds was able to activate the expression of transfected reporter genes bearing synthetic simple GREs[26]. In this report, we used these structurally related compounds as tools to examine ligand selectivity in regulating the transcription of primary GR target genes in their normal chromosomal settings. Our strategy was to first investigate whether these compounds selectively modulate GR-regulated biological phenotypes in different cell types. We then determined whether these compounds induced differential gene expression programs in a given cell type, and tested

by chromatin immunoprecipitation (ChIP) whether the selective ligand effects correlated with GR occupancy at the target gene GREs.

Chapter 1 Results

Arylpyrazole compounds differentially affect GR-regulated proliferation and differentiation

Table 1.1 shows the chemical structures of the arylpyrazole compounds used in this study. Notably, the compounds differ only in the substituents attached at "C-11" of the arylpyrazole nucleus, a position thought to be equivalent to C-11 in the C-ring of the steroid nucleus (see dexamethasone structure in Table 1 inset for comparison). In every case, the compounds were bound by the closely related androgen receptor (AR) and progesterone receptor (PR) with affinities at least 100-fold lower than GR (Table 1.1). Similarly, the compounds failed to trigger transcriptional activation by the mineralocorticoid receptor (MR), cotransfected into CV-1 cells with a reporter gene bearing multiple mineralocorticoid response elements, whereas GR was strongly activated in parallel assays (data not shown). Thus, this series of arylpyrazoles is highly selective for GR.

We then tested the biological effects of these compounds in three glucocorticoid-responsive cell types. First, we examined the effects of a saturating concentration (1 μM) of the compounds in A549, a human lung epithelial cell line that responds strongly to proinflammatory signals, and, as with many cells involved in inflammatory responses, is growth inhibited by dexamethasone and prednisolone (Fig. 1.1A). To monitor cell viability and proliferation, we measured relative ATP levels in cells treated with the various compounds; ATP can be measured sensitively, rapidly, and precisely, and correlates closely with [^{3}H]-thymidine incorporation assays[27]. We found that ligand **2** was

comparable to dexamethasone and prednisolone in suppressing cell proliferation, whereas ligands **1, 3, 4, 6–12,** and **14** had weaker effects; notably, this assay is highly sensitive, such that even the weak effects reflect significant activity. In contrast, ligands **5, 13,** and **15** had no effect (Fig. 1.1A).

Table 1.1 *GR Ligands*

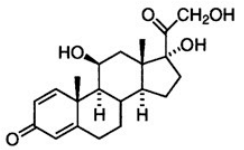

prednisolone (PRED)

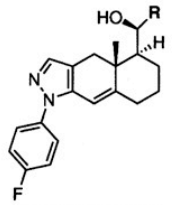

arylpyrazoles **1-15**

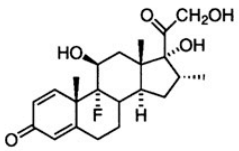

dexamethasone (DEX)

compound	R	GR Binding IC_{50}(nM)	PR IC_{50}(nM)	AR IC_{50}(nM)
DEX	-	1.4 ± 0.3	>1000	>1000
PRED	-	4.1 ± 1.2	ND	ND
PROG	-	ND	12.7 ± 3.8	ND
DHT	-	ND	ND	5.1 ± 1.8
1		4.9 ± 3.8	>1000	>1000
2		0.7 ± 0.2	>1000	>1000
3		8.6 ± 5.0	>1000	>1000
4		2.3 ± 1.1	>1000	>1000
5	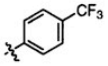	14.0 ± 3.7	>1000	>1000
6		7.9 ± 1.1	650	>1000
7		9.2 ± 2.8	>1000	>1000
8		7.0 ± 2.0	>1000	>1000
9		2.5 ± 0.3	>1000	>1000
10		5.5 ± 1.1	>1000	>1000
11		1.8 ± 0.3	>1000	>1000
12		2.4 ± 0.6	>1000	>1000
13	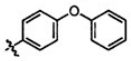	15.5 ± 7.6	>1000	>1000
14		5.2 ± 2.4	1000	>1000
15		6.6 ± 0.7	>1000	>1000

Next, we tested the compounds in mouse 3T3-L1 preadipocytes, where dexamethasone, insulin, and IBMX act together to drive adipocyte differentiation. We assessed the ability of the arylpyrazole compounds to replace dexamethasone in the differentiation cocktail. As shown in Figure 1.1B, most compounds (at 1 μM) were able to substitute for dexamethasone to induce differentiation. The effects of ligands 2–4 and 6–10 were similar to those of dexamethasone, whereas ligands 1, 5, 11, and 14 had weaker effects. Three compounds—ligands 12, 13, and 15—did not induce 3T3-L1 differentiation (Fig. 1.1B). Notably, this pattern of ligand effects differed substantially from the pattern of effects of observed in A549 cells.

Finally, we determined the actions of the compounds in mouse MC3T3-E1 preosteoblasts, where dexamethasone and prednisolone inhibit differentiation to osteoblasts[28,29]. Strikingly, none of the compounds inhibited MC3T3-E1 preosteoblast differentiation as measured by alizarin red staining (Fig. 1.1C). When we monitored the levels of calcium and phosphate, two indicators of osteoblast differentiation, ligands 2 and 9, had modest effects (data not shown). Again, this pattern of ligand effects differed markedly from the patterns observed in A549 or 3T3-L1 cells. Thus, the various arylpyrazole compounds clearly function differentially in different cell types (Table 1.2). For example, ligand 2 induced 3T3-L1 differentiation and inhibited A549 cell proliferation but did not efficiently suppress MC3T3-E1 differentiation.

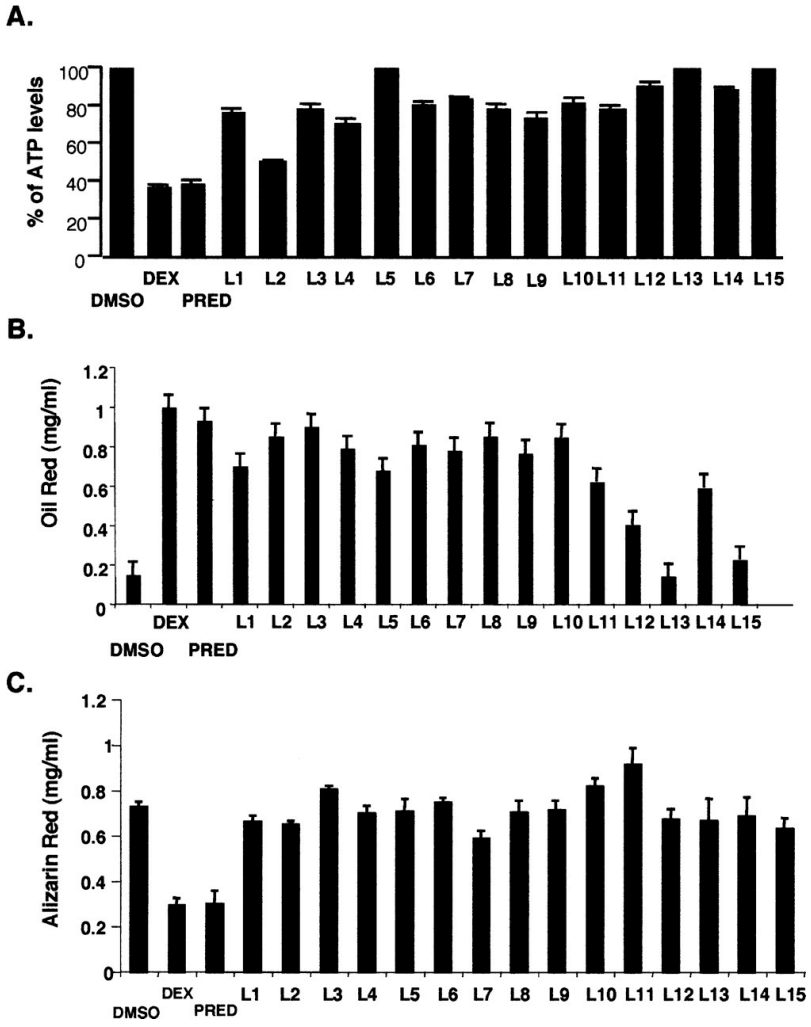

Figure 1.1 Arylpyrazole compounds differentially affect cell growth and differentiation. (*A*) Effects of arylpyrazole compounds on A549 cell proliferation. A549 cells were treated with either DMSO, dexamethasone (0.1 μM), or arylpyrazole compounds (1 μM) for 5 d, and the relative ATP levels were measured. The data represent the mean (standard error of the mean, SEM) of the percent of ATP levels (dexamethasone or arylpyrazole compound-treated divided by the DMSO-treated) from four experiments. (*B*) Effects of arylpyrazole compounds on 3T3-L1 adipocyte differentiation. Confluent cultures of 3T3-L1 cells were placed in differentiation medium that contained IBMX, insulin with either DMSO, dexamethasone (1 μM), prednisolone (1 μM), or various arylpyrazole compounds (1 μM) as indicated. Oil Red staining was used to measure the extent of adipocyte differentiation. The data represent the mean (SEM) of Oil Red concentration from three experiments. (*C*) The effects of arylpyrazole compounds on MC3T3-E1 osteoblast differentiation. MC3T3-E1 cells were grown to confluence and then placed in differentiation medium that contained either DMSO, dexamethasone (1 μM), prednisolone (1 μM), or various arylpyrazole compounds (1 μM) as indicated. Alizarin Red staining was used to measure the extent of osteoblast differentiation. Data are averaged (with SEM) from four independent experiments.

Table 1.2 Comparison of biological effects of arylpyrazole compounds in three cell types

	Inhibition of A549 cell proliferation	Induction of 3T3-L1 preadipocyte differentiation	Repression of MC3T3-E1 preosteoblast differentiation
Dexamethasone	++	++	++
L1	+	+	−−
L2	++	++	−−
L3	+	++	−−
L4	+	++	−−
L5	−−	+	−−
L6	+	++	−−
L7	+	++	−−
L8	+	++	−−
L9	+	++	−−
L10	+	++	−−
L11	+	+	−−
L12	+	−−	−−
L13	−−	−−	−−
L14	+	+	−−
L15	−−	−−	−−

Distinct arylpyrazole compounds induced differential gene expression patterns in a single cell type

The selective functions of distinct ligands in different cell types suggested that each arylpyrazole compound may regulate a specific gene expression program. In order to test this model, we compared the gene expression profiles regulated by arylpyrazole compounds in a single cell type. A549 cells were chosen because dexamethasone-responsive genes had already been defined by microarray analysis, and >10 of these had been shown to be primary regulatory targets, as defined by demonstration of GR occupancy in vivo at the GREs of each gene[30]; in contrast, few primary GR target genes have been identified in 3T3-L1 and MC3T3-E1. A549 cells express functional GR and display characteristics of type II alveolar epithelial cells, which are glucocorticoid target cells in vivo; regulation of various primary GR target genes, such as those involved in sodium transport and lung homeostasis (ENaCα), cell proliferation (Kip2), and the inflammatory response (IL-8 and GM-CSF), has been studied in these cells[31-36].

We chose 17 representative A549 GR target genes and used quantitative real-time PCR (qPCR) to compare gene expression patterns induced by arylpyrazole compounds, dexamethasone, and prednisolone. These 17 genes were selected because they are highly regulated by glucocorticoids and/or their GREs were previously identified. As shown in Figure 1.2, A–C, the different arylpyrazole compounds induced distinct patterns of gene expression. For example, ligands 2, 4, 8–12, and 14 activated all of the genes that were activated by dexamethasone; ligand 2 showed the strongest activities among these compounds (Fig. 1.2A). In contrast, ligands 1, 3, and 5–7 induced only a subset of the dexamethasone-induced genes, and ligand 15 did not activate any target gene (Fig. 1.2A).

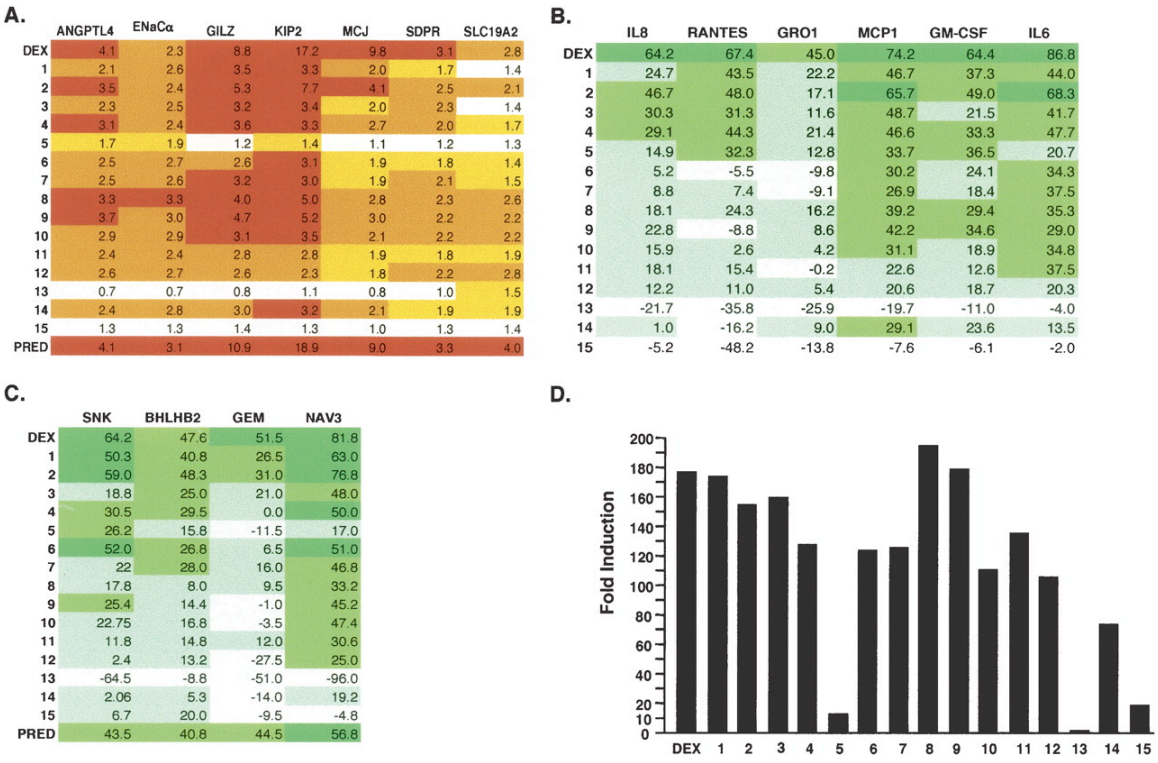

Figure 1.2 Arylpyrazole compounds differentially affect the expression of GR target genes in A549 cells. (*A*) Effects of arylpyrazole compounds on dexamethasone-induced genes. A549 cells were treated with dexamethasone or various arylpyrazole compounds for 4–5 h. Total RNA was prepared and subjected to cDNA synthesis. The cDNA was then analyzed by qPCR to measure the relative mRNA levels of distinct target genes using gene-specific primers. Red bars represent induction greater than threefold. Orange represents induction between two- and threefold. Yellow represents induction between 1.5-fold and twofold. (*B*) Effects of arylpyrazole compounds on TNFα-induced dexamethasone-suppressed genes. A549 cells were treated with TNFα and either dexamethasone or arylpyrazole compounds for 4 h. Total RNA was prepared and subjected to cDNA synthesis. The cDNA was then analyzed by qPCR to measure the relative mRNA levels of distinct target genes using gene-specific primers. Green represents percent inhibition >50%. Medium green represents percent inhibition between 25% and 50%. Light green represents percent inhibition between 0% and 25%. (*C*) Effects of arylpyrazole compounds on dexamethasone-suppressed genes. A549 cells were treated with TNFα and dexamethasone or various arylpyrazole compounds for 4 h. Total RNA was isolated and subjected to cDNA synthesis. The cDNA was then analyzed by qPCR to measure the mRNA levels of distinct target genes. The representative colors are as described above. The data in *A*–*C* represent the mean of the fold induction (DEX-treated responses divided by the DMSO-treated responses) from at least three experiments. The SEM is shown in the Supplemental Material. (*D*) The effects of arylpyrazole compounds on reporter genes containing simple GRE. Seventy-five nanograms of TAT3 reporter plasmids were transfected with 100 ng of RSV-βGal into A549 cells in a 24-well plate. After 24 h, cells were washed with PBS and treated with 0.1 μM DEX for an additional 16–20 h. Cells were then lysed and subjected to assays for luciferase and β-Gal activities. One representative data set from three independent transfection experiments is shown.

Glucocorticoids act as potent anti-inflammatory agents by suppressing the expression of various cytokine and chemokine genes. We tested the effects of our arylpyrazole compounds on six cytokines whose expression is induced by TNF-α (Fig. 1.2B). We found that ligands **1, 2,** and **4** inhibited the expression of most of the TNF-α-induced genes, whereas ligands **12–15** had little effect (Fig. 1.2A). Ligands **3** and **6–10** inhibited only a subset (two or three) of the genes (Fig. 1.2B); in contrast, ligand **5,** which induced only a single target gene of our test set, repressed three of the cytokine genes, although the effect was relatively modest (Fig. 1.2B). Furthermore, the six TNF-α-regulated genes could be divided into two groups with respect to their responses to ligands **6–10**: MCP-1, GM-CSF, and IL-6 were somewhat inhibited, whereas IL-8, RANTES, and GRO1 were largely unaffected (Fig. 1.2B).

The final group of target genes in our test set was glucocorticoid-repressed but not TNFα-induced. Ligands **1, 2, 4,** and **6** generally mimicked the effects of dexamethasone and prednisolone on these four genes; ligands **3** and **7** repressed two target genes; ligands **5** and **8–11** inhibited only one; and ligands **12–15** failed to repress (Fig. 1.2C). Interestingly, most of the compounds repressed NAV3 gene expression, but only ligands **1–3** repressed GEM, and then only weakly (Fig. 1.2C).

In summary, our results showed that modest changes in ligand chemistry can cause dramatic effects on gene expression profiles. Strikingly, when these same 15 compounds were tested for regulation of a transfected reporter gene containing synthetic GREs in A549 cells, all but ligand **13** activated transcription, although ligands **5** and **15** were weaker than the others (Fig. 1.2D). Thus, the differential effects of modest changes in

ligand chemistry are greatly amplified in the context of natural response elements in their normal chromosomal settings.

Ligand 15 is a competitive inhibitor of prednisolone and dexamethasone effects

As ligands **13** and **15** bound GR with high affinities in vitro (Table 1.1), yet failed to regulate any glucocorticoid-responsive genes or influence A549 cell growth, we tested whether they potentiate GR activities prior to changes in gene expression, such as nuclear localization. Cells that stably express rat GR fused to enhanced GFP (eGFP–rGR) were treated with DMSO, dexamethasone, and ligand **13** or ligand **15** for 4 h, and the localization of eGFP–rGR was monitored. As shown in Figure 3A, eGFP–rGR was cytoplasmic in the control (DMSO-treated) cells and nuclear in the dexamethasone-, ligand **13**-, or ligand **15**-treated cultures (Fig. 1.3B–D). Thus, these experiments demonstrate that ligands 13 and 15 differ from dexamethasone in their effects on GR function at some step after ligand binding and nuclear localization.

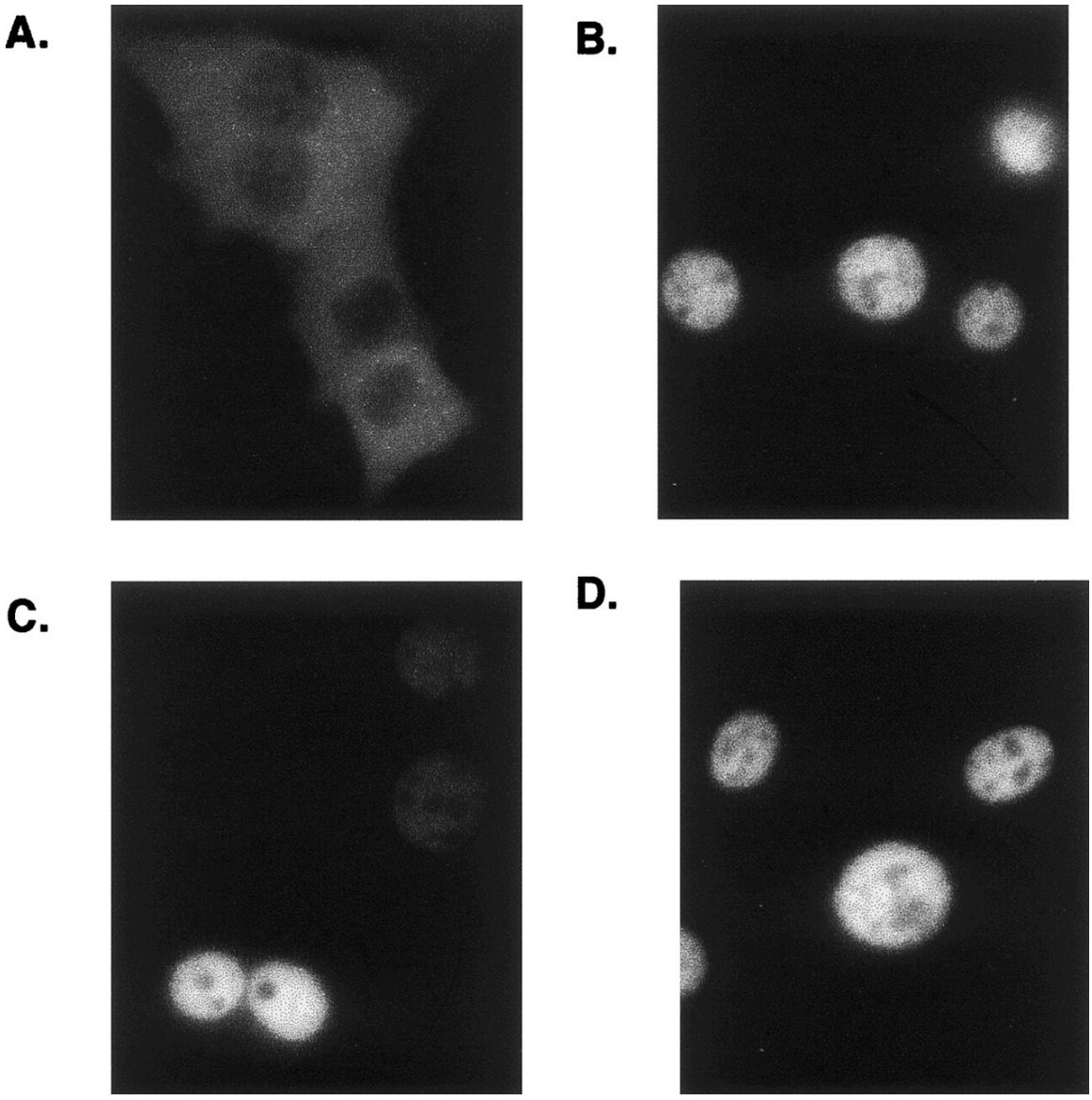

Figure 1.3 Ligands **13** and **15** induce GR nuclear localization. Subconfluent eGFP–rGR cells were treated with DMSO (vehicle control) (*A*), 100 nM dexamethasone (*B*), 1 μM ligand **13** (*C*), and 1 μM ligand **15** (*D*) for 4 h. Localization of eGFP–rGR protein was then monitored. Representative data from two experiments are shown.

We then tested whether these two compounds are competitive inhibitors of dexamethasone and prednisolone. For these experiments, we cotreated A549 cells with 1 μM ligand 13 or 15 and 1 or 0.1 μM prednisolone, and monitored the effects on GR-responsive genes. As shown in Figure 1.4A, ligand 15 but not 13 significantly

antagonized the 0.1 μM prednisolone-induced expression of Kip2, GILZ, and MCJ genes, whereas ligand 13 had no effect. Ligand 15 also modestly inhibited the induction of these three genes by prednisolone (Fig. 1.4A). We further showed that 1 μM ligand 15 but not 13 significantly decreased the antiproliferative effect of 0.1 μM prednisolone (Fig. 1.4B), whereas neither ligand competed with 1 μM prednisolone (Fig. 1.4B). Taken together, our findings establish that ligand 15 is a competitive inhibitor of prednisolone in A549 cells.

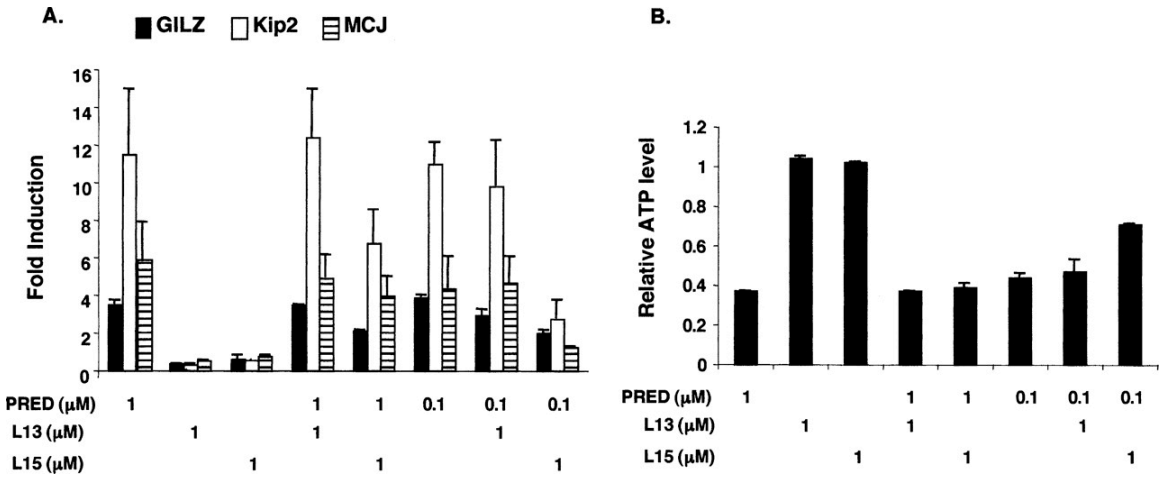

Figure 1.4 Ligand **15** inhibits prednisolone-regulated cell proliferation and gene expression in A549 cells. (*A*) A549 cells were treated as indicated for 4–5 h. Total RNA was isolated and subjected to cDNA synthesis. The cDNA was then analyzed by qPCR to measure mRNA levels of distinct GR target genes: GILZ (solid bar), Kip2 (open bar), and MCJ (hatched bar). The data represent the mean (SEM) of the fold induction (relative to DMSO-treated responses) from four experiments. (*B*) A549 cells were treated with distinct ligands as indicated for 5 d. The relative ATP levels of cells were then measured. The data represent the mean (SEM) of the fold induction (relative to DMSO-treated responses) from three experiments.

GR:GRE binding in vivo is differentially regulated by ligands

The failure of ligands **13** and **15** to affect GR target gene transcription could reflect either a loss of GRE occupancy by GR bound to either of these two compounds, or GR:GRE binding by GR that is inactive for transcriptional regulation. To test this model, we performed ChIP assays to detect the in vivo GR occupancy at three GREs: ENaCα, GILZ, and SLC19A2 (Wang et al. 2004). We found that ligand **13**-bound GR (denoted as GR:**13**) did not occupy any of these three GREs (Fig. 1.5A–C). GR:**15** was recruited to the GILZ and the SLC19A2 GREs, but the occupancy was lower than that of GR:prednisolone (Fig. 1.5B,C). Interestingly, the occupancy of GR:**15** and GR:prednisolone at ENaCα GRE was comparable (Fig. 1.5A), despite the failure of ligand **15** to activate ENaCα gene transcription.

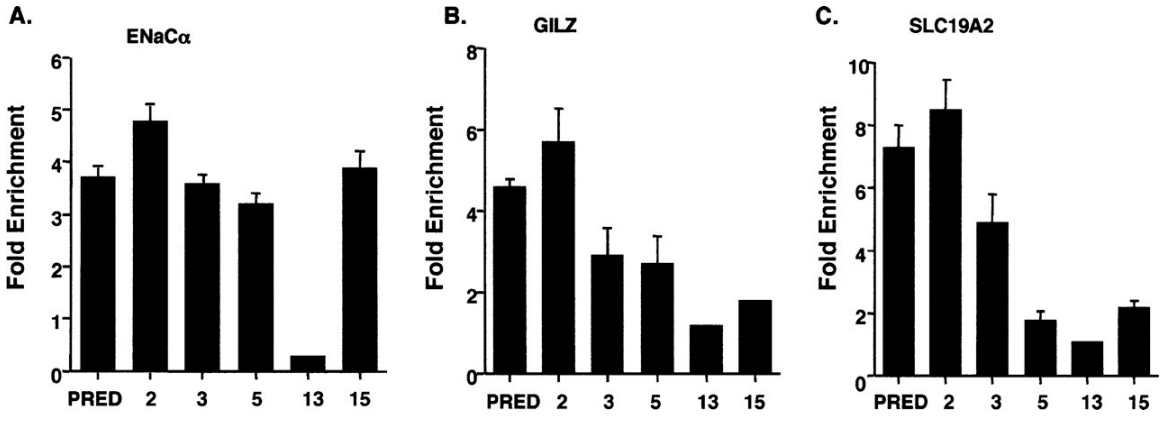

Figure 1.5 Arylpyrazole compounds differentially affect GR occupancy at distinct GREs. A549 cells were treated with prednisolone or various arylpyrazole compounds for 1 h, and ChIP experiments were performed to assess occupancy by GR. The results for the following genes are shown: ENaCα (*A*), GILZ (*B*), and SLC19A2 (*C*). The fold enrichment values for the experimental regions are determined by normalizing to the control hsp70 value. The data represent the mean (SEM) of the fold enrichment (relative to DMSO-treated responses) from at least three experiments.

We also tested the occupancy of ligands GR:**2,** GR:**3,** and GR:**5** at these three GREs. At the ENaCα GRE, the recruitment of GR was comparable when A549 cells were treated

with prednisolone or ligands **2, 3,** or **5** (Fig. 1.5A); in parallel, the ENaCα gene was induced by prednisolone and these three compounds (Figs. 1.2A, 1.5A). While the occupancy of GR:**2** was comparable to that of GR:prednisolone at the GILZ and the SLC19A2 GREs, the occupancy of GR:**5** was much weaker (Fig. 1.5B,C), and ligand **5** failed to induce transcription of either gene (Fig. 1.2A). The weaker occupancy of GR:**3** relative to GR:prednisolone at the GILZ GRE appeared to correlate with a lower magnitude of induction of GILZ gene expression by ligand **3** (Fig. 1.5B). In contrast, whereas GR:**3** significantly occupied SLC19A2 GRE, it did not activate SLC19A2 gene transcription (Figs. 1.2A, 1.4C).

Taken together, our results indicated that GR:GRE occupancy commonly correlated with receptor-mediated induction. Importantly, however, we defined two distinct mechanisms by which ligands selectively regulate GR target gene transcription. First, GR:**13** complexes failed to occupy three GREs at genes that are strongly induced by GR:prednisolone. Second, GR:**3** and GR:**15** occupied successfully the GREs at the SLC19A2 and ENaCα genes, respectively, but they were inactive in transcriptional regulation, implying a functional difference in the regulatory complexes at these genes at a step downstream of GRE occupancy.

***Prednisolone, not ligand* 15, induces histone acetylation of the ENaCα gene**

Among the first events following GR:GRE occupancy are modifications of chromatin structure, such as histone acetylation. We surveyed the effects of prednisolone and ligand **15** on histone acetylation of the ENaCα gene by monitoring eight genomic regions spanning 1.5 kb on either side of the transcription start site (Fig. 1.5A). Time-course

experiments with prednisolone revealed that maximal increases of acetylated histone H3 and H4 levels were observed upon 30 min of treatment in many of these regions (data not shown). For histone H3, prednisolone increased acetylation levels in three genomic regions (Fig. 1.6B, regions 1, 5, 7, and 8); in contrast, ligand **15** did not increase AcH3 levels in these regions (Fig. 1.6B). Furthermore, prednisolone increased the levels of acetylated histone H4 (AcH4) in all genomic regions tested except region 3, which includes the GRE (Fig. 1.6C). Ligand **15,** however, failed to induce significant AcH4 levels in these seven regions (Fig. 1.6C). Overall, these results demonstrated that although GR:**15** is recruited to the ENaCα GRE, it is unable to stimulate efficient histone acetylation.

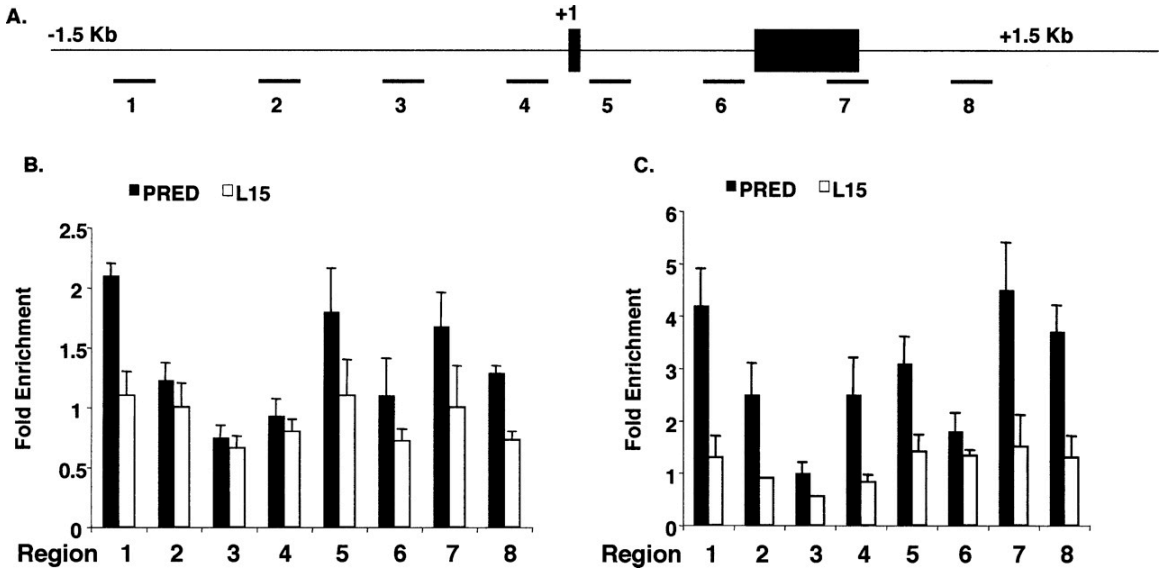

Figure 1.6 Prednisolone but not ligand **15** increases histone acetylation at the ENaCα gene. (*A*) Schematic diagram of the ENaCα gene; closed boxes indicate exons, and the transcription start site is indicated as +1. Amplified genomic regions are underlined and numbered. (*B*) A549 cells were treated with prednisolone (1 μM) or ligand **15 (**1 μM) for 30 min, and actylated histone H3 was measured in each numbered region by ChIP. (*C*) A549 cells were treated with prednisolone (1 μM) or ligand **15** (1 μM) for 30 min, and actylated histone H4 was measured in each numbered region by ChIP. Fold enrichment values in *B* and *C* were determined by normalizing to a control gene, hsp70. The data represent the mean (SEM) of the fold enrichment (relative to DMSO-treated responses) from at least three experiments.

Discussion

Previous studies have shown that ligands for various intracellular receptors can dictate the actions of their cognate receptors. Most notably, ER ligands such as estradiol, tamoxifen, and raloxifene display distinct functions in different cell types, and induce dramatically different gene expression profiles in a single cell type[20,37,11]. Although these results are striking, the chemical structures of these ER ligands are significantly different, thus complicating inferences of potential relationships between chemical structure and biological response. In this study, we applied a series of structurally related compounds (Table 1.1), that differ at only a single position on an arylpyrazole scaffold, to systematically analyze their effects on GR actions.

Our closely related arylpyrazole compounds displayed remarkable differences in their effects on GR target genes (Table 1.2; Fig. 1.2B). For example, ligands **14** and **15** differ only in the position of a single hydroxyl group (Table 1.1); however, they evoked markedly distinct GR-regulatory activities, both in A549 and in 3T3-L1 cells. In A549 cells, ligand **14** effectively induced the expression of several prednisolone-activated genes, whereas ligand **15** failed to activate any. Similarly, ligands **4** and **9** differ only by a single oxygen atom, yet ligand **4** represses the Rantes gene nearly as effectively as dexamethasone, whereas ligand **9** is inactive. Thus, our studies demonstrate that slight differences in ligand structure can drastically affect the activities of intracellular receptors; moreover, ligand activities clearly depend on response element and cellular context. By comparing chemically similar ligands in well-defined response element and

cellular (or cell-free) environments, it should eventually be possible to discern structure–function relationships for ligands and, in turn, to define how changes in the topology of the ligand-binding pocket determine specific receptor actions.

Our ChIP experiments showed that the different arylpyrazole compounds produced strikingly distinct enrichments of GR-binding fragments from different genes. We have assumed here that the differential enrichments are proportional to GR occupancy in vivo; an alternative explanation is that differential ChIP signals reflect variations in epitope accessibility or affinity resulting from distinct GR conformations or regulatory complex compositions. It may prove possible in future work to distinguish these possibilities, for example, by testing whether the arylpyrazole compounds affect intrinsic GR:GRE-binding affinities. Whatever the case may be, our present findings establish that differences in ligand chemistry give rise to a host of functionally distinct GR-containing regulatory complexes. Indeed, these results using synthetic ligands suggest that the conventional idea that GR uses only a single ligand in vivo perhaps should be re-evaluated; particular precursors or metabolites of cortisol, for example, may be functional GR ligands in specific cell or gene contexts.

Although our ChIP results generally indicate a rough correspondence between GR:GRE occupancy and the magnitude of regulation, this correspondence is clearly violated at certain GREs. This might be explained in some settings by ligand-selective effects on the actions of GREs as allosteric regulators of GR activity[38]. In addition, GR-binding sequences associated with normal chromosomal genes are commonly embedded within clusters of factor-binding sites that collectively comprise “composite” GREs. These elements include binding sites for non-GR regulators that participate in a GRE-specific

manner in the hormone response. At some composite GREs, such as that for the rat phosphoenolpyruvate carboxykinase (PEPCK) gene, the nonreceptor regulators are required for GR recruitment to its DNA-binding sites[39]; at others, such as that for the proliferin gene, GR binds to the GRE independently but depends on nonreceptor regulators to define its activity[40,41]. Furthermore, GR also can act from "tethering" GREs, at which the receptor fails to bind DNA, and instead associates through protein–protein interaction with a DNA-bound nonreceptor regulator[14,32]. Remarkably, even a 1-base-pair difference in a regulator-binding site can result in the recruitment of distinct cofactors to regulatory complexes[32,42]. In the limit, this implies that each GR target gene might nucleate the assembly of a GRE-specific regulatory complex to mediate its glucocorticoid response; Rogatsky et al.[43] have, in fact, detected GRE-specific patterns of GR functional domains, each conferring glucocorticoid activation of a different gene.

Thus, GR integrates signaling information from both ligands and GREs to determine its conformation and regulatory function. Notably, because ligand binding precedes the potential GRE interaction, the GR conformation induced by a particular arylpyrazole compound may promote binding to only a subset of GREs, and regulatory activity at only a subset of the occupied sites. In our study, we used dexamethasone to identify an initial set of GR target genes; it seems likely that the arylpyrazole compounds may regulate additional genes not controlled by dexamethasone or prednisolone. Moreover, our initial assays measured the effects of the arylpyrazole ligands on the expression of a reporter gene bearing a simple synthetic GRE. Because each reporter represents only a certain GRE context, reporter analyses greatly oversimplify the ligand effects on endogenous gene regulation. Notably, ligand **15,** which was inactive on several endogenous target

genes induced by prednisolone, was able to activate reporter gene expression. Thus, ligand **15** may in fact regulate a subset of endogenous genes whose GRE sequences and architecture yield functional ligand **15**-induced regulatory complexes in appropriate cell contexts in vivo.

Our results indicate that multiple mechanisms underlie ligand-regulated gene transcription. Thus, ligands can differentially affect the capacity of GR to bind to particular GREs. In addition, ligands can selectively affect events downstream of GR:GRE association, such as histone acetylation. In the simplest model, these downstream events may reflect ligand-directed differences in the subunit composition of the regulatory complexes. Alternatively, the complexes may be compositionally identical, but conformationally distinct in ways that affect their specific functions. Interestingly, for the ENaCα genes we found that p300, a universal coactivator, was recruited to the GRE upon either prednisolone or ligand **15** treatment (data not shown). In future studies, it will be interesting to determine whether the differential effect of these two ligands on GR regulation of EnaCα resides in differences in subunit occupancy or conformation.

In conclusion, we suggest that subtle differences in ligand structure induce or stabilize particular "surfaces" of intracellular receptors that alter their interactions with chromosomal response elements and effect differential gene regulation. Specifically, our series of arylpyrazole compounds are valuable tools for dissection of cellular and molecular functions of GR. For example, detailed analyses of ligand-specific regulatory complexes at distinct GREs will advance our understanding of the context-dependence that contributes to the remarkable range of physiological actions of GR and other

intracellular receptors. Moreover, these compounds may provide a potential resource for therapeutic development.

Chapter 1 Materials and Methods

qPCR

Total RNA was isolated from cells by using QIAshredder and RNeasy kits (Qiagen). To synthesize random-primed cDNA, 0.5 μg of total RNA (10 μL), 4 μL of 2.5 mM dNTP, and 2 μL of random primers (New England Biolabs) were mixed and incubated at 70°C for 10 min. A 4-μL cocktail containing 25 U of Moloney Murine Leukemia Virus (M-MuLV) Reverse Transcriptase (New England Biolabs), 10 U of RNasin (Promega), and 2 μL of 10× reaction buffer (New England Biolabs) was then added, and incubated at 42°C for 1 h. The reaction was then incubated at 95°C for 5 min.

The resultant cDNA was diluted to 200 μL, and 4–5 μL was used per 35-μL reaction containing 1.25 U of *Taq*DNA polymerase (Promega), 1× reaction buffer, 1.5 mM $MgCl_2$, 0.5 mM dNTP (Invitrogen), 0.2× SYBR green I dye (Molecular Probes), and 357 nM each primer. qPCR was performed in an Opticon-2 DNA Engine (MJ Research) and analyzed by using the Ct method (Applied Biosystems Prism 7700 Users Bulletin No. 2) and Rpl19 as an internal control for data normalization.

For ChIP experiments, samples from 1×10^8 to 2×10^8 A549 cells were used for 40 qPCR reactions. Primers that correspond to the promoter region of the hsp70 gene were used for data normalization.

All primers used in this report are available upon request.

ChIP

A549 cells (1×10^8 to 2×10^8 cells) were cross-linked by adding 10% (v/v) of a formaldehyde stock solution (50 mM HEPES-KOH at pH 8; 1 mM EDTA; 0.5 mM EGTA; 100 mM NaCl; 4.1% formaldehyde) at room temperature for 10 min. After 5 min, 0.125 M glycine (final concentration) was added to stop the cross-linking, cells were rinsed with phosphate-buffered saline (PBS), harvested by scraping, and collected by centrifugation (5 min at 600*g*). Pellets were resuspended in Lysis Buffer (50 mM HEPES-KOH at pH 8; 1 mM EDTA; 0.5 mM EGTA; 140 mM NaCl; 10% glycerol; 0.5% NP-40; 0.25% Triton X-100; 1 mM PMSF; 5 μg/mL each of leupeptin, pepstatin A, and aprotinin) and nutated for 10 min at 4°C. The crude nuclei were collected by centrifugation (600*g* for 5 min at 4°C) and resuspended in Wash Buffer (10 mM Tris-HCl at pH 8; 1 mM EDTA; 0.5 mM EGTA; 200 mM NaCl; 1 mM PMSF; 5 μg/mL each of leupeptin, pepstatin A, and aprotinin) and nutated again. Washed nuclei were centrifuged as above and resuspended in 1× RIPA Buffer (10 mM Tris-HCl at pH 8; 1 mM EDTA; 0.5 mM EGTA; 140 mM NaCl; 1% Triton X-100; 0.1% Na-deoxycholate; 0.1% SDS; 1 mM PMSF; 5 μg/mL each of leupeptin, pepstatin A, and aprotinin).

Samples were sonicated (power setting 5–6) with a Branson Sonifier 250 with a microtip in 20-sec bursts followed by 1 min of cooling on ice for a total sonication time of 120–150 sec per sample. This procedure produced DNA fragment sizes of 0.3–0.8 kb. Samples were then centrifuged in a microfuge at maximal speed for 10 min at 4°C. N499 antibody raised against GR (Nissen and Yamamoto 2000) or AcH3 or AcH4 antibody (Upstate) was added to this cleared chromatin extract and incubated overnight with rotation at 4°C. Samples were then centrifuged again, and supernatants were transferred to fresh tubes containing 20 μL of precleared 50% slurry Protein A/G agarose beads (for

GR, Santa Cruz) or Protein A agarose beads (for AcH3 and AcH4, Upstate) in 1× RIPA containing 100 μg/mL sonicated salmon sperm DNA. After 3 h with beads, samples were centrifuged and the pellets were washed once with 1× RIPA buffer, three times with 1× RIPA containing 100 μg/mL salmon sperm DNA for 5 min with rotation, twice with 1× RIPA containing 500 mM NaCl final plus 100 μg/mL salmon sperm DNA for 5 min with rotation, and once with 1× RIPA buffer. Then 100 μL of digestion buffer was added (50 mM Tris at pH 8; 1 mm EDTA; 100 mM NaCl; 0.5% SDS; 100 μg/mL proteinase K) and placed at 55°C for 3 h, followed by overnight at 65°C to reverse cross-links. DNA was phenol-$CHCl_3$ extracted once, $CHCl_3$ extracted once, and ethanol precipitated in the presence of 20 μg of glycogen. Pellets were resuspended in TE and used to perform qPCR.

Cell lines

A549 human lung adenocarcinoma cells (ATCC and UCSF cell cultural facility) were cultured in DMEM with 10% fetal bovine serum (FBS; GIBCO). When cells were treated with dexamethasone, prednisolone, or arylpyrazole compounds, DMEM with 10% charcoal stripped FBS (Omega) was used.

3T3-L1 preadipocytes (ATCC) were cultured in DMEM with 10% calf serum (GIBCO). Confluent cultures were induced to differentiate by changing the medium to DMEM with 10% FBS, 1 μg/mL insulin, 0.5 mM isobutyl-1-methylzanthin, and 1 μM dexamethasone, prednisolone, or distinct arypyrazole compounds. After 2 d, this medium was replaced with DMEM supplemented with 10% FBS plus 1 μg/mL insulin, and cells were maintained in this medium until processing for analysis.

MC3T3-E1 cells (a gift of Dr. Tamara Alliston, University of California at San Francisco, San Francisco, CA) were grown in α-MEM with 10% FBS. For osteoblast differentiation, these cells were switched to differentiation medium upon reaching confluence. This medium consisted of α-MEM, 10% FBS, 100 mg/mL ascorbic acid, and 5 mM β-glycerophosphate.

Cell viability assay

Cell viability was monitored using the CellTiter-GloTM luminescence assay (Promega) according to the manufacturer's recommended protocols. This assay uses luciferase to measure ATP, an indicator of viable cells. The luminescent signal produced is proportional to the number of viable cells present in culture.

Oil Red O staining

3T3-L1 cells were washed three times with PBS and fixed in 10% formalin in PBS for 1 h. After washing the cells twice with PBS, cells were stained with Oil Red staining solution (0.5% Oil Red [Sigma] in isopropanol, diluted 3:2 in water and filtered with a 0.22-μm filter). After staining, cells were washed three times with water. Isopropanol was then added into culture wells for 15 min. The extracting dye was monitored at the optical density 500 nm[44].

Alizarin red staining

Confluent cultures of MC3T3-E1 cells in 12-well plates were rinsed in Ca^{2+}/Mg^{2+}-free phosphate-buffered saline and fixed for 5 min in 10% formalin/saline. The cells were then incubated with alizarin red (0.1% in saline) solution for 3–7 min followed by several

washes with water. For quantitation, the stained cells were destained for 3–4 h with ethylpyridinium chloride (Sigma), and the extracted stain was measured by absorbance at 562 nm[45].

GR-GFP cell line and imaging analysis

The eGFP–rGR cell line expressing enhanced GFP-rat GR under control of the Tet-Off synthetic promoter was obtained as a stably transfected derivative of the Tet-Off murine mammary adenocarcinoma cell line 5858[46]. The eGFP–rGR construct was cloned into pTRE-tight (Clontech), and the resulting construct was transfected along with a puromycin-resistance plasmid into Tet-Off cell line 5858. Colonies were selected in media supplemented with 1.5 μg/mL puromycin and isolated by single-cell cloning of strongly GFP-positive cells. Cells were maintained in DMEM (GIBCO) supplemented with 10% FBS, 0.1 mM nonessential amino acids, 2 mM L-glutamine, 1 mM sodium pyruvate, 1 mg of G418/mL, 1.5 μg/mL puromycin, and 10 μg/mL tetracycline at 37°C in 5% CO_2 in a humidified incubator. To induce eGFP–rGR expression for imaging, cells were transferred to Lab-Tek II chambers (Nalge Nunc International) 3 d prior to imaging and grown in media without tetracycline. One day prior to imaging, cells were switched to phenol red-free DMEM supplemented with 0.1 mM nonessential amino acids, 2 mM L-glutamine, 1 mM sodium pyruvate, 1 mg of G418/mL, 1.5 μg/mL puromycin, and 10 μg/mL tetracycline, and with 10% charcoal-stripped FBS (Omega). Cells were treated with ligand (1 μM) for 4 h before imaging using a Zeiss Axiovert 200M microscope with a Zeiss Apochromat 63×/1.4-numerical-aperture oil immersion objective.

Transfection

Transfection of A549 lung adenocarcinoma cells used lipofectamine 2000 (Invitrogen) according to the technical manual; cells were harvested 24 h post-transfection. Assays for β-galactosidase and luciferase activity have been described previously[47]. The TAT3 reporter plasmid was previously described[47].

Ligand-binding assays

Ligand binding was determined by fluorescence polarization using GR, AR, and PR Competitor Assay Kits (Invitrogen) according to the manufacturer's recommended protocol[26].

Acknowledgments

We thank Drs. Lisa Choy, Tamara Alliston, and Fred Schaufele for providing MC3T3-E1 preosteoblasts and 3T3-L1 preadipocytes. We thank Drs. Rik Derynck, Brian Black, Kevan Shokat, Hans Luecke, Eric Bolton, Neal Freedman, and Inez Rogatsky for reviewing the manuscript. J.-C.W. is supported by a post-doctoral fellowship of the American Heart Association. S.H.M. is supported by a post-doctoral fellowship from the Leukemia and Lymphoma Society. C.P. is supported by a predoctoral fellowship from the American Heart Association. This work is supported by grants from the NIH to K.R.Y. and T.S.S.

Chapter 2: Selective Glucocorticoid Receptor-Mediated Therapies for Asthma

Chapter 2 Introduction

Asthma is a chronic inflammatory disease responsive to glucocorticoid therapy and characterized by airway hyperreactivity, mucus overproduction and eosinophilic inflammation. The molecular mechanisms that initiate and maintain the disease state have not been completely determined, but it has become clear that understanding of asthma pathogenesis and the development of new therapies will require the identification and study of the disease modifying genes that act downstream of the signaling pathways that contribute to the disease.

Glucocorticoids have been used as the main drugs for asthma treatment for almost six decades. Indeed, inhaled corticosteroids and long-acting bronchodilators are currently the mainstay therapy for most asthma patients. Despite improvements in the pharmacokinetic and pharmacodynamic profiles of inhaled corticosteroids, adverse effects are still of great concern to clinicians. Systemic effects of inhaled corticosteroids include adrenal suppression, reduction of growth velocity in children and loss of bone mineral density.

Both the positive therapeutic effects of corticosteroids, and their adverse side effects, are mediated via regulation of gene transcription by the glucocorticoid receptor (GR), which binds selectively to cognate ligands, such as the hormone cortisol or the synthetic agent fluticasone. Upon ligand binding, GR migrates to the nucleus, binds to specific genomic sites termed glucocorticoid response elements (GREs) and regulates transcription from nearby genes. GREs are surprisingly diverse: GR binds selectively to a broad range of DNA sequences and can also tether through protein-protein contact to nonreceptor DNA-bound factors. The precise molecular mechanisms of regulation by GR are not fully

understood, but they too are diverse: GR controls distinct circuits of genes in different tissues, and it can activate some genes and repress others even within a single cell. Its tissue-specific regulatory circuits create gene networks that produce global physiologic, pathologic or pharmacologic consequences, such as those seen in the treatment of asthma.

Despite intense efforts in pharma and biotech, no GR ligands have been described that retain certain activities while losing others. In particular, there are no compounds or treatment regimens that are efficacious for the treatment of asthma without accompanying adverse effects. Recent observations showing that GRE architecture and ligand structure strongly affect the nature and mechanisms of GR regulation imply that the development of corticoids (*i.e.,* GR ligands, not necessarily steroidal, that modulate GR activities *in vivo*) with desired selectivity is likely within reach, but will require a better understanding of the molecular events that underlie GR signaling and regulation at particular target genes in particular cell types.

Glucocorticoid treatment affects multiple cell types in the lungs of asthmatic patients. Corticosteroids inhibit cytokine secretion by macrophages, reduce circulating eosinophils, inhibit activation of T-lymphocytes, decrease mucosal mast and dendritic cell number, and also inhibit the transcription of several cytokines in epithelial airway cells. Corticosteroids seem to regulate a network of inflammatory genes across multiple cell types. Steroid treatment increases the levels of the anti-inflammation genes lipocortin-1, secretory leukocyte protease inhibitor, the anti-inflammatory cytokine interleukin 10 (IL-10), and IκB-α, a negative regulator of the NFκB pathway. Finally, steroid treatment inhibits the transcription and secretion of several cytokines, including IL-1β, TNF-α, granulocyte-macrophage colony-stimulating factor (GM-CSF), IL2, IL-3,

IL-4, IL-5, IL-6, IL-11 and the chemokines IL-8, RANTES, MCP-1, MCP-3, MIP-1α, and eotaxin. Unfortunately, the primary target genes that contribute to the various effects of corticoids remain largely unidentified.

To approach this problem, Woodruff et al.[48] performed a microarray-based clinical study in which genomewide expression patterns were obtained from bronchoepithelial cells (BEC) of healthy controls and asthmatic patients before and after therapy with the inhaled corticosteroid fluticasone. Bronchoepithelial cells were used for their ease of isolation through bronchoscopy, their involvement in asthma pathogenesis and because they are the first cell type to be exposed to inhaled glucocorticoid therapeutics and to allergens that provoke asthma pathogenesis.

Three genes (CLCA1, SERPINB2 and POSTN) were identified that displayed increased expression in BECs of asthmatic patients when compared to healthy controls and whose levels were decreased after treatment with fluticasone. Importantly, these three genes were linked to asthma in animal and cell culture models, and their transcript levels correlated with the clinical response to fluticasone. These results suggest that POSTN, CLCA1 and SERPINB2 may contribute to asthma pathogenesis and that their downregulation by fluticasone may be linked causally to the efficacy of glucocorticoid therapy. To investigate the transcriptional regulation of CLCA1, SERPINB2 and POSTN by glucocorticoids we established a cell culture system that recapitulated the results of the Woodruff et al. clinical study.

Chapter 2 Materials and Methods

In Vitro Studies

BEAS-2B cells were maintained on DME-H16 10% FBS medium and changed to DME-H16 medium containing 10% activated charcoal-stripped FBS the day before they reached confluence. All further experiments are carried out in stripped serum medium. Cells were treated with IL-13 (50 ng/ml) for 4 days, with the addition of dexamethasone at a dose range in the last 24 h before cell lysis and RNA extraction using the Qiagen RNeasy mini-kit (Qiagen, Valencia, CA). All conditions were performed in triplicate.

Whole lungs were frozen in liquid N_2 and disrupted in the presence of RLT buffer. RNA was extracted using the Qiagen RNeasy mini-kit (Qiagen, Valencia, CA). Human bronchial epithelial cells were obtained at autopsy (courtesy of Walter Finkbeiner, University of California, San Francisco) by enzymatic digestion as described previously in ref. 42 and plated in a 1:1 mixture of DMEM/Ham's F-12 plus 5% FBS, penicillin (100 units/ml), streptomycin (1 mg/ml), fungizone (2.5 μg/ml), gentamicin (50 μg/ml) (PSFG), and onto polycarbonate inserts (0.4-μm pore size; Costar, Corning, MA) coated with 20 μg/ml human placental collagen at 9.1×10^5 cells per filter. For 2 successive days, filters and wells were rinsed twice with PBS with PSFG, and 1 ml of ALI medium[49] was added to each well. Then, the medium was changed every other day. On days 13 and 14, medium was switched to ALI (−) hydrocortisone/(+) 50 ng/ml IL-13 excepting four control filters, which were switched to ALI (−) hydrocortisone. On day 15, either 1 μM dexamethasone (Sigma–Aldrich, St. Louis, MO) reconstituted in DMSO or 100 nM budesonide (AstraZeneca, Wilmington, DE) diluted in PBS were added as appropriate.

All conditions were performed in quadruplicate. On day 16, cells were lysed, and RNA was extracted as described above.

MC3T3-E1 cells were maintained in α-MEM with 10% FBS. Osteoblast differentiation was induced after confluence was reached. The differentiation medium consisted of α-MEM, 10% FBS, 100 mg/mL ascorbic acid, and 5 mM β-glycerophosphate. Cells were maintained in differentiation medium for 2 weeks in the presence or absence of ligand before staining was performed. Confluent cultures of MC3T3-E1 cells in 12-well plates were rinsed in Ca^{2+}/Mg^{2+}-free phosphate-buffered saline and fixed for 5 min in 10% formalin/saline. The cells were then incubated with alizarin red (0.1% in saline) solution for 3–7 min followed by several washes with water.

Real-Time PCR (qPCR)

For analysis of epithelial brushings and primary human airway epithelial cells, two-step qPCR was performed as described previously in ref. 47. cDNA synthesis was carried out by using 20 ng of total RNA and BD Clontech (Mountain View, CA) Powerscript Reverse Transcriptase with random hexamers for priming. Then, multiplex preamplification was performed by using one-fifth of the resultant cDNA, Advantage 2 Polymerase (BD Clontech), and 5 pmol of each outflanking primer. Multiplex hot-start amplification was done for 5, 10, 15, and 20 cycles to ensure that the reaction remained in the exponential phase of PCR and the substrates were not limiting[50]. Real-time PCR gene quantification was then performed on the amplified cDNA by using TaqMan probes (Applied Biosystems, Foster City, CA) and Universal Master Mix (Platinum Quantitative PCR SuperMix-UDG with ROX; Invitrogen, Carlsbad, CA). Transcript quantification

was run on an ABI Prism 7900 Sequence Detection System (Applied Biosystems). Cycle threshold values obtained for each gene were then converted into relative transcript copy numbers based on logarithmic transformation and linear regression of prior data, as described previously[50]. Transcript copy numbers were normalized by using a two-step approach. First, the amount of amplification product used in TaqMan profiling was normalized on the basis of housekeeping gene expression. Then a panel of four housekeeping genes was measured during TaqMan profiling (GAPDH, ubiquitin, EEF1A1, and PPIA), and the geometric mean value of the two housekeeping genes most stably expressed across the samples was used for normalization[51]. For BEAS-2B cells, qPCR was performed without multiplex preamplification. First-strand cDNA synthesis was carried out by using 10 μg of starting RNA, and then one-fourth of the resultant cDNA was used for qPCR gene quantification by using the methods described above (including the same four housekeeping genes for normalization).

Sensitization and challenge with OVA

Age- and sex-matched 6–8-wk-old mice were sensitized by i.p. injection of OVA (Sigma-Aldrich) on days 0, 7, and 14 as reported previously[52]. The sensitizing emulsion consisted of 50μg OVA and 10 mg of aluminum potassium sulfate in 200μl of saline. On days 21, 22, and 23, the sensitized mice were lightly anesthetized by isoflurane inhalation and challenged with 100μg OVA in 30μl of saline administered intranasally. Dexamethasone and ligand 2 were solubilized in 50μl of DMSO and administered by i.p. injection 24h before OVA challenge on days 21, 22, and 23. Prednisolone and ligand 5 were solubilized in methylcellulose solution and administered by gavage 24h before OVA

challenge on days 21, 22, and 23. Control mice were treated in the same way, except that OVA was omitted during both the sensitization and challenge phases.

Assessment of airway reactivity, inflammation

Airway reactivity was measured as previously reported. Briefly, on day 24, mice were anesthetized, intratracheally intubated, mechanically ventilated, and paralyzed, and airway resistance was measured at baseline and following i.v. administration of increasing doses of acetylcholine (0.03, 0.1, 0.3, 1, and 3 μg/g body weight). Bronchoalveolar lavage (BAL) fluid leukocytes and serum OVA-specific IgE levels were measured as previously described[52]. All animal experiments were performed at the Sandler Center for Basic Research in Asthma.

Chapter 2 Results

IL-13 is a Th2 cytokine that is released by activated CD4+ T-lymphocytes. IL-13 is elevated in the sputum of asthmatic patients and can induce airway hyperresponsiveness and mucus overproduction when overexpressed in the BECs of transgenic mice. In addition, recent clinical studies suggest that inhibition of Th2 responses via a common inhibitor of IL-13 and IL-4 signaling may be beneficial for asthma control. IL-13 binds to a transmembrane receptor that activates the JAK/STAT6, PI3K and MAP kinase pathways. The effects of IL-13 during asthma induction seem to be mediated by the transcription factor STAT6, since a STAT6 KO mouse is resistant to IL13-induced airway hyperresponsiveness and mucus overproduction.

We found that treatment of the human bronchoepithelial cell line BEAS-2B with IL-13 (50 ng/ml) for 72hr induced SERPINB2 and POSTN transcription and that the glucocorticoid dexamethasone (72hr treatment) inhibited this activity in a dose-dependent manner (fig. 2.1a); the BEAS-2B cell line does not express CLCA1. Interestingly, induction of SERPINB2 and POSTN by IL-13 and repression by dexamethasone had slower kinetics when compared with the regulation of the genes IL-6 and MCP-1, which are also induced by IL-13 and repressed by glucocorticoids. The latter genes only required 4hr of treatment for induction or repression (data not shown). Importantly, we found that treatment of primary human bronchoepithelial cells (HBECs) for 72hr with IL-13 (50 ng/ml) induced CLCA1, SERPINB2 and POSTN mRNA levels and that dexamethasone again inhibited this activity (fig. 2.1b). Thus, the BEAS-2B cell line recapitulates some but not all aspects of the biology of bronchoepithelial cells. To probe the specificity of this response we tested the lung carcinoma cell line A549, and found

that CLCA1, SERPINB2 or POSTN were not expressed in those cells under basal conditions or after treatment with IL-13. We concluded that regulation of these genes by IL-13 is specific to bronchoepithelial cells (collaboration with Prescott Woodruff).

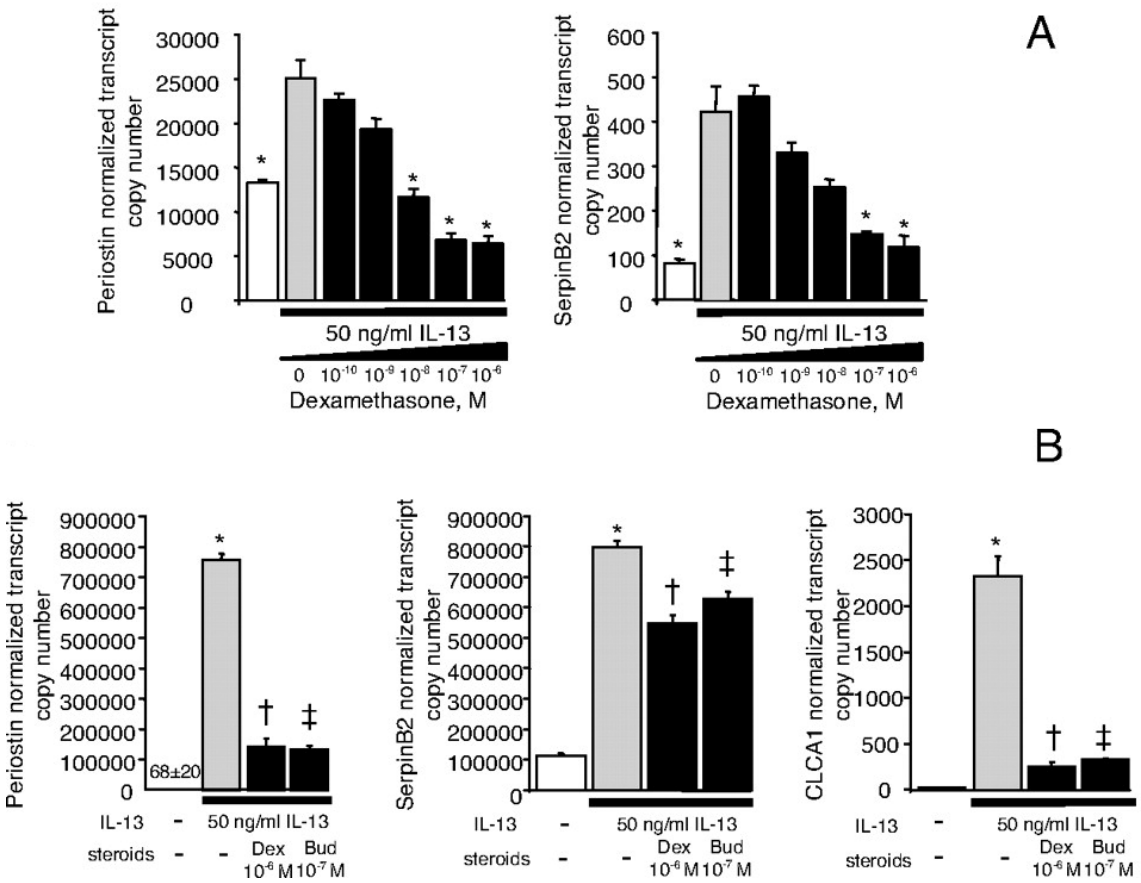

Figure 2.1 *In vitro* effects of IL-13 and corticosteroids on lung epithelial cells. (*A*) Dexamethasone inhibits induction of *periostin* and *serpinB2* by IL-13 in BEAS-2B cells grown in monolayer (*, $P < 0.05$ compared with IL-13-exposed cells without dexamethasone). (B) Dexamethasone (Dex) and budesonide (Bud) inhibit induction of *periostin* and *serpinB2* and *CLCA1* by IL-13 in primary airway epithelial cells grown at an ALI (*, $P < 0.05$ compared with all other groups; †, $P < 0.05$ compared with all groups except Bud; ‡, $P < 0.05$ compared with all groups except Dex). (Adapted from Woodruff, PG et al., 2007)

The SERPINB2 gene codes for a serine protease inhibitor and is located on chromosome 18 as part of a gene cluster that contains 6 other serpinB family genes. These genes appear to function in apoptotic cascades, metastasis and possibly asthma. We found that 5

of the 7 serpinB family genes of this cluster (SERPINB13, 4, 3, 7 and 2) are regulated in tandem by IL-13 and budesonide in BEAS-2B (fig. 2.2a). We confirmed these findings in primary HBECs. Although the repression of IL-13-induced SERPINB3 and SERPINB7 mRNA levels by budesonide did not reach statistical significance in HBECs we observed a trend towards significance (fig. 2.2b). Two serpinB genes (SERPINB5 and 8) reside on either side of the regulated cluster and are expressed under basal conditions. However, SERPINB5 is not affected by IL-13 or IL-13+glucocorticoid treatment, while SERPINB8 mRNA levels are slightly increased by either IL-13 or IL-13+glucocorticoid treatment in BEAS-2Bs and HBECs (fig. 2.2). We tested whether the SerpinB node of cross-talk between the IL-13 and glucocorticoid pathways is determined by direct transcriptional regulation by STAT6 and GR, respectively. First, we used bioinformatics to identify three putative glucocorticoid response elements (GREs) present in the 500kb spanning the serpinB locus, and showed that only one of them is conserved between rat and mouse. Secondly, we used chromatin immunoprecipitation to interrogate these genomic regions for GR binding after treatment with dexamethasone. We failed to detect binding of GR within these regions, despite detection of GR at the IL-8 GRE under the same conditions (data not shown). We are currently testing the hypothesis that GR may downregulate the transcription of the serpinB genes by a tethering mechanism that involves STAT6.

To identify additional asthma candidate genes regulated by the glucocorticoid and IL-13 pathways we carried out a literature search focusing on animal and human models of asthma. We found that in addition to SERPINB2, CLCA1 and POSTN, the genes ITLN1, GPX2, CEACAM5 and MUC5AC are also induced by IL-13 and repressed by glucocorticoid treatment in primary HBECs (data not shown). One or more of these genes

may function to promote asthma and respond to glucocorticoid treatment. We are currently investigating their molecular mechanisms of regulation by GR and STAT6.

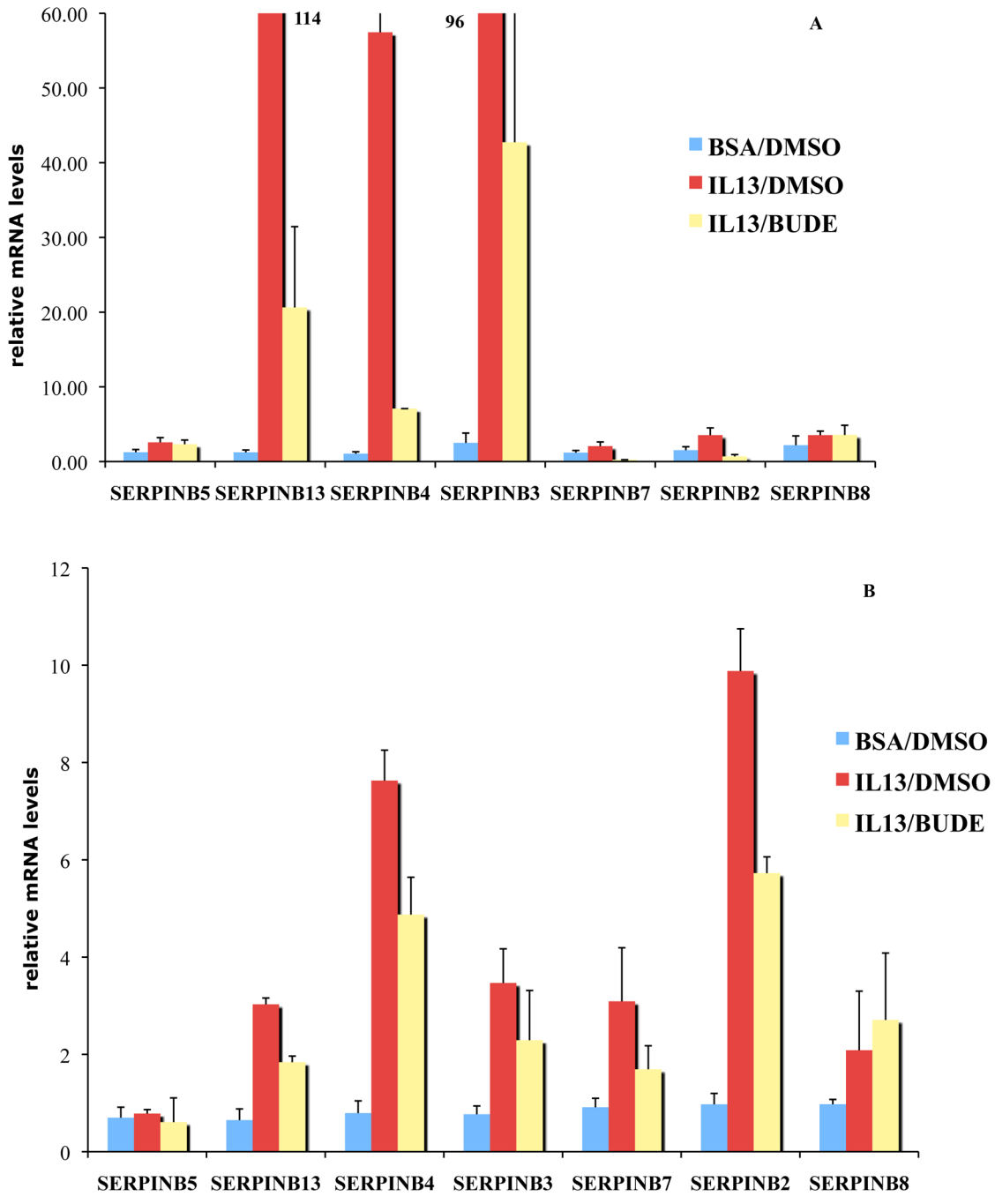

Fig. 2.2 Regulation of SERPINB cluster by IL-13 and dexamethasone. (A) BEAS-2B cells treated for 72hrs with IL-13 (50 ng/ml) and with dexamethasone for the last 24hrs. (B) HBECs treated for 72hrs with IL-13 (50 ng/ml) and with dexamethasone for the last 24hrs.

Our collaborator Tom Scanlan synthesized a novel series of nonsteroidal arylpyrazole GR ligands, which we have characterized in three biological activity assays. The striking result is that none of the arylpyrazoles strongly inhibits osteoblast differentiation, whereas some of them display inhibition of A549 cell proliferation and cytokine expression. This provocative biological activity profile (BAP) invites speculation that such ligands, or derivatives of them, might control the inflammatory aspects of asthma without inducing the associated decrease in bone density observed during chronic treatment with conventional glucocorticoids. Importantly, ligands 1, 2 and 5 were shown to have anti-inflammatory activity comparable to dexamethasone when administered as ointments in a standard mouse paw assay (Thomas Scanlan, unpublished results).

To determine if the arylpyrazole ligand series contains ligands of potential use towards asthma treatment we tested their abilities to prevent IL-13 induced transcription of the asthma candidate genes identified by Woodruff et al. We treated primary HBECs with IL-13 (50 ng/ml) for 72hr and added saturating concentrations of dexamethasone (1 μM), budesonide (100 nM) and arylpyrazole GR ligands (1, 2, 5, 9, 17) (1 μM) during the last 24hr of treatment. We found that all ligands were able to repress the transcription of POSTN (fig. 2.3). Ligand 9 was able to repress the transcription of SERPINB2, and ligand 2 was able to repress the transcription of CLCA1. Notably, ligand 2 had efficacy similar to the potent glucocorticoids dexamethasone and budesonide in the repression of SERPINB2.

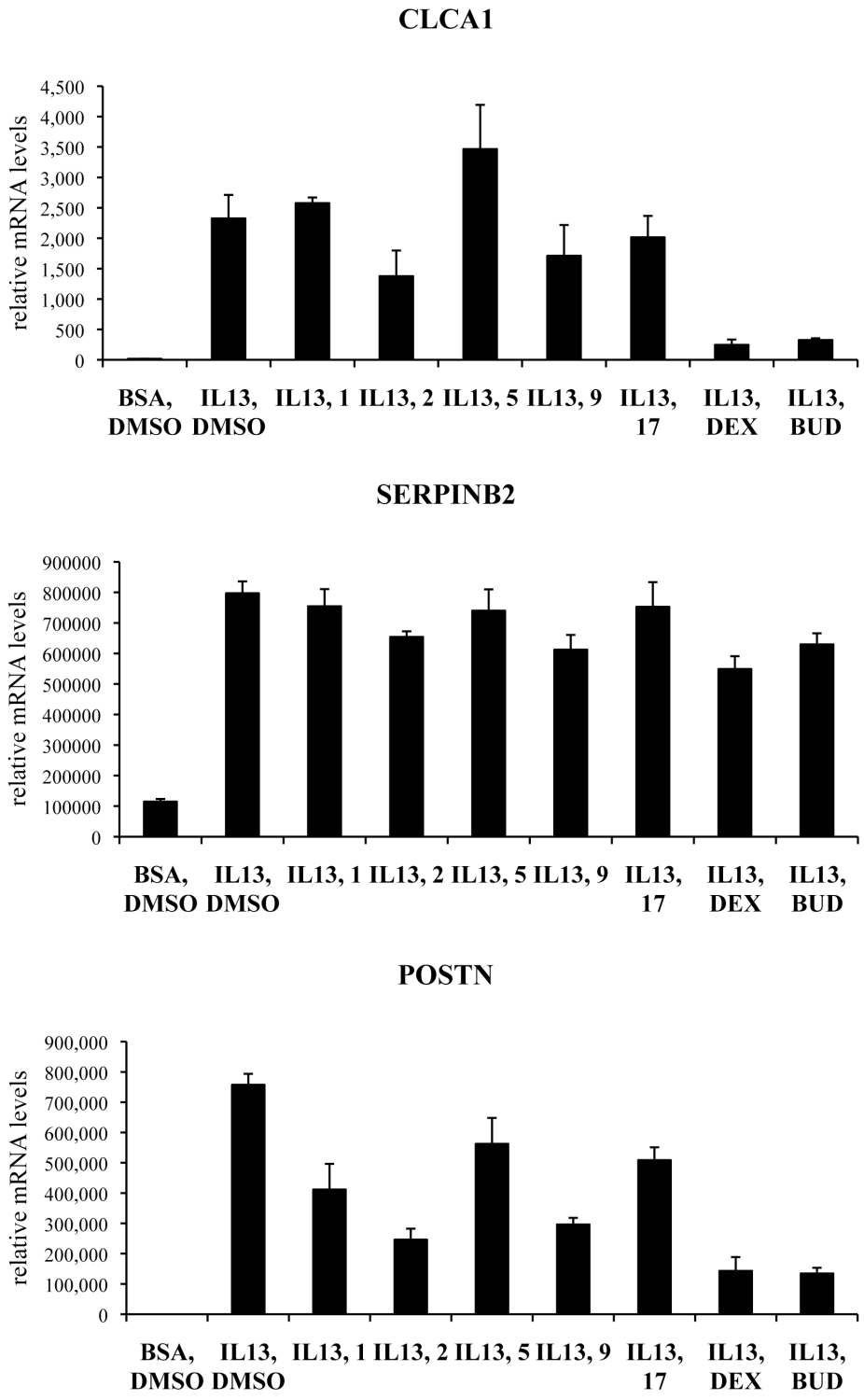

Fig. 2.3 Regulation of SERPINB2, POSTN and CLCA1 IL-13 dexamethasone, budesonide and arylpyrazole ligands. Primary HBECs were treated for 72hrs with IL-13 (50 ng/ml); and with ligands for the last 24hrs.

To further characterize ligand 2 we performed dose-response experiments testing the ability of ligand 2 to inhibit osteoblast differentiation of MC-3T3E1 preosteoblasts and to inhibit the transcription of asthma marker genes in primary HBECs when compared to dexamethasone. We found that while ligand 2 inhibited preosteoblast differentiation with an estimated IC50 ≅ $5*10^{-6}$, dexamethasone displayed an estimated IC50 ≅ 10^{-8} (fig. 2.4). Importantly, ligand 2 failed to fully block differentiation even at the highest dose used (1 μM), whereas the asthma drug budesonide had an IC50 similar to dexamethasone in this assay.

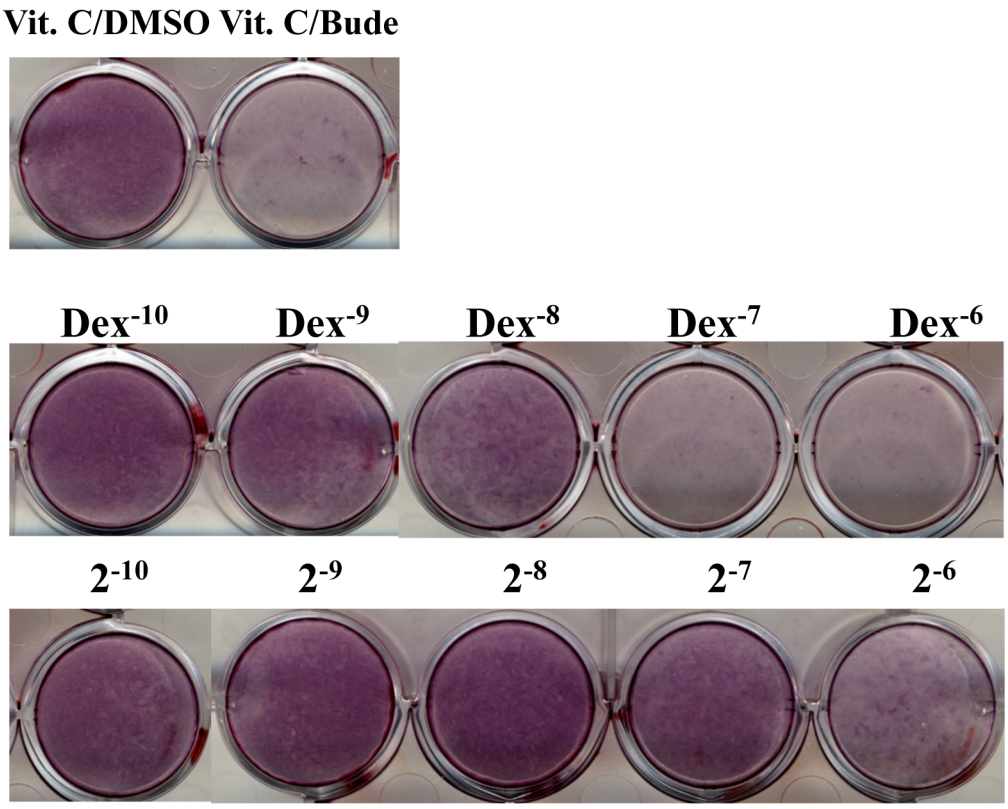

Fig. 2.4 *In vitro* effects of glucocorticoids on preosteoblasts. MC3T3-E1 cells treated every 48hrs with Vit. C, beta-glycerolphosphate and ligand. Cells were stained at the end of 2 weeks with Alizarin Red.

These results led us to hypothesize that ligand 2 might provide effective asthma therapy with bone sparing properties. To test the first part of this hypothesis we turned to the ovalbumin (OVA)-induced model of acute lung inflammation. This experimental model is an imperfect but useful proxy of human asthma. Importantly, OVA-induced eosinophilic inflammation, airway hyperreactivity and mucus overproduction are all glucocorticoid-responsive in this model. OVA-treated mice were treated IP, daily for the 3 days during the OVA challenge with dexamethasone (5mg/kg) or ligand 2 (5mg/kg). Dexamethasone treatment partially prevented the OVA-induced increase in airway hyperreactivity (fig. 2.5a), mucus overproduction as assessed by the increase in inflammatory cells obtained by broncholavage (fig. 2.6) and histology (data not shown). Ligand 2 prevented the increase in eosinophils observed in the OVA-treated mice. However, ligand 2 did not affect significantly any of the inflammation parameters when compared to control treated OVA-induced animals.

Next, we tested ligand 5 of the arylpyrazole series for therapeutic activities in the OVA-mouse model of asthma. Similarly to ligand 2, ligand 5 fails to inhibit osteoblast differentiation at saturating doses, represses the IL-13-induced transcriptional activation of POSTN and has anti-inflammatory activity when administered as an ointment. We administered ligand 5 (5 and 30 mg/kg) and prednisolone (5 and 30 mg/kg) IP, daily for the 3 days during the OVA challenge. We decided to use the glucocorticoid prednisolone because its affinity to GR is more similar to ligand 5's affinity. Dexamethasone has an affinity higher than either ligand and similar to ligand 2. We observed that prednisolone at 30 mg/kg was able to partially prevent the OVA-induced increase in airway hyperreactivity (fig. 2.5b), mucus overproduction as assessed by histology and the

increase in inflammatory cells obtained by broncholavage (data not shown). Prednisolone at 5 mg/kg or ligand 5 at the two doses tested did not exert therapeutic effects.

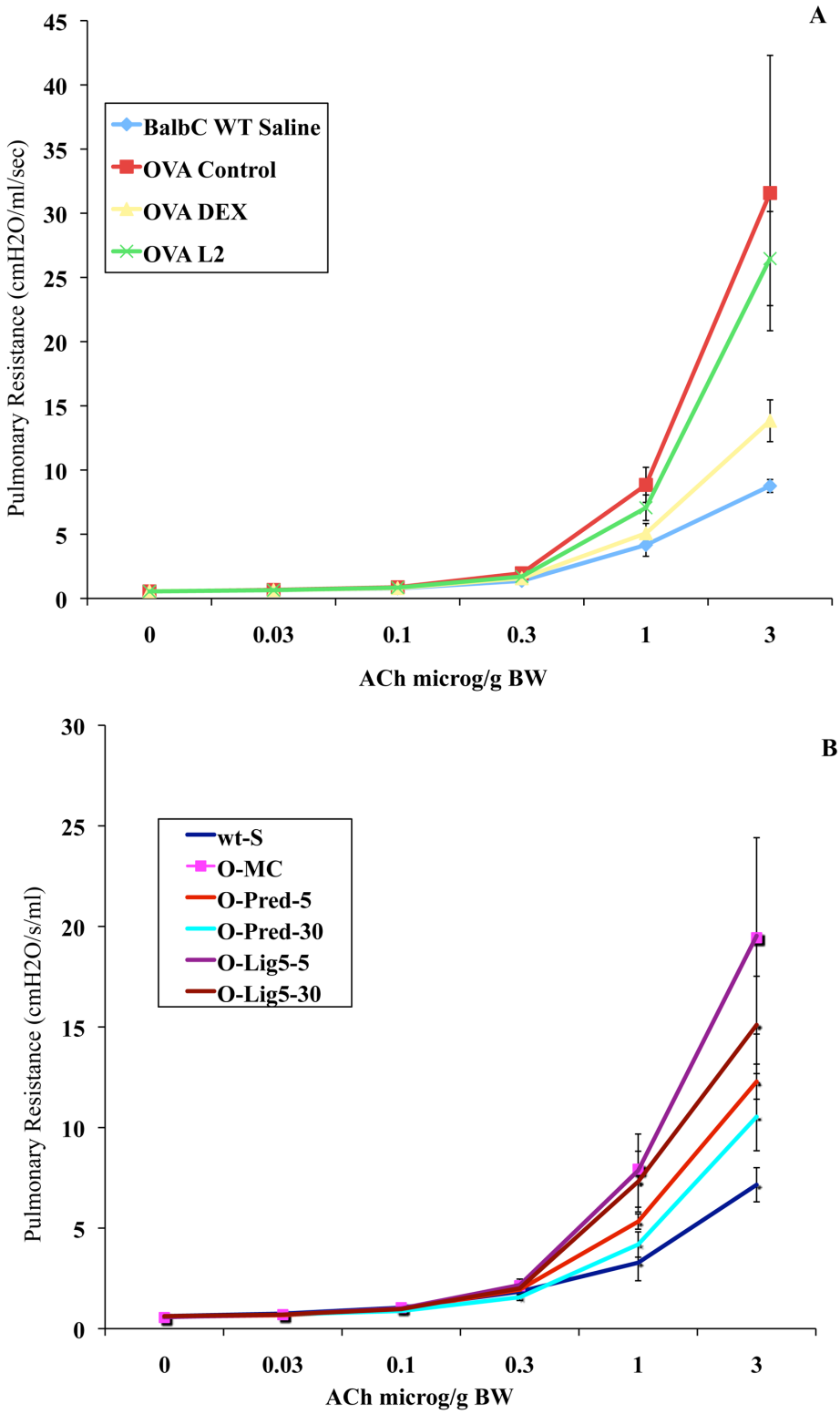

Fig. 2.5 Effect of dexamethasone, prednisolone, ligand 2 and ligand 5 on OVA-induced airway hyperresponsiveness. (A) OVA-induced mice were treated with dexamethasone or ligand 2 (5 mg/kg) for three days during OVA-challenge. (B) OVA-induced mice were treated with prednisolone or ligand 5 (5 and 30 mg/kg) for three days during OVA-challenge.

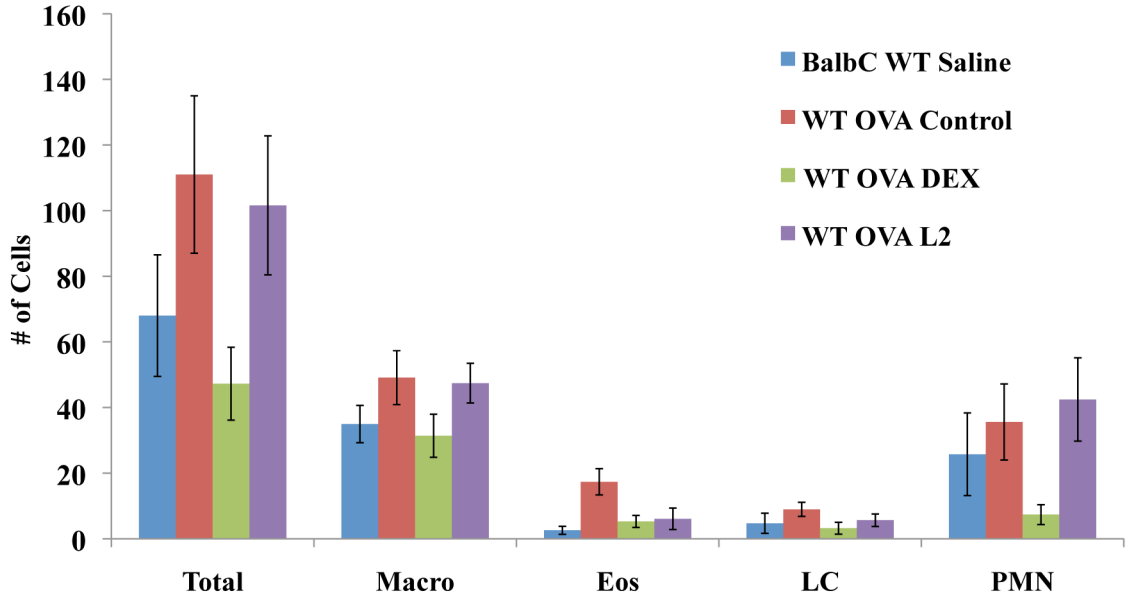

Fig. 2.6 Effect of dexamethasone and ligand 2 on OVA-induced inflammatory cell broncholavage counts. OVA-induced mice were treated with dexamethasone or ligand 2 (5 mg/kg) for three days during OVA-challenge. Cells obtained by broncholavage were counted and classified; macrophages (Macro), Eosinophils (Eos), Lymphocytes (LC), Neutrophils (PMN).

Next, we evaluated the ability of prednisolone and ligand 5 to reach pulmonary tissue. We evaluated if treatment with GR ligands affected GR target genes in the lungs of OVA-challenged animals. We used qPCR to measure relative transcript levels of periostin and mucin 5AC (Muc5AC) (fig. 2.7). Muc5AC is a member of the mucin gene family and is induced by inflammation in the airways of asthmatic patients[53]. Moreover, Muc5ac contains two GR binding regions upstream of the transcription start site and is likely a primary target gene of GR[54]. We found that Muc5ac was highly upregulated in the lungs of OVA-challenged animals. Prednisolone treatment substantially inhibited OVA-induced Muc5ac, but ligand 5 had no effect. Periostin mRNA levels were not changed in OVA-animals when compared to control and were not affected by prednisolone or ligand 5 treatment.

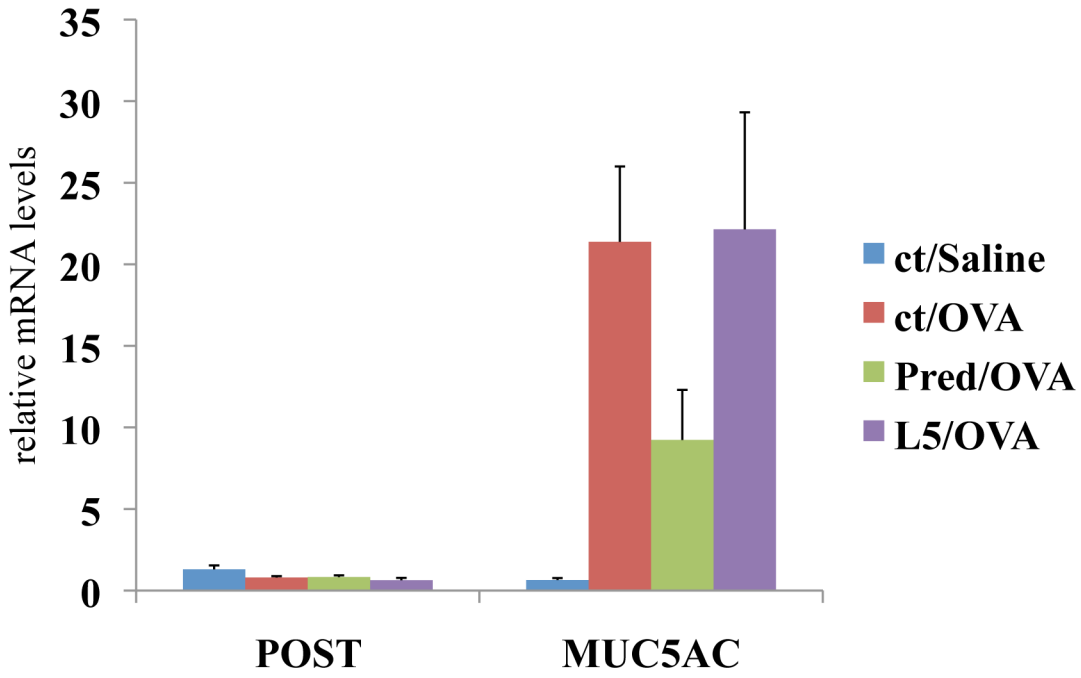

Fig. 2.7 Regulation of Periostin and MUC5AC in the lung by prednisolone and ligand 5. WT mice were subjected to the OVA model of lung inflammation or treated with saline. During 3-day challenge with OVA animals were treated with ligand 5, prednisolone or control. qPCR performed with RNA isolated from whole lungs. Data shows average of 6 animals, +/-SE.

Chapter 2 Discussion

Glucocorticoids were introduced as asthma therapies in the fifties and today remain the most effective approach to asthma control. The introduction of inhaled corticosteroids greatly decreased the incidence and severity of adverse effects associated with glucocorticoid therapy. However, inhaled corticosteroids are not completely free of side effects and are still used cautiously in the pediatric population. Advances in the understanding of the molecular actions of the glucocorticoid receptor spurred the search for compounds that dissociate therapeutic and adverse effects of corticosteroids. To facilitate the finding of such compounds it is paramount to define the transcriptional networks and associated genes that act downstream of GR in affected tissues.

We developed a cell culture-based model to study the regulation of glucocorticoid-regulated asthma candidate genes. We used this model to identify a cluster of serpinB genes that are regulated in tandem by IL-13 and glucocorticoids and to find novel genes that may act downstream of glucocorticoids to promote therapeutic activities. Moreover, we employed a cell culture-based strategy to identify GR ligands that may be novel asthma therapies with bone-sparing properties. We were not able to demonstrate a therapeutic activity of ligands 2 and 5 despite their ability to regulate asthma candidate genes. Additionally, ligand 5 did not regulate GR target genes in the pulmonary tissue of treated animals. We hypothesize that this first generation of arylpyrazole ligands suffers from unfavorable pharmacokinetic properties.

We could not determine the IC50s related to inhibition of asthma genes in primary HBECs of either dexamethasone or ligand 2. We and others (Prescott Woodruff and John

Fahy, pers. commun.) have experienced difficulties with data reproducibility and data noise when working with primary HBECs. These may be related to donor source and the intrinsic variability of handling protocols when material is obtained from human subjects (e.g. epithelial brushing vs. lung resection). Rough approximations from our experiments suggest that ligand 2 is able to repress IL-13-induced transcription of POST, CLCA1 and SERPINB2 with efficacies similar to dex.

Interestingly, we did not observe upregulation of periostin transcripts in the lungs of OVA-treated animals. Periostin is induced by IL-13 and is increased in the lungs of asthmatic patients[55]. The absence of periostin increase in the OVA-model suggests that this model does not fully recapitulate asthma as it presents in humans. Asthma is a chronic disease and the 3-day OVA challenge may not be sufficient to induce periostin when compared to the months or years of chronic inflammation in the lungs of asthmatic patients. Additional studies employing chronic mouse models of lung inflammation may be necessary to resolve this discrepancy.

Chapter 2 Acknowledgments

We greatly benefited from the experience of the center personnel and from discussions with Xiaozhu Huang, David Erle and Dean Sheppard, and enjoyed a fruitful, highly beneficial and ongoing collaboration with Prescott Woodruff.

Chapter 3. Glucocorticoid signaling defines a novel commitment state during adipogenesis *in vitro*

Chapter 3 Introduction

The ability to store excess energy for future use has been strongly selected during evolution. In mammals, adipocytes comprise a tissue responsible for this function. These cells store excess energy in the form of triglycerides that are contained inside lipid droplets, organelles composed of a neutral lipid core surrounded by a protein-coated single phospholipid layer. Excess adipose tissue is associated with numerous diseases including cancer, diabetes, hypertension and cardiovascular disease[56]. Indeed, it has been established that fat cells, in addition to their role in energy storage, also perform endocrine functions. Adipocytes are intimately involved in metabolic homeostasis by secreting and responding to hormones and cytokines that regulate energy intake and expenditure. Notably, differentially located human fat depots display distinct metabolic characteristics, perhaps accounting for the strong association of excess visceral fat, but not subcutaneous fat, with cardiovascular disease[57].

The apparent functional distinction between visceral and subcutaneous fat raises the question of whether these cells represent two distinct terminal differentiation fates. Fat depots are thought to arise during development from mesenchymal/mesodermal stem cells (MSC) and neural crest stem cells that differentiate through the process of adipogenesis. Work during the past two decades has identified a large number of signaling pathways (e.g., WNT, bone morphogenetic proteins, fibroblast growth factors, glucocorticoids) that regulate alternative cell fates of mesodermal lineages (bone, cartilage, muscle or fat) during development or postnatal periods. Despite this accumulated knowledge, we have no definitive view of mammalian fat ontogenesis[58,59]. Indeed, it is unknown to what degree adipogenesis follows the paradigm established by

studies of the hematopoietic system: the hematopoietic stem cell gives rise to distinct lineages through a series of commitment steps mediated by specific signaling events that lead to stereotypic changes in the complement of genes expressed in the committed cell type. The identity of cells within these lineages is defined by distinct cell surface markers and transcriptional regulatory factors. Additionally, the hormones and signals that promote differentiation at each step have been largely determined[60]. In contrast, the preadipocyte remains the only described intermediary cellular type during differentiation of adipocytes. Preadipocytes are operationally defined as cells isolated from the stromovascular fraction of fat depots that possess the ability to progress towards an adipocytic cell fate when stimulated with "adipogenic cocktails". Recent studies have begun to define molecular markers specific to preadipocytes[61,62]. However, we do not know the signals that induce preadipocyte commitment or if there are markers that clearly distinguish preadipocyte populations resident in the various fat depots of mammals. Furthermore, the existence of putative intermediary cellular states between preadipocytes and adipocytes has not been determined. Finally, the rules that govern preadipocyte/MSC differentiation to generate adipocytes with varied metabolic phenotypes remain for the most part unknown.

Here, we have begun to explore these questions using cell culture models of adipogenesis. The 3T3-L1 cell line is one of the most robust cell culture adipogenesis systems, and its relevance has been repeatedly confirmed in mouse models. 3T3-L1 preadipocytes are normally differentiated into adipocytes by a two-step protocol: First, cells are grown to confluence and maintained for two days in a post-confluent state in the presence of medium containing calf serum (CS). Next, cells are exposed for another two

days to a differentiation cocktail (DIM) that contains the glucocorticoid dexamethasone (dex), the growth factor insulin, the phosphodiesterase inhibitor methylisobutylxanthine (IBMX) and fetal bovine serum (FBS). This signaling protocol launches a transcriptional cascade that, once initiated, is independent of DIM and culminates in the formation of mature adipocytes after 6-8 days of culture[63]. Terminal differentiation is typically assessed using lipid dyes, and by monitoring metabolic activities and gene expression specific to adipocytes.

Individually, some of the components of the DIM cocktail are known to influence adipogenesis *in vivo*. Repeated injection of insulin for diabetes control, for example, has been shown to induce local adipogenesis at the sites of injection[64]. In addition, excess glucocorticoids are responsible for the excess visceral adipose tissue observed in patients with Cushing's syndrome[65]. Finally, the downstream effector of IBMX actions, cAMP, appears to modulate polyunsaturated fatty acid-induced obesity in mice[66]. Collectively, these observations suggest that the pathways activated by the DIM cocktail could induce adipogenesis by mechanisms that are potentially separable and independent from one another. In particular, it seemed possible that the signaling pathways activated by DIM treatment could encompass distinct commitment stages in the progression from preadipocyte to adipocyte. To begin to examine this hypothesis, we temporally uncoupled the activities of the four signaling components of the DIM cocktail and determined if sequential treatment might reveal distinct intermediates during preadipocyte differentiation. Furthermore, we sought to identify cellular factors that participate in defining such intermediates.

Chapter 3 Materials and Methods

Cell culture lines and differentiation

3T3-L1 preadipocytes (ATCC) were cultured in DMEM with 10% calf serum (HyClone). C3H10T1/2 cells (UCSF Cell Culture Facility) were cultured in DMEM with 10% FBS (GIBCO). Mouse MSCs were obtained from 2-3 month old mice. The bone marrow was extracted with a 23 gauge needle by flushing the femur marrow cavity with 2 ml Iscove's media supplemented with 2% fetal bovine serum per bone. Flushed bone marrow was cultured in mesenchymal stem cell enrichment media (Stem Cell Technologies). Media was changed daily during 3 days to remove the hematopoietic non-adherent cells, and then every other day thereafter. At the appearance of large circular colonies of MSCs, cells were trypsinized and passaged to enrich for MSCs.

Primary bone marrow derived mesenchymal stem cells, 3T3-L1 preadipocytes and C3H10T1/2 cells were induced to differentiate by treatment with various combinations of 1-10 μg/ml insulin (UCSF Cell Culture Facility), 0.5 mM 3-isobutyl-1-methylxanthine (Sigma), 1 μM dexamethasone (Sigma) and 1 μM rosiglitazone (BioMol). After treatment, cells were maintained in cell culture medium until processing for analysis.

Insulin-stimulated glucose uptake

Day-10 post-treatment 3T3-L1 cells cultured in 12-well plates were serum starved in DME-H21 medium for 4 h. Each treatment group consisted of 3 wells that were washed with PBS at 37°C and incubated for 10 min with 500 mL of PBS; PBS with insulin (10 mg/ml); or PBS, insulin and cytochalasin B (20 mM). Next, cells were incubated with 2-

deoxyglucose (50 mM) and [^{3}H]-2-deoxyglucose (2 mCi/ml) in PBS, for 10 min at 37°C. Reaction was stopped by washing wells with PBS at 4°C. Cells were lysed in 200 ml of 0.1% SDS and combined with 3.5 ml of biodegradable scintillation counting cocktail. [^{3}H]-2-deoxyglucose uptake was determined in a multipurpose-scintillation counter (Beckman LS6500). Insulin-stimulated uptake was determined by calculating the count number ratio of PBS-insulin over PBS group, after subtraction of non-specific uptake (cytochalasin B group). We used the two-tailed, unpaired Welch's t-test, adjusted for multiple tests by Bonferroni correction, to generate p-values.

Triglyceride content determination

Triglyceride levels of day 10 post-treatment cells were measured by colorimetric detection of glycerol produced by triglyceride hydrolysis, according to manufacturer's instructions. Triglyceride assay kit (TG-1-NC), Zen-Bio, Inc. We used the two-tailed, unpaired Welch's t-test, adjusted for multiple tests by Bonferroni correction, to generate p-values.

Lipolysis

Lipolysis rates of day 10 post-treatment cells were determined by detection of free glycerol release, according to manufacturer's instructions. Cells were exposed to isoproterenol (10 mM) or control solvent for 3 h before measurement. Lipolysis assay kit (LIP-3), Zen-Bio, Inc. We used the two-tailed, unpaired Welch's t-test to generate the p-value comparing isoproterenol-induced lipolysis rates for DIM and dex-then-IBMX differentiated cells after normalizing each to the mean lipolysis rate without isoproterenol addition.

Oil Red O staining

3T3-L1 cells were washed three times with PBS and fixed in 10% formalin in PBS for 1 h. After washing the cells twice with PBS, cells were stained with Oil Red O staining solution (0.5% Oil Red O (Sigma) in isopropanol, diluted 3:2 in water and filtered with a 0.22-µm filter). After staining, cells were washed three times with water. Representative images of treated cells were obtained with a Zeiss Axiovert 40 CFL inverted microscope or by scanning of stained plates (Epson Perfection 2450 photo scanner). The objectives LD A-Plan 20x and A-Plan 10x were used for microscopy.

Immunoblot

3T3-L1 cells were washed with PBS at 4°C and lysed on RIPA buffer (10 mM Tris-HCl, pH 8.0, 1 mM EDTA, 150 mM NaCl, 5% glycerol, 0.1% sodium deoxycholate, 0.1% SDS, 1% Triton X-100, supplemented with protease inhibitors) at 4°C. Cell lysates were rotated for 15 min at 4°C and cleared by centrifugation (21000g for 15 min at 4°C). Protein lysates were resolved by SDS-PAGE and transferred to PVDF (Millipore) membranes using semi-dry transfer (Bio-Rad). Membranes were blocked for 1 h at 22°C with 5% (w/v) non-fat powder milk on TBS-T (10 mM Tris-base, 150 mM NaCl, 0.1% Tween-20, pH 7.6). Membranes were incubated overnight with primary antibodies in TBS-T, 1% (w/v) milk at 4°C, followed by 1 h at 22°C in the presence of secondary antibody in TBS-T 1% (w/v) milk. Proteins were detected by chemiluminescence (ECL PLUS Western Blot Detection System, Amersham). The following antibodies were used: C/EBPd (sc-151), C/EBPb (sc-150), C/EBPa (sc-61), PPARg (sc-7196), Pref-1 (sc-8625),

actin (sc-1616), anti-goat IgG-HRP (sc-2020) Santa Cruz Biotechnology; ECL Anti-rabbit IgG-HRP (NA934V), GE Healthcare.

Microarrays and qPCR

Total RNA was isolated from cells by using QIAshredder and RNeasy kits (Qiagen). For microarray experiments, cDNA was generated by one cycle of reverse transcription (Superscript II, Invitrogen) using 15 mg of total RNA. Experiments were performed using the Mouse Exonic Evidence Based Oligonucleotide (MEEBO) microarray oligo set. Experimental samples labeled with cy5 were hybridized against cy3 labeled experimental pool samples. Arrays were gridded with SpotReader (Niles Scientific). Microarray data will be made available at the Gene Expression Omnibus website (http://www.ncbi.nlm.nih.gov/geo/). All linear models for differential gene expression were constructed with *limma*[67] in BioConductor[68]. Probes were normalized without background subtraction using the 'printtiploess' method of *limma*[69]. A linear model for dex was constructed to compare 4 biological replicates of mock DMSO treatment with dex treatment at either 2 or 36 h. The single-color DIM time course data[70] were normalized without background subtraction and summarized by Tukey biweight using the 'threestep' method of *affyplm* in Bioconductor[71]. A linear model for DIM was constructed to compare the 2 biological replicates at each time point to the time 0 controls. Genes were considered differentially expressed if at least one probe had log-odds greater than 50:50 in the linear model. Furthermore, overlap of dex and DIM differential expression was for genes differentially expressed both at 2 h or 36 h of dex treatment and at some point in the DIM time course and with a fold-change greater than 2

in at least one of the conditions. Gene ontology enrichments were generated using DAVID Bioinformatics Resources 2008[72].

To generate cDNA for qPCR, 1 μg of total RNA, 4 μL of 2.5 mM dNTP, and 2 μL of 15 μM random primers (New England Biolabs) were mixed and incubated at 70°C for 10 min. A 4 μl cocktail containing 25 U of Moloney Murine Leukemia Virus (M-MuLV) Reverse Transcriptase (New England Biolabs), 10 U of RNasin (Promega), and 2 μl of 10x reaction buffer (New England Biolabs) was added, and incubated at 42°C for 1 h. The reaction was incubated at 95°C for 5 min. The resultant cDNA was diluted to 100 μl, and 4 μl were used for each 35 μL reaction containing 1.25 U of *Taq* DNA polymerase (Applied Biosystems), 1x reaction buffer, 1.5 mM $MgCl_2$, 0.5 mM dNTP (Invitrogen), 0.4x SYBR green I dye (Molecular Probes), and 357 nM each primer. qPCR was performed in the 7300 Real-Time PCR System (Applied Biosystems) and analyzed by using the Ct method (7300 System SDS Software). Rpl19 was used as an internal control for data normalization. All primers used in this report are available upon request.

Chapter 3 Results

Effect of temporal uncoupling on the ability of DIM cocktail components to induce adipogenesis of 3T3-L1 preadipocytes

To test the hypothesis that components of the DIM cocktail perform distinct and separable actions, we treated post-confluent cells for 48 h with one, two or three components of DIM followed by treatment with combinations of the remaining factors for another 48 h. We evaluated differentiation levels by staining with the neutral lipid dye Oil Red O.

Surprisingly, we found that the insulin and FBS components of the cocktail were dispensable for complete adipogenesis (>90%) when the 3T3-L1 preadipocytes were treated sequentially, first with dex for 48 h followed by IBMX for 48 h. In contrast, treatment with IBMX followed by dex did not induce significant differentiation (<5%). Most unexpectedly, simultaneous treatment with dex and IBMX for 48 h led to low adipogenesis levels (10-20%). Moreover, pretreatment of 3T3-L1 cells with IBMX rendered preadipocytes partially resistant to differentiation induced by the full DIM cocktail, whereas pretreatment with dex had no such effect (Figure 3.1).

We conclude from these results that dex and IBMX can induce full adipogenesis by performing actions that are essential and separable, but non-commutative. In addition, the full differentiation observed with dex followed by IBMX treatment, coupled with the reduced differentiation upon simultaneous treatment with dex and IBMX suggests that IBMX action may depend upon a prior process mediated by dex. For example, dex treatment may lead to the accumulation of a product that is needed for IBMX action or it

may decrease the levels of an inhibitor of differentiation. Indeed, simultaneous treatment of 3T3-L1 preadipocytes with dex and IBMX for 96 h, instead of 48 h, was capable of inducing full differentiation (Supplemental Figure 3.1). Thus, when preadipocytes are induced to differentiate with the full DIM cocktail, FBS and insulin might accelerate the kinetics of a rate-limiting step.

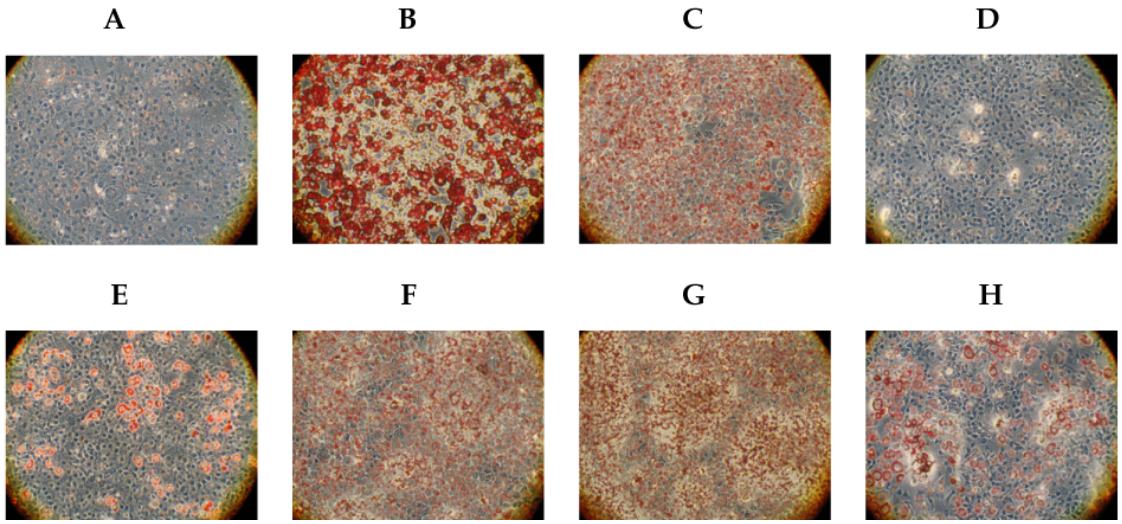

Figure 3.1. Oil Red O stained 3T3-L1 cells treated under different differentiation conditions. 2-day confluent 3T3-L1 cells were treated for the indicated times and stained 8 days later with oil Red O. Cells were observed with light microscopy, 20X magnification. (A) No treatment control. (B) Treatment with DIM (0.5 mM IBMX, 1 μM dex, 1 μg/ml INS and 10% FBS) for 48 h followed by treatment with INS for 48 h. (C) Treatment with 1 μM dex for 48 h followed by treatment with 0.5 mM IBMX for 48 h. (D) Treatment with 0.5 mM IBMX for 48 h followed by treatment with 1 μM dex for 48 h. (E) Simultaneous treatment with 1 μM dex and 0.5 mM IBMX for 48 h. (F) Treatment with vehicle for 48 h followed by treatment with DIM for 48 h. (G) Treatment with dex for 48 h followed by treatment with DIM for 48 h. (H) Treatment with 0.5 mM IBMX for 48 h followed by treatment with DIM for 48 h.

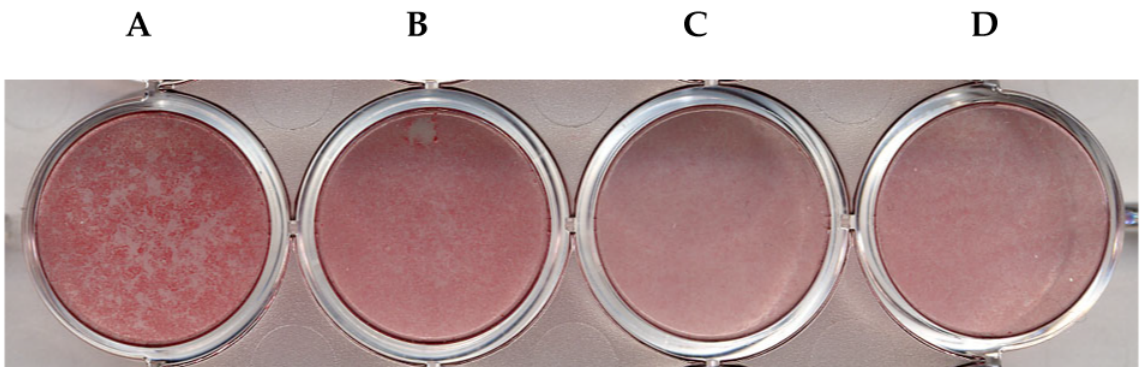

Supplemental Figure 3.1. Oil Red O stained 3T3-L1 cells treated under different differentiation conditions. 2-day confluent 3T3-L1 cells were treated for the indicated times and stained 8 d later with oil Red O. Cell culture plates were scanned. (A) Treatment with DIM (0.5 mM IBMX, 1 μM dex, 1 μg/ml INS and 10% FBS) for 48 h followed by treatment with INS for 48 h. (B) Simultaneous treatment with 1 μM dex and 0.5 mM IBMX for two periods of 48 h. (C) Treatment with 0.5 mM IBMX for 48 h followed by treatment with 1 μM dex for 48 h. (D) Treatment with 1 μM dex for 48 h; followed by treatment with 0.5 mM IBMX for 48 h; followed by treatment with 1 μM dex for 48 h.

Sequential treatment of C3H10T1/2 and primary mesenchymal stem cells with dexamethasone and IBMX induces adipogenesis

Importantly, the capacity for sequential exposure to dex followed by IBMX to induce adipogenesis is not restricted to 3T3-L1 cells. The mesenchymal stem cell line C3H10T1/2 and primary mouse mesenchymal stem cells (MSCs), both of which undergo adipogenesis in response to the classic DIM cocktail[63], also differentiated to adipocytes with sequential dex and IBMX treatment, albeit at lower efficiency than with the full DIM cocktail (Figure 3.2); conversely, treatment of C3H10T1/2 cells or primary MSCs with IBMX followed by dex failed to induce differentiation. Dex-treated MSCs, however, required insulin to differentiate into adipocytes upon subsequent treatment with IBMX.

These findings indicate that under these circumstances, insulin is required for differentiation of MSCs, but not preadipocytes. Dex, in contrast, is necessary for differentiation of both cell types and provides a signal that primes preadipocytes towards

differentiation, but is not sufficient to bring MSCs to the same stage during adipogenesis. These results support the hypothesis that components of the DIM cocktail can perform actions that are discrete and separable. Furthermore, our results are consistent with a model in which glucocorticoids establish a novel cellular intermediate, the "dex-primed preadipocyte", in the progression from preadipocytes toward adipocytes.

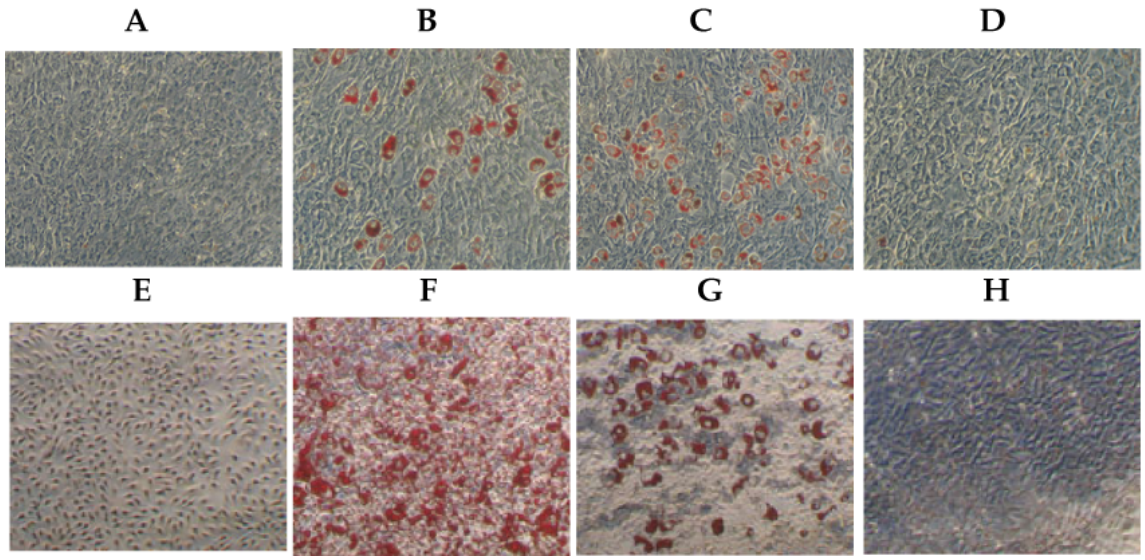

Figure 3.2. Oil Red O stained C3HT101/2 and primary mesenchymal stem cells (MSC) cells treated under different differentiation conditions. 2-day confluent C3HT101/2 (A-D) and primary MSCs (E-H) cells were treated for the indicated times and stained 8 days later with oil Red O. Cells were observed with light microscopy, 20X magnification. (A) Control. (B) Treatment with 0.5 mM IBMX, 1 μM dex, 1 μg/ml INS and 10% FBS for 48 h followed by 48 h of INS treatment. (C) Treatment with 1 μM dex and 1 μg/ml INS for 48 h followed by 0.5 mM IBMX treatment for 48 h. (D) Treatment with 0.5 mM IBMX and 1 μg/ml INS for 48 h followed by 1 μM dex treatment for 48 h. (E) Control. (F) Treatment with 0.5 mM IBMX, 1 μM dex, 1 μg/ml INS and 1 μM rosiglitazone for 48 h two times. (G) Treatment with 1 μM dex and 1 μg/ml INS for 48 h followed by 0.5 mM IBMX treatment for 48 h. (H) Treatment with 0.5 mM IBMX and 1 μg/ml INS for 48 h followed by 1 μM dex treatment for 48 h.

Expression profile of dex-primed preadipocytes

We further characterized dex-primed preadipocytes by determining the dose response and time-course properties of the glucocorticoid signal during priming of 3T3-L1

preadipocytes. We found that complete priming required dex treatment for 36 h, and that under these conditions, dex had an EC50 ≅ 100 nM (Supplemental Figure 3.2). To examine this commitment state at the molecular level we used genomewide microarrays to interrogate gene expression in 2-day confluent 3T3-L1 preadipocytes, with or without dex treatment. We found that dex treatment for 2 h or 36 h significantly affected 94 and 163 genes, respectively, by more than 2 fold.

Next, we compared the expression profile of dex-primed preadipocytes with that from published data of preadipocytes treated with DIM for 4 days to induce full adipogenesis (Figure 3.3 and Supplemental Material)[70]. We found that approximately 80% of the genes affected by dex treatment alone were also modulated by DIM treatment during the 4-day time-course (Figure 3.3A). Additionally, cluster analysis revealed that the set of genes regulated by dex includes genes modulated throughout the 4-day DIM time course (Figure 3.3B). We then performed gene ontology analysis comparing the genes modulated by dex alone with the genes modulated by DIM, but not dex. Notably, dex selectively modulates the expression of genes that participate in extracellular matrix processes, immune processes and the transforming growth factor-beta (TGFb), WNT and MAP kinase pathways; in contrast, genes regulated by DIM, but not affected by dex alone, impact intracellular processes, mitochondrial function, lipid synthesis, glucose and NAD metabolism, oxidative phosphorylation and the citrate cycle (Figure 3.3C). Thus, dex-primed preadipocytes express a genetic program distinct from that of adipocytes and appear to represent a discrete intermediate between the preadipocyte and the adipocyte.

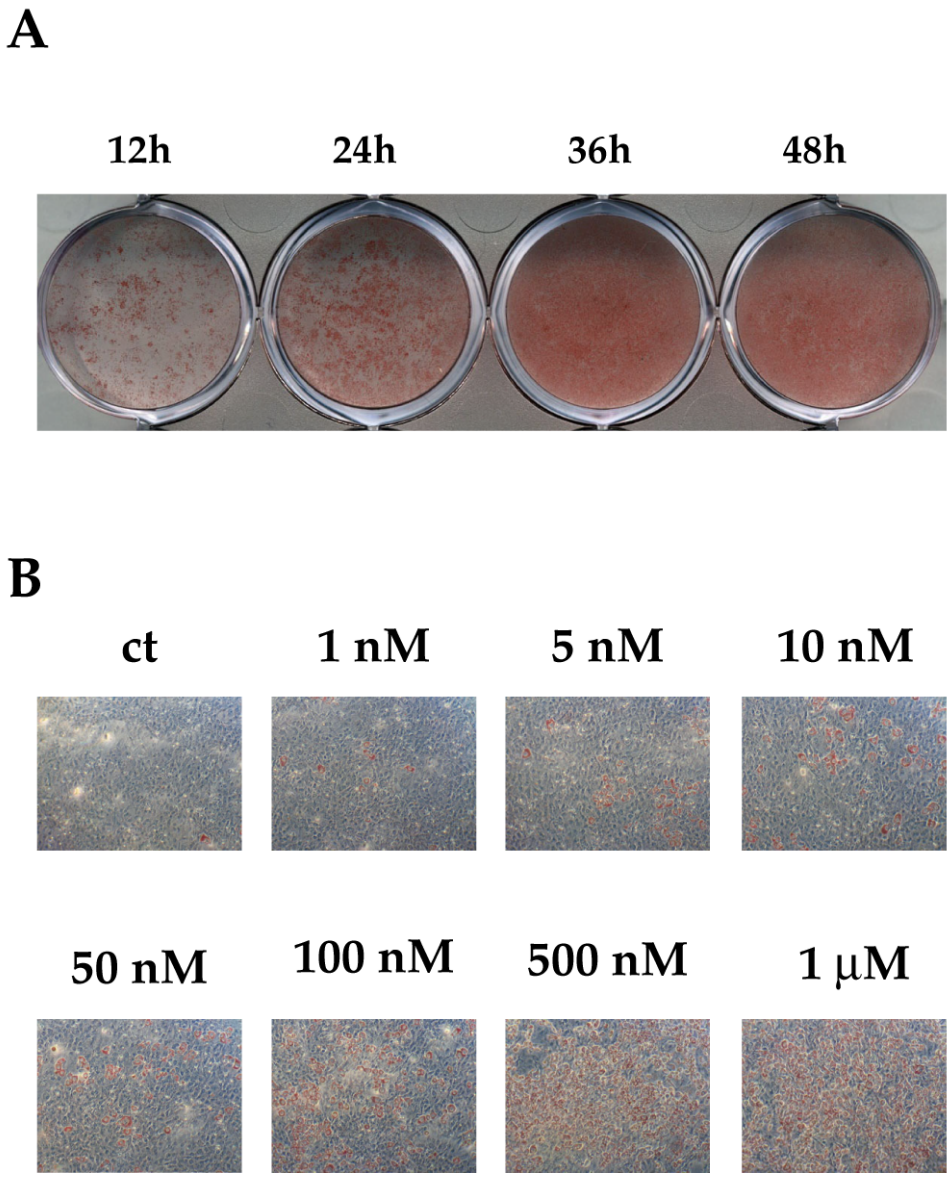

Supplemental Figure 3.2. 2-day confluent 3T3-L1 cells treated under different differentiation conditions were stained 8 d later with oil Red O. (A) Treatment with 1 μM dex for 12, 24, 36 or 48 h, followed by treatment with 0.5 mM IBMX for 48 h. (B) Treatment with 1 nM, 5 nM, 10 nM, 0.5 μM, 1 μM dex or control for 48h, followed by treatment with 0.5 mM IBMX for 48 h.

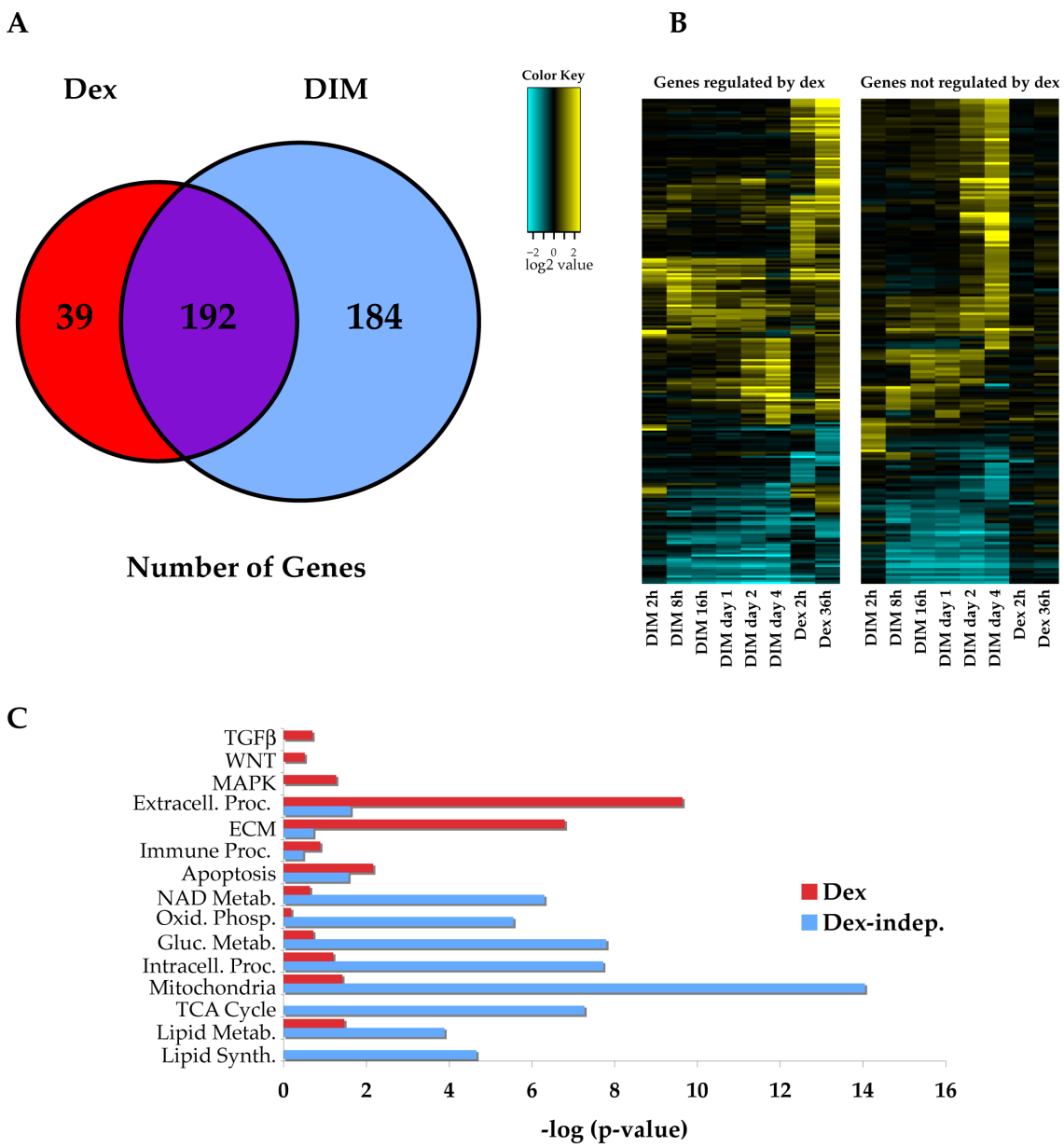

Figure 3.3. Expression profiles of dex-treated preadipocytes and DIM-induced adipogenesis. (A) Overlap of genes affected by dex treatment at 2 or 36 h (red) and genes affected during 4 d of DIM-induced adipogenesis (blue). (B) Hierarchical clustering of genes affected by dex (left) or those affected by DIM, but not dex (right). Genes (rows) were clustered using non-centered Pearson correlation distance and average linkage agglomeration. (C) The expression profile of dex treatment of preadipocytes at 2 or 36 h was compared to a published dataset of DIM-induced adipogenesis over 4 days[70]. P-values of select gene ontology categories from DAVID 2007[72] are shown for genes affected by dex (red) or those affected by DIM, but not dex (Dex-indep., blue).

Effect of differentiation by sequential treatment with dexamethasone and IBMX on the metabolic properties of adipocytes

To further characterize the metabolic properties of preadipocytes treated sequentially with dex followed by IBMX and *vice versa*, we assessed in 3T3-L1 cells functional parameters characteristic of adipocytes: insulin-stimulated glucose uptake, lipolysis and total triglyceride levels (Figure 3.4).

Adipocytes treated with insulin respond by increasing rates of glucose transport; thus, the amount of glucose internalized after insulin treatment is a measure of insulin sensitivity. We found that the insulin sensitivity of adipocytes generated by sequential treatment of 3T3-L1 preadipocytes with dex and IBMX was equal to that of DIM adipocytes. Cells treated with IBMX followed by dex behaved similar to control cells and did not increase their glucose uptake after insulin treatment (Figure 3.4A).

Adipocytes store energy as triglycerides in fat droplets. The energy stores can be mobilized in times of need by signals that increase lipolysis rates. At the organismal level the sympathomimetic system generates such signals by producing adrenergic stimuli. The beta-adrenergic agonist isoproterenol (ISO) can be used in cell culture to simulate these conditions; preadipocytes, unlike adipocytes, do not respond to ISO. Adipocytes differentiated by sequential treatment with dex and IBMX displayed basal lipolysis rates equivalent to DIM adipocytes (212±5 vs. 212±7 μmol of glycerol/ h). DIM adipocytes increased their rates of lipolysis by 127±15 % above the basal rate, while dex-IBMX adipocytes increased their rates by 82±2% above basal after isoproterenol treatment, representing a significantly lower increase in lipolysis (p-value = 1.7e-2). Once again,

cells treated with IBMX followed by dex did not differ from control preadipocytes (Figure 3.4B).

Measurement of total triglyceride levels showed that DIM adipocytes stored approximately four times more triglycerides than preadipocytes. Dex-IBMX adipocytes stored approximately 1.8 fold more triglycerides than preadipocytes. IBMX-dex treated preadipocytes contained the same amount of triglycerides as control preadipocytes (Figure 3.4C). These data are consistent with the lower retention of Oil Red O by the dex-IBMX adipocytes as compared to the DIM adipocytes.

These results revealed an unexpected interaction between the signaling pathways modulated by dex and IBMX as part of the DIM cocktail. In that context, dex and IBMX seem to act synergistically and are both required for robust adipogenesis. However, when dex and IBMX activities were temporally uncoupled, preadipocytes were able to detect the order in which these pathways signal and only differentiated if dex acted before IBMX. To investigate the mechanism by which preadipocytes distinguished between the different orders of exposure to dex and IBMX, we characterized the pattern of expression of some key adipogenic regulatory factors after sequential treatment.

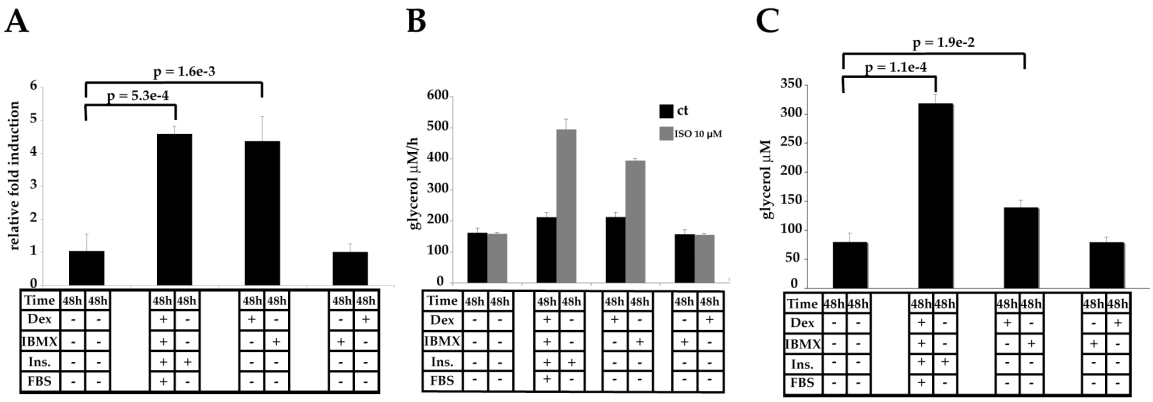

Figure 3.4. Effect of differentiation conditions on the metabolic properties of 3T3-L1 cells. 3T3-L1 preadipocytes on day 2 post-confluence were treated with combinations of 0.5 mM IBMX, 1 μM dex, 1 μg/ml INS or 10% FBS. (A) Insulin-induced glucose uptake. Day 10 post-treatment 3T3-L1 cells were treated with 10 μg/ml insulin for 10 min. Uptake of 2-DG was measured by scintillography. Data are means +/- SD. n ≥ 3. (B) Isoproterenol-stimulated lipolysis. Day 10 post-treatment 3T3-L1 cells were treated with 10 μM ISO for 3 h. Measurement of glycerol secretion in the medium was used to determine rate of ISO-induced lipolysis. Data are means +/- SD of three independent experiments. (C) Triglyceride storage. Total triglyceride levels of day 10 post-treatment 3T3-L1 cells were measured through an enzymatic colorimetric assay. Data are means +/- SD of three independent experiments.

Effect of differentiation mode on the expression of adipogenic transcriptional regulatory factors

Treatment of preadipocytes with the DIM differentiation cocktail induces a cascade of transcription factors that is responsible for the initiation and establishment of the adipogenic cell fate. The initial step of the adipogenic transcriptional cascade is the transient induction of the transcriptional regulatory factors CCAAT/enhancer binding protein beta and delta (C/EBPβ and C/EBPδ). Previous studies using 3T3-L1 cells have demonstrated that in the DIM cocktail dex is the main inducer of C/EBPδ while IBMX is responsible for the induction of C/EBPβ. Next, C/EBPβ and C/EBPδ act together to activate expression of C/EBPα and peroxisome proliferator-activated receptor gamma (PPARγ). Various other transcription factors are known to modulate adipogenesis, but

they all seem to act by modulating the expression of either PPARγ or of one of the C/EBPs[58].

We used quantitative real-time PCR (qPCR) and immunoblotting to monitor the levels of C/EBPα, β, δ and PPARγ at 2, 4, 6, 8 and 10 days after treatment with DIM, after sequential treatment with dex followed by IBMX, or after sequential treatment with IBMX followed by dex (Figure 3.5). We sought to determine if the disparate differentiation outcomes induced by the two sequential treatments were reflective of differential patterns of expression of C/EBPα, β, δ and PPARγ.

qPCR analysis revealed the following differences between sequential treatments and the standard, DIM-induced pattern of expression: [1] Treatment of 3T3-L1 preadipocytes with dex followed by IBMX transiently induced C/EBPδ on day 2, and then C/EBPβ on day 4; the pattern of expression of PPARγ and C/EBPα mRNAs was similar to DIM-treated cells (Figure 3.5A). [2] Treatment of 3T3-L1 preadipocytes with IBMX followed by dex transiently increased the levels of C/EBPβ mRNA by 3-fold on day 2; C/EBPd expression was delayed, increasing above control levels only on day 6; PPARγ and C/EBPα mRNA levels were above control (3-13-fold) during days 4-10 (Figure 3.5A). Interestingly, despite induction of PPARγ and C/EBPα mRNAs, the IBMX-dex treatment did not promote substantial adipogenesis.

Immunoblot analysis revealed that preadipocytes treated with dex for 48 h followed by IBMX for 48 h displayed an increase in C/EBPδ levels with dex treatment at day 2 followed by a decline in protein levels following IBMX treatment on day 4. C/EBPβ reached levels above untreated cells on day 4 post-treatment and decreased after day 6.

C/EBPα and PPARγ protein levels started to increase on day 4 and reached levels equivalent to DIM-treated cells on day 6 post-treatment (Figure 3.5B).

Treatment of 3T3-L1 preadipocytes with IBMX followed by dex led to increases in the protein levels of C/EBPβ and C/EBPδ relative to untreated cells. C/EBPβ reached its highest levels on day 6 post-treatment. C/EBPδ levels surpassed untreated cells on day 6 and increased slightly thereafter. Notably, the increases in C/EBPβ and C/EBPδ levels were not associated with increased protein levels of C/EBPα or PPARγ. This may indicate that a threshold level of C/EBPβ and C/EBPδ was required to achieve C/EBPα and PPARγ expression, and subsequent adipogenesis.

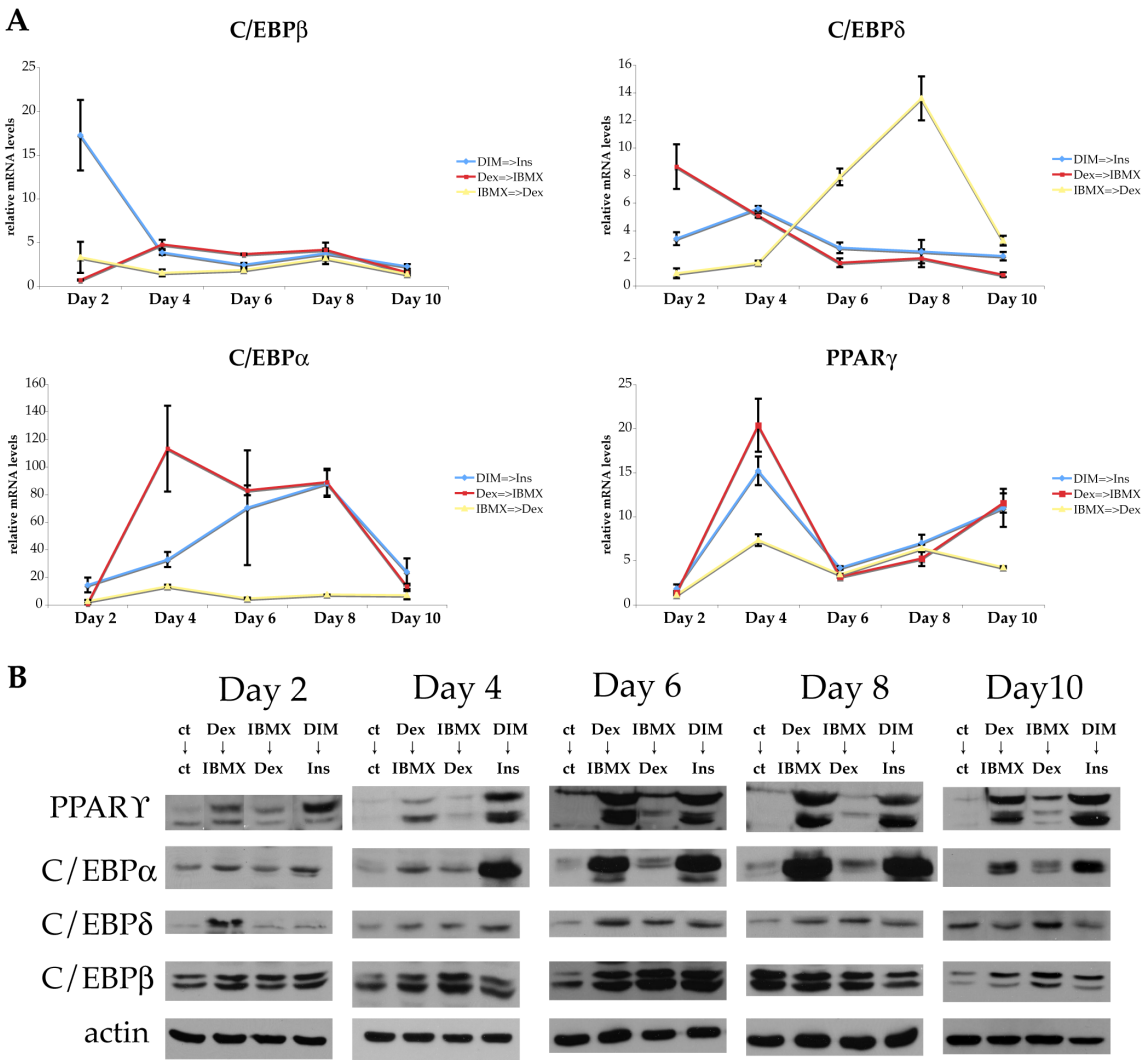

Figure 3.5. Levels of adipogenic transcription factors during differentiation induced by sequential treatment with dexamethasone and IBMX. (A) RNA was extracted from 3T3-L1 cells 2,4,6,8 and 10 d after induction of differentiation by treatment with the DIM cocktail, dex for 48 h followed by IBMX for 48 h and IBMX for 48 h followed by dex for 48 h. mRNA levels were quantified by quantitative real-time PCR. Data were normalized relative to untreated cells mRNA levels and show mean +/- SD. (B) Protein lysates were prepared from 3T3-L1 cells 2,4,6,8 and 10 d after induction of differentiation by treatment with the DIM cocktail, dex for 48 h followed by IBMX for 48 h and IBMX for 48 h followed by dex for 48 h. Proteins were separated by SDS-page, transferred and immunoblotted with specific primary antibodies directed against PPAR gamma, C/EBP alpha, C/EBP delta, C/EBP beta or b-actin.

Preadipocyte factor 1 (Pref-1) is a sensor of dexamethasone and IBMX signaling

Pref-1 is related to the Notch/Delta/Serrate family of secreted epidermal growth factor-like repeat-containing proteins and is one of the most highly expressed mRNAs in 3T3-L1 preadipocytes. During differentiation induced by the DIM cocktail, Pref-1 levels decline dramatically and it has been demonstrated that Pref-1 is an inhibitor of adipogenesis *in vitro* and *in vivo*[73]. Forced expression of Pref-1 in preadipocytes inhibits differentiation, while knockdown enhances it. Moreover, mice overexpressing the soluble form of Pref-1 display decreased adipose tissue mass, whereas Pref-1 knockout mice possess increased adipose tissue mass. The downregulation of Pref-1 during DIM-induced adipogenesis is conferred by dexamethasone, which inhibits Pref-1 transcription in a dose and time-dependent manner that correlates with glucocorticoid-promoted differentiation[74]. We hypothesized that this repression of Pref-1 by dex may be somehow affected by IBMX.

To test our hypothesis we used qPCR and immunoblots to monitor mRNA and protein levels of Pref-1 after treating 3T3-L1 preadipocytes with the DIM cocktail, dex followed by IBMX, and IBMX followed by dex. We found that treatment of 3T3-L1 preadipocytes with dex followed by IBMX or with the DIM cocktail decreased Pref-1 mRNA levels by up to 10 fold relative to control cells. In contrast, treatment with IBMX followed by dex was relatively ineffective at repressing Pref-1 (Figure 3.6A). Pref-1 protein levels paralleled the Pref-1 mRNA findings. Treatment with dex followed by IBMX or with the DIM cocktail reduced Pref-1 protein to almost undetectable levels. 3T3-L1 preadipocytes treated with IBMX-dex maintained levels of Pref-1 expression similar to untreated cells, despite being slightly repressed on day 4 of IBMX-dex treatment (Figure 3.6B).

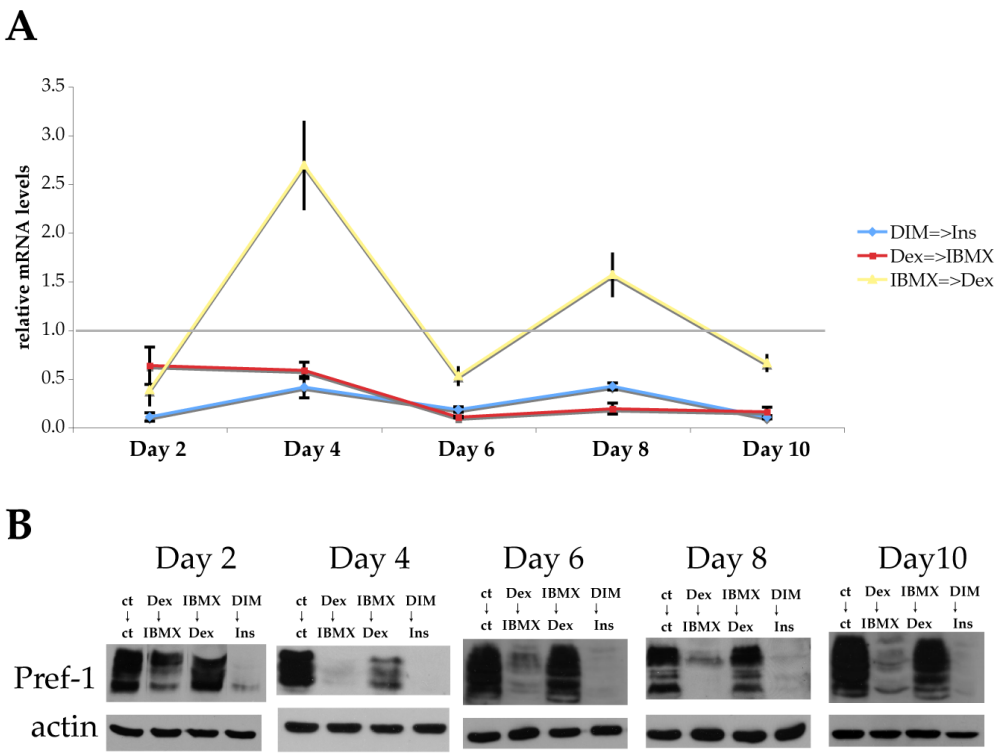

Figure 3.6. Effect of differentiation condition on the levels of Pref-1. (A) RNA was extracted from 3T3-L1 cells 2,4,6,8 and 10 d after induction of differentiation by treatment with the DIM cocktail, dex for 48 h followed by IBMX for 48 h and IBMX for 48 h followed by dex for 48 h. mRNA levels were quantified by quantitative real-time PCR. Data were normalized relative to untreated cells mRNA levels and show mean +/- SD. (B) Protein lysates were prepared from 3T3-L1 cells 2,4,6,8 and 10 d after induction of differentiation by treatment with the DIM cocktail, dex for 48 h followed by IBMX for 48 h and IBMX for 48 h followed by dex for 48 h. Proteins were separated by SDS-page, transferred and immunoblotted with specific primary antibodies directed against Pref-1 or b-actin.

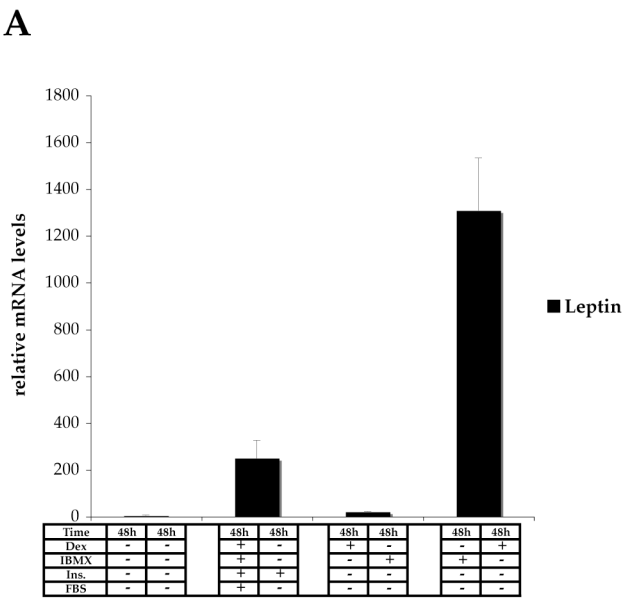

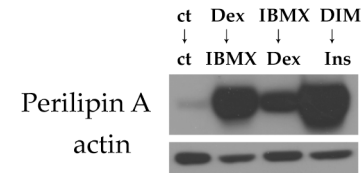

Supplemental Figure 3.3. Effect of differentiation condition on the levels of leptin and perilipin A. (A) RNA was extracted from 3T3-L1 cells 8 d after induction of differentiation by treatment with the DIM cocktail, dex for 48 h followed by IBMX for 48 h and IBMX for 48 h followed by dex for 48 h. mRNA levels were quantified by quantitative real-time PCR. Data were normalized relative to untreated cells mRNA levels and show mean +/- SD. (B) Protein lysates were prepared from 3T3-L1 cells 10 d after induction of differentiation by treatment with the DIM cocktail, dex for 48 h followed by IBMX for 48 h and IBMX for 48 h followed by dex for 48 h. Proteins were separated by SDS-page, transferred and immunoblotted with specific primary antibodies directed against perilipin A or b-actin.

Supplemmental Table 3.1. *Log2 fold values of dex-regulated genes*

Gene	DIM 2h	DIM 8h	DIM 16h	DIM day 1	DIM day 2	DIM day 4	Dex 2h	Dex 36h
Ncf4	0.04	0.06	0.05	0.03	0.03	-0.08	1.63	3.52
Ctla2a	-0.02	-0.08	-0.05	0.02	-0.05	-0.07	1.58	3.31
Ctla2b	0.21	0.13	-0.07	-0.06	-0.08	-0.03	1.56	3.20
Copg	0.13	0.20	0.31	0.08	0.12	0.04	1.36	3.15
Mthfd2	0.05	0.10	0.06	0.01	0.06	0.21	0.74	1.88
Cav1	0.00	0.23	0.08	-0.06	-0.09	0.36	0.64	1.98
Pbef1	0.13	-0.37	-0.26	-0.39	-0.01	0.20	0.98	2.17
Ptk2b	0.09	-0.12	-0.07	-0.12	0.10	0.27	0.61	1.63
Dbn1	0.11	-0.11	-0.12	-0.12	-0.09	-0.11	0.57	1.16
Glul	0.13	0.17	0.23	0.29	0.57	0.27	3.09	3.84
Vldlr	0.04	0.06	0.11	0.04	0.11	0.01	1.06	1.25
Aqp2	0.08	0.09	0.09	0.13	0.01	-0.13	1.27	1.88
Fabp4	-0.05	-0.08	-0.22	0.04	-0.07	0.27	1.60	2.59
2310005P05Rik	0.01	-0.02	-0.10	-0.06	-0.03	0.11	0.75	1.18
Sult1a1	0.04	0.01	0.04	0.01	0.08	0.31	1.28	2.07
Rab3d	0.06	-0.13	-0.18	-0.09	-0.13	0.54	1.89	2.29
Clca1	-0.12	-0.11	-0.09	-0.44	0.09	-0.41	0.45	2.02
Ifi203	-0.17	-0.34	-0.35	-0.30	-0.39	-0.30	0.69	1.63
Bcl2l1	0.12	0.15	-0.20	-0.21	-0.21	-0.19	0.52	1.04
Aldh1a1	0.09	0.00	0.01	0.03	0.06	-0.02	0.68	3.41
Amelx	0.00	0.04	-0.03	0.02	0.08	0.01	0.23	1.27
Ap1b1	-0.03	0.03	-0.07	-0.06	-0.01	-0.03	0.30	1.34
Krt8	0.03	0.08	0.05	0.03	0.11	-0.04	0.28	1.15
Kctd9	-0.01	-0.02	-0.01	0.12	0.03	0.05	0.16	1.05
Ndrg2	-0.01	-0.03	0.01	-0.05	-0.04	0.10	0.11	1.34
Lama2	0.03	-0.06	-0.02	-0.02	-0.03	0.01	0.12	1.06
Cd36	0.01	0.01	0.01	0.02	0.03	0.26	0.13	1.45
Terf2	-0.08	0.09	0.05	-0.01	0.10	0.07	0.09	1.10
Dpep1	0.15	0.51	0.36	0.36	0.50	0.28	0.76	2.95
Stim1	0.05	0.19	0.17	0.22	0.21	0.07	0.24	1.18
Glud1	0.01	0.13	0.19	0.09	0.31	0.06	0.11	1.31
S100a10	-0.03	0.29	0.20	0.10	0.17	-0.19	0.22	1.01
Lgals3	0.34	0.07	0.18	-0.02	-0.24	0.21	-0.24	2.04
Ly6f	0.00	0.05	-0.12	0.04	0.00	0.01	-0.15	1.01
Cp	-0.06	-0.10	-0.19	-0.15	-0.08	0.48	0.18	1.21
Capn6	-0.09	0.03	0.26	0.01	0.24	-0.44	0.23	1.01
Nusap1	-0.29	-0.10	0.00	0.25	-0.07	-0.30	0.37	1.21
Cdh13	-0.15	-0.08	0.23	0.49	0.31	-0.30	0.03	1.04
Ear2	-0.05	0.15	0.47	0.72	2.01	0.55	0.63	2.29
Anxa8	0.19	0.01	0.53	0.90	1.52	0.54	0.32	2.48
Ear1	0.04	0.16	0.24	0.27	1.10	0.24	0.28	2.23
Cd24a	0.04	1.09	0.84	0.60	0.49	-0.01	0.70	1.84
Idh2	0.35	0.56	0.57	0.51	0.68	0.08	0.24	1.37
Rnh1	0.27	0.51	0.41	0.36	0.17	-0.25	0.06	1.17
Furin	0.02	0.44	0.40	0.38	0.32	0.09	-0.18	1.17
Gja1	0.03	0.67	0.33	0.23	0.30	-0.16	-0.60	1.07
Map3k6	0.49	0.98	0.40	0.39	0.66	0.31	1.62	2.07
Tead4	0.32	1.00	0.44	0.39	0.55	0.12	1.51	1.68
Fdx1	0.16	0.38	0.07	0.11	0.24	0.42	0.79	1.42
Zbtb16	-0.06	0.25	0.34	0.47	0.71	0.57	2.67	2.60

Klf9	0.26	0.03	-0.05	0.12	0.18	0.23	1.07	1.04
1190002H23Rik	0.12	0.21	0.16	0.22	0.66	1.11	1.12	1.27
Cdo1	0.12	0.58	-0.14	0.15	0.59	0.83	1.45	1.27
Rhob	0.88	1.07	-0.15	-0.29	0.42	0.96	2.32	2.05
Apcdd1	0.13	0.23	-0.13	-0.25	0.04	0.54	1.02	0.86
Myc	0.93	0.34	0.33	0.10	0.66	0.23	1.02	1.24
Nfkbia	0.65	0.16	0.03	0.10	0.38	0.31	1.24	0.96
Per1	0.74	0.29	0.19	0.27	0.14	0.09	1.06	0.48
Gadd45g	0.94	0.06	-0.05	0.35	0.97	0.22	1.75	0.54
Sesn1	0.39	-0.11	-0.05	0.01	0.34	0.12	1.47	0.56
Pdk4	0.75	-0.05	0.10	0.25	-0.05	-0.19	1.73	1.44
Gem	0.48	-0.18	0.06	0.08	0.06	-0.58	1.04	0.65
Mt4	0.08	0.24	0.09	0.07	0.04	0.07	1.55	0.61
Snta1	0.18	0.26	0.05	0.09	0.06	0.01	1.03	0.40
Fjx1	0.11	0.35	0.15	0.26	0.19	0.18	1.12	0.31
Peli1	-0.02	0.02	0.10	-0.09	0.01	-0.14	1.35	0.39
Adamts1	0.06	-0.07	0.00	-0.07	-0.09	-0.07	1.42	0.24
Pfkfb3	0.13	0.05	0.00	0.09	0.09	0.13	1.03	0.09
Preb	0.00	0.07	-0.01	0.01	0.03	0.02	1.01	0.09
Acvrl1	0.07	0.07	-0.10	0.03	-0.05	-0.01	1.84	1.04
Ampd3	-0.04	-0.08	-0.03	-0.01	-0.10	-0.08	1.19	0.60
Arfl4	-0.02	0.08	-0.01	0.02	-0.07	-0.13	1.72	1.31
Foxo3a	0.06	0.21	-0.07	-0.08	-0.06	-0.38	1.41	0.66
Mertk	0.13	0.03	-0.41	-0.19	-0.12	-0.12	1.22	0.62
Mras	0.07	0.07	-0.07	-0.09	-0.16	-0.35	1.29	0.01
Fst	0.19	0.78	0.26	0.20	0.24	-0.21	1.24	-0.11
Rgs2	2.42	1.01	1.42	1.60	1.48	0.49	0.79	0.74
Cebpb	2.17	1.45	1.34	1.26	1.33	0.08	1.02	0.87
Klf5	1.45	1.15	1.30	1.49	1.38	0.30	0.60	0.28
Tsc22d1	1.39	0.92	0.52	0.55	0.48	0.07	0.19	0.65
Sdc4	0.80	1.30	0.70	0.95	0.82	0.47	0.86	0.38
Dusp1	2.88	2.07	1.33	0.77	0.72	-0.14	2.50	1.58
Nfil3	1.60	0.81	0.59	0.65	0.48	0.16	0.91	0.39
Mt2	1.46	2.38	1.31	1.14	0.82	-0.61	1.74	2.22
Mt1	1.11	1.58	0.77	0.96	0.75	-0.45	1.37	1.65
Fkbp5	1.37	2.80	1.85	2.11	2.73	0.74	2.36	3.11
Vdr	1.22	1.69	1.08	0.67	0.19	-0.16	0.86	0.95
Pdxk	0.91	1.16	0.89	0.53	0.24	0.04	0.41	0.41
Mcl1	0.54	1.14	0.59	0.24	0.16	-0.07	0.21	0.51
Prdx6	0.57	1.98	1.01	0.07	0.22	-0.19	0.71	0.26
Hsp110	0.24	1.71	0.67	0.16	0.47	0.20	0.41	0.55
Xdh	0.28	2.21	1.67	1.46	1.24	0.02	0.35	0.85
Samhd1	0.09	1.43	0.69	0.60	0.57	0.00	0.24	0.48
Top1	0.22	1.18	0.56	0.50	0.48	0.35	0.32	0.39
Itga5	0.37	1.31	0.81	0.53	0.26	-0.12	0.07	0.37
Srm	0.28	1.59	0.96	0.44	1.24	0.67	0.26	0.57
Ptges	0.54	1.08	0.76	0.41	0.81	0.39	0.28	0.54
Bzw2	0.31	0.89	0.87	0.45	1.13	0.63	-0.08	0.48
AI553587	0.52	2.46	1.58	0.35	1.34	1.60	0.78	-0.21
Clic4	0.16	1.04	0.52	0.20	0.46	0.68	0.58	0.87
Rasa3	0.39	1.45	1.45	1.39	1.25	0.46	0.50	0.98
Col4a2	-0.13	1.18	1.42	1.38	1.28	0.90	0.32	0.72
Col4a1	0.06	1.36	1.40	1.19	1.26	0.98	0.42	1.60
H2afx	0.40	0.75	0.69	1.36	1.30	0.53	0.10	0.94

Gas6	0.06	0.69	1.31	1.40	1.21	-0.11	0.28	1.38
Wnt4	0.11	0.89	1.13	0.89	0.52	-0.23	-0.22	0.53
Tmem167	0.25	0.41	1.03	0.80	0.93	0.04	0.44	0.06
Mcm7	0.04	-0.14	1.26	0.92	0.90	0.02	0.10	0.25
Fosl1	0.70	1.78	1.22	0.87	0.68	0.24	-0.84	0.00
Slc35e4	0.19	0.45	0.09	0.28	1.01	0.37	0.59	0.18
Cebpd	2.47	0.14	0.31	0.63	0.76	-0.74	0.93	0.87
Nr4a1	2.57	0.13	0.00	0.03	-0.30	-0.54	1.16	0.06
Serpine1	1.70	0.88	0.62	0.22	0.27	-0.49	0.42	1.32
Thbd	1.03	0.89	0.11	-0.22	-0.11	-0.19	0.19	0.50
Abhd5	0.31	0.79	0.82	0.68	1.43	2.03	0.12	0.61
Fasn	0.22	0.58	0.54	0.33	0.96	1.70	0.19	0.46
Retsat	0.17	0.47	0.33	0.34	0.56	1.06	0.06	0.23
Gys1	-0.01	0.24	0.24	0.46	0.74	1.32	-0.04	0.31
Fh1	0.15	0.17	0.31	0.30	0.68	1.16	0.05	0.59
Atp5a1	0.23	0.22	0.22	0.21	0.76	1.00	0.03	0.54
Prps1	0.03	0.50	0.43	0.22	0.87	1.69	0.15	0.72
Aldoa	0.39	0.15	0.05	0.28	0.71	1.29	-0.15	0.33
Cox5b	0.36	0.11	0.09	0.26	0.59	1.28	0.00	0.34
Uqcrc1	0.42	0.03	0.13	0.22	0.56	1.09	0.01	0.53
Pnpla2	0.17	0.01	-0.09	0.46	2.27	4.19	0.13	0.59
Uqcrc2	0.22	-0.10	0.03	0.07	0.84	1.63	0.05	0.46
Prdx3	0.18	0.10	0.07	0.09	0.68	1.30	0.08	0.53
C3	-0.04	-0.03	0.24	0.65	2.30	2.88	0.12	0.93
Pparg	-0.05	-0.34	0.01	0.24	1.32	1.89	0.00	0.61
Sfxn1	-0.18	-0.07	0.33	0.26	0.88	1.56	0.02	0.58
Scp2	-0.28	-0.11	0.28	0.04	0.82	1.43	-0.18	0.64
Bcat2	0.14	-0.04	-0.05	0.00	0.49	2.06	-0.07	0.81
Etfdh	-0.01	-0.08	0.16	0.10	0.46	1.18	-0.08	0.66
Col6a2	-0.05	0.44	0.76	1.30	1.30	1.82	0.12	0.93
Zfp385	-0.08	0.69	0.62	0.95	0.98	1.07	-0.15	0.81
Mknk2	0.44	1.12	0.78	0.60	1.01	1.43	0.08	1.20
G6pdx	0.01	0.53	0.73	0.37	0.81	1.03	0.05	0.76
Agt	0.21	0.49	0.89	1.48	3.03	2.74	0.02	1.68
Mapk6	-0.18	0.36	0.46	0.49	1.64	1.45	0.18	0.48
Pim3	0.85	0.11	0.27	0.49	1.34	1.12	-0.13	0.90
Cebpa	-0.16	-0.12	0.23	0.45	2.16	2.95	-0.49	-0.04
Lpl	-0.56	-0.12	-0.10	-0.31	1.21	2.66	-0.33	0.18
Cdkn2c	-0.09	-0.35	-0.11	0.19	0.51	1.37	-0.64	0.31
Lcn2	-0.02	0.39	1.21	1.53	1.26	2.48	1.57	3.19
Map4k4	-0.01	0.28	0.37	0.30	0.29	0.58	0.46	1.02
Orm2	0.09	0.15	0.24	0.34	0.51	0.96	0.07	1.61
Hp	-0.02	0.13	0.19	0.28	0.51	2.07	0.52	1.34
Orm1	-0.04	0.01	0.09	0.24	0.37	1.64	0.57	1.64
Lpin1	0.10	-0.17	-0.16	0.09	0.94	1.64	1.03	0.87
Nrip1	0.00	0.05	0.16	0.14	0.73	1.19	0.96	0.66
Nnmt	0.35	-0.24	-0.31	-0.29	-0.01	1.70	-0.15	0.47
Scarb1	-0.09	-0.44	-0.36	-0.31	0.12	1.86	0.00	0.70
Acaa2	0.24	-0.28	-0.25	-0.13	0.45	1.06	-0.05	0.58
Impdh1	0.12	0.49	0.04	-0.29	0.14	1.15	-0.05	0.14
Lum	-0.02	-0.02	-0.27	0.17	0.58	1.71	-0.19	-1.35
Arl4c	1.05	0.38	-0.07	-0.09	-0.17	-0.25	-0.68	-0.12
Cxcl1	1.34	-0.34	-0.18	-0.32	-0.71	-0.42	-0.88	-0.85
Id2	2.51	0.21	-0.49	-0.65	-1.23	-1.49	-0.61	-1.50
Map4k3	-0.05	-0.06	-0.10	-0.02	-0.03	-0.01	0.58	-1.05

Postn	-0.44	0.06	-0.03	-0.51	-0.16	-0.02	0.34	-1.49
Mmp3	0.13	-0.04	-0.28	-0.22	0.14	-0.07	-0.04	-1.22
Ptn	0.01	0.20	-0.03	-0.44	-0.39	-0.25	0.07	-1.54
Tnc	0.00	0.22	-0.10	-0.13	-0.10	-0.25	-0.27	-1.25
H2-T18	-0.12	0.10	0.01	0.01	-0.07	-0.22	-0.04	-1.11
Fmod	-0.12	-0.01	-0.17	-0.12	-0.22	-0.28	-0.05	-1.03
Sema3c	-0.11	-0.13	-0.05	0.02	-0.11	-0.18	-0.02	-1.13
Ikzf2	-0.08	-0.03	-0.16	-0.02	-0.13	-0.12	-0.09	-1.06
Chst2	-0.10	-0.12	-0.10	-0.13	-0.16	-0.15	-0.11	-1.08
Angptl4	-0.07	-0.04	0.16	0.37	0.55	0.39	-1.57	-0.49
Has2	-0.29	-0.58	0.18	0.35	0.39	0.07	-1.66	-1.03
Cxcl5	0.37	-0.21	0.06	0.00	-0.78	-1.08	-2.45	-1.78
Mafb	0.01	-0.03	0.01	-0.03	-0.02	0.02	-0.66	-1.68
Gata2	-0.12	-0.08	-0.09	-0.06	-0.14	-0.13	-0.91	-1.36
Edg1	-0.02	0.02	0.00	0.02	-0.03	0.01	-1.02	-0.89
Enc1	-0.02	-0.06	-0.03	-0.09	-0.09	-0.07	-1.38	-1.40
Bnc1	-0.11	-0.15	-0.28	-0.33	-0.30	-0.37	-1.23	0.06
Ppp1r3c	-0.39	-0.27	-0.11	-0.20	0.04	-0.16	-1.03	-0.03
Irf1	-0.55	-0.42	-0.35	-0.39	-0.34	-0.21	-1.30	-0.39
Socs3	-0.18	0.08	-0.01	0.10	-0.16	-0.31	-1.11	-0.30
Cxxc5	-0.20	-0.26	0.09	-0.16	-0.34	-0.41	-1.55	-0.26
Adam19	-0.28	-0.13	-0.17	-0.14	0.02	0.04	-1.06	-0.55
Rgs16	0.05	-0.23	-0.30	-0.28	-0.26	-0.18	-1.21	-0.58
Hic1	-0.19	-0.26	-0.28	-0.20	-0.16	-0.38	-1.18	-0.53
Plac8	0.34	0.69	0.56	0.11	-0.38	-1.74	0.53	0.17
Serpinb6a	0.47	-0.03	-0.14	-0.27	-0.78	-1.43	0.14	0.48
Sgk	1.42	-0.22	-0.29	-0.59	-0.62	-0.80	0.63	0.75
Adm	1.64	-0.82	-0.94	-0.94	-0.95	-0.94	1.39	0.68
Id3	1.65	-0.39	-0.66	-0.64	-0.87	-1.55	0.21	0.37
Dok1	0.51	-0.45	-0.74	-0.65	-0.73	-0.98	1.59	0.65
Cyr61	0.66	-0.99	-1.14	-1.21	-1.20	-1.46	1.10	0.86
Anxa4	-0.14	-0.02	0.04	-0.38	-0.56	-0.83	0.12	1.10
Cndp2	0.05	-0.15	-0.34	-0.49	-0.30	-0.20	0.03	1.02
Ifi202b	-0.50	-0.32	-0.23	-0.39	-0.41	-0.72	-0.02	1.59
G6pd2	-0.35	-0.46	-0.42	-0.37	-0.45	-0.34	-0.16	1.13
Anxa1	0.27	-0.35	-0.76	-1.04	-1.30	-0.71	-0.23	0.87
Anxa3	0.12	-0.10	-0.90	-1.13	-1.25	-1.29	-0.12	0.65
Gas1	-0.46	-1.42	-0.63	-0.33	-0.58	-1.09	-0.52	0.62
Bhlhb2	0.05	-0.76	-0.46	-0.64	-0.18	-0.56	-1.11	0.00
Ccl7	0.14	-0.97	-0.63	-0.93	-1.26	-1.39	-1.87	0.32
Marcksl1	0.15	0.00	0.05	-0.27	-0.42	-1.00	-0.11	-0.51
Dlk1	0.12	0.14	0.00	0.01	-0.58	-1.36	0.01	-0.76
Fgf7	-0.46	-0.38	-0.20	-0.77	-1.42	-1.58	-1.02	-1.07
Phldb2	-0.66	-0.67	-0.91	-1.17	-1.47	-1.57	-1.35	-1.25
Efnb2	-0.04	0.13	-0.22	-0.39	-0.56	-1.06	-0.30	-1.29
Fzd1	0.04	-0.01	-0.18	-0.51	-0.60	-0.99	-0.52	-1.13
Vcam1	-0.32	-0.37	-0.45	-0.70	-0.95	-1.11	0.01	-1.20
Sfrp2	-0.19	-0.63	-0.94	-1.09	-1.43	-1.16	-0.28	-1.67
Egr1	0.08	-0.95	-0.84	-0.87	-0.74	-0.56	0.13	-1.63
D0H4S114	-0.39	-1.34	-1.20	-1.06	-0.88	-0.58	-0.09	-1.42
Anxa6	0.23	-0.85	-1.37	-1.28	-0.89	0.00	0.06	-0.39
Hmox1	-0.06	-1.31	-1.26	-1.18	-0.81	-0.25	-0.81	-0.18
F3	-0.15	-1.72	-1.34	-0.99	-0.60	-0.78	-0.40	-0.82
Bdnf	0.14	-0.46	-0.31	-0.80	-1.03	-1.56	-0.01	0.09
Tmsb10	0.13	-0.10	-0.34	-0.57	-0.94	-1.29	-0.05	-0.45

Pltp	0.07	-0.17	-0.63	-0.83	-1.86	-1.44	0.05	-0.43
Col5a2	-0.41	-0.15	-0.57	-1.11	-0.68	-0.99	-0.08	-0.39
Timp3	-0.41	-0.46	-0.89	-0.81	-1.18	-1.49	0.13	-0.53
Acta2	0.01	-0.49	-2.01	-2.74	-2.89	-2.64	-0.02	-0.71
Amot	-0.48	-0.93	-0.43	-0.55	-0.50	-1.02	-0.07	-0.50
Marcks	-0.78	-1.75	-0.86	-0.72	-0.79	-0.89	-0.39	-1.11
Gadd45a	-0.96	-1.47	-1.16	-1.12	-1.16	-1.00	-0.85	-0.21
Snai2	-0.87	-1.23	-1.44	-1.38	-1.64	-1.58	-0.23	-0.96
Tpm1	-0.17	-1.21	-1.66	-1.76	-2.11	-1.74	-0.14	-1.60
Cnn2	-0.07	-0.93	-1.16	-1.27	-1.48	-1.23	-0.14	-0.48
Plat	-0.15	-0.86	-0.83	-0.97	-0.83	-1.18	-0.32	-0.61
Gas2	0.00	-0.91	-0.92	-0.95	-1.09	-0.96	-0.38	-0.60
Fzd2	0.00	-0.93	-0.94	-0.69	-0.78	-1.26	-0.69	-0.39
Ccl2	0.11	-1.80	-1.22	-1.63	-2.22	-2.24	-1.83	-0.92
Wisp1	-0.42	-0.70	-0.89	-0.83	-0.69	-1.10	-0.72	-0.01
Csf1	-0.54	-1.10	-1.28	-1.40	-1.59	-1.54	-0.62	-0.45
Plk2	-0.63	-1.70	-1.89	-2.10	-2.48	-2.76	-1.68	-0.69

Supplemental Table 3.2. *Log2 fold values of DIM-regulated genes, not affected by dex treatment*

Gene	DIM 2h	DIM 8h	DIM 16h	DIM day 1	DIM day 2	DIM day 4	Dex 2h	Dex 36h
Taldo1	0.35	0.03	0.28	0.40	1.40	2.00	-0.12	0.13
1100001G20Rik	0.08	0.04	0.27	0.57	1.33	1.89	-0.10	0.18
Cox6a1	0.30	0.13	0.32	0.60	0.84	1.49	0.06	0.19
Sdhd	0.11	0.08	0.39	0.47	0.89	1.33	-0.07	0.30
Hibadh	0.30	0.18	0.15	0.18	0.80	1.58	0.02	0.32
Suclg1	0.16	0.13	0.16	0.13	0.64	1.39	-0.06	0.43
Alad	0.24	-0.02	0.25	0.09	0.63	1.43	-0.09	0.23
Aco2	0.22	0.47	0.35	0.39	1.00	1.48	-0.10	-0.05
Mrpl12	0.25	0.33	0.26	0.25	0.93	1.51	-0.13	-0.05
Grpel1	0.22	0.23	0.10	0.07	0.81	1.13	0.09	0.00
Uqcrh	0.37	0.38	0.37	0.42	1.06	1.13	-0.03	0.03
Atp5o	0.31	0.16	0.10	0.31	0.76	1.33	-0.30	-0.05
Dgat1	0.27	0.14	0.01	0.18	0.83	1.59	-0.26	-0.21
Ndufb8	0.44	0.14	0.16	0.36	0.74	1.27	-0.09	0.09
0910001A06Rik	0.23	0.30	0.24	0.07	0.42	1.10	-0.03	-0.05
Slc25a10	0.42	0.23	0.19	0.52	1.27	2.58	0.03	-0.13
Cox7a2	0.11	-0.03	0.12	0.26	0.53	1.23	0.06	-0.04
Uqcr	0.10	0.09	0.16	0.29	0.51	1.01	0.07	0.02
Mrpl51	0.03	-0.04	0.29	0.42	0.55	1.37	-0.07	-0.06
Txndc14	0.11	-0.07	0.24	0.28	0.55	1.08	-0.03	-0.10
Psen2	0.23	0.07	0.14	0.29	0.30	1.14	-0.05	-0.11
Uqcrq	0.12	0.13	0.33	0.39	0.57	1.44	0.37	-0.07
Dhrs7b	0.16	-0.06	0.21	0.35	0.32	1.17	0.16	-0.15
Gnpat	0.03	0.01	0.12	0.12	0.44	1.19	0.21	-0.06
Hsd11b1	-0.18	0.13	0.31	0.59	1.08	2.45	0.06	0.41
Cox7b	-0.12	-0.03	0.33	0.26	0.48	1.32	-0.16	0.18

Ndufc1	-0.08	-0.32	0.26	0.34	0.47	1.23	-0.06	0.10
Ogdh	0.09	0.34	0.37	0.36	0.54	1.28	-0.16	-0.06
S100a8	0.08	0.38	0.51	0.46	0.34	1.24	-0.37	0.07
Pcyox1	-0.19	0.23	0.51	0.31	0.43	1.21	-0.05	0.20
Lipe	-0.05	0.08	0.28	0.62	2.68	3.56	0.21	0.50
Acsl1	-0.18	-0.10	-0.02	0.08	2.16	3.11	0.27	0.21
Acadm	-0.09	-0.26	0.17	0.24	0.88	1.39	0.08	0.22
Dbi	0.04	-0.22	-0.21	0.20	1.35	2.23	-0.09	-0.21
2010100O12Rik	0.03	-0.12	-0.05	0.18	0.63	1.01	0.06	-0.01
Fabp5	0.04	-0.14	-0.29	-0.07	1.61	1.82	0.62	0.53
Pex11a	-0.08	-0.13	-0.11	0.04	0.97	1.43	0.33	0.27
Slc5a6	-0.05	0.08	-0.07	0.08	1.91	1.54	0.01	0.29
Ormdl3	-0.26	0.30	0.38	0.20	0.81	1.18	-0.01	0.02
Aifm1	-0.42	0.17	0.45	-0.02	0.72	1.14	0.19	0.30
1110020P15Rik	0.22	0.01	0.06	0.34	0.58	1.16	0.08	0.66
Tpi1	0.46	-0.16	0.04	0.48	0.55	1.04	-0.15	0.19
Tkt	0.49	-0.16	-0.04	0.17	0.43	1.03	-0.08	-0.11
Adipoq	0.06	0.04	0.02	0.17	2.77	5.91	0.13	0.19
Cidec	-0.02	0.01	0.00	0.12	2.10	4.77	-0.19	0.19
G0s2	-0.13	-0.02	-0.11	0.00	1.32	2.65	-0.32	0.37
Retn	-0.13	-0.21	-0.18	-0.22	1.24	4.00	-0.37	-0.03
Hipk2	0.06	0.18	0.14	0.03	0.68	2.15	-0.20	0.12
Itga6	-0.07	0.14	0.19	0.01	0.40	1.51	-0.19	0.32
Dld	-0.19	0.05	0.25	-0.05	0.50	1.37	0.02	0.31
Cfd	-0.01	0.08	0.02	0.11	1.35	4.83	-0.02	0.00
BC054059	0.00	0.11	0.01	0.08	0.53	2.75	0.12	0.03
Gpd1	-0.07	-0.04	0.06	-0.06	0.29	2.43	0.10	-0.18
Thrsp	-0.05	-0.02	-0.01	-0.03	0.09	2.56	-0.02	0.24
Apoc1	0.01	0.08	0.02	0.05	0.11	1.33	0.00	0.27
Nr1h3	0.14	-0.10	-0.02	0.00	0.54	2.31	0.05	0.47
Coq5	-0.02	-0.02	-0.04	-0.10	0.29	1.08	0.06	0.18
Alas1	0.16	-0.01	-0.02	0.04	0.30	1.27	0.27	0.29
Cs	0.06	-0.04	0.09	0.08	0.26	1.19	-0.01	0.40
Lonp2	0.04	-0.17	-0.09	0.04	0.59	1.09	0.08	0.35
Ndufb5	0.05	-0.13	-0.06	0.07	0.37	1.09	-0.02	0.30
Sdhc	0.23	-0.16	-0.07	0.08	0.53	1.06	-0.12	0.13
Chchd3	0.08	-0.27	0.11	0.05	0.41	1.15	-0.21	0.26
Ndufa9	0.34	-0.09	-0.08	0.05	0.32	1.15	-0.20	0.42
Dhcr7	0.18	-0.08	-0.24	-0.08	0.07	1.24	-0.03	0.61
Mosc2	0.04	-0.06	-0.33	-0.17	0.17	1.36	-0.02	0.34
Tspan12	0.01	0.11	0.13	0.09	0.13	1.11	-0.42	0.12
Mgst1	0.18	-0.33	-0.32	-0.20	0.50	1.33	0.00	0.26
Qdpr	0.19	-0.39	-0.25	-0.20	0.58	1.09	0.02	0.01
Cib2	0.26	-0.14	-0.26	-0.16	0.61	1.05	-0.12	-0.02
Gstz1	0.41	-0.53	-0.30	-0.18	0.20	2.08	-0.13	-0.03

1110001J03 Rik	0.31	-0.34	-0.39	0.12	0.36	1.15	-0.11	-0.01
Col15a1	-0.11	-0.09	-0.05	0.09	0.59	1.66	0.06	-0.67
Mtx2	-0.34	-0.48	0.11	-0.01	0.54	1.14	-0.11	-0.20
Camp	0.05	0.14	0.11	0.17	0.09	1.32	0.48	-0.09
Ak2	0.03	0.74	0.59	0.63	1.25	1.84	0.12	0.30
Mdh2	0.18	0.51	0.51	0.49	0.91	1.48	0.06	0.29
Timm23	0.16	0.55	0.45	0.29	0.81	1.07	0.13	0.24
Xbp1	0.08	0.95	0.62	0.47	1.35	1.62	-0.08	0.02
Bcap31	0.29	0.29	0.54	0.64	0.78	1.03	-0.06	0.28
Psma1	0.09	0.24	0.38	0.60	0.86	1.05	0.04	0.15
Pcx	0.16	0.37	0.92	0.84	2.03	1.78	-0.03	0.40
Ldha	0.25	0.53	0.85	0.99	1.05	1.12	0.02	0.05
Srebf1	-0.17	-0.06	0.42	0.61	1.21	0.97	-0.06	0.24
Nola3	0.25	0.39	0.73	0.69	1.04	0.49	0.01	0.15
Eif2b1	0.12	0.61	0.54	0.38	1.05	0.69	-0.03	0.25
2310028O1 1Rik	0.03	0.34	0.72	0.50	1.06	0.64	0.51	0.08
Scd1	-0.03	1.62	1.42	0.95	1.49	3.11	1.45	-0.18
9130213B0 5Rik	0.06	0.84	0.68	0.40	0.47	1.40	0.36	0.45
Pfkl	0.04	0.25	0.29	0.70	0.70	1.09	0.51	-0.12
Psat1	0.18	0.25	0.20	-0.09	-0.35	1.25	0.01	0.32
Hsd17b12	-0.05	0.03	0.08	-0.42	-0.06	1.00	0.03	0.32
Bckdhb	-0.07	-0.40	-0.42	-0.59	0.47	1.54	0.12	0.15
Sdpr	-0.31	-0.51	-0.67	-0.61	0.07	1.48	-0.14	0.39
Aoc3	-0.01	-0.44	-0.57	-0.47	-0.23	2.01	0.20	-0.48
Nol5a	0.23	1.31	1.19	0.78	1.37	0.33	0.10	0.08
Lxn	0.42	1.23	1.09	0.98	1.10	-0.23	0.07	-0.03
Rrm2	0.58	1.07	1.73	1.41	1.27	0.50	-0.01	0.19
Impdh2	0.66	0.86	0.93	1.05	1.19	-0.07	-0.14	0.67
Osmr	-0.17	1.21	1.55	1.26	0.65	-0.03	-0.07	0.27
Pcna	0.17	0.50	1.22	0.59	0.53	-0.04	-0.02	0.22
Cdc45l	0.05	0.03	1.01	0.89	0.67	0.40	-0.23	0.22
Cdc2a	-0.02	-0.14	0.97	1.46	0.56	0.23	-0.25	0.21
Tcf19	0.06	-0.09	1.37	1.06	0.61	0.09	0.14	-0.01
Top2a	-0.15	0.04	1.00	1.37	0.70	-0.14	0.03	0.72
Mcm4	-0.18	-0.08	1.11	0.61	0.20	-0.28	-0.09	0.07
Saa3	0.02	0.16	0.45	0.78	1.34	0.25	0.21	0.14
H19	0.07	0.10	0.06	0.44	1.21	0.07	0.13	0.09
Ly6a	0.18	0.19	1.06	1.33	0.49	-1.88	-0.11	0.48
Ugdh	1.31	2.32	1.16	0.78	0.04	-0.60	-0.08	-0.06
Il1rl1	0.82	1.57	1.23	0.48	-0.19	-0.28	0.25	0.17
Ramp3	0.21	1.37	0.62	0.33	-0.04	0.05	-0.08	-0.27
Kcnn4	0.06	1.09	0.54	0.36	0.07	-0.11	0.00	-0.01
Pttg1ip	0.29	1.21	0.24	0.11	0.19	0.09	0.25	0.23
Cd164	0.15	1.34	0.88	0.40	0.55	0.57	0.35	0.42
Hspa5	0.08	1.17	0.71	0.09	0.39	0.87	-0.03	0.03

Prnp	0.65	1.00	0.47	0.29	0.78	0.27	0.01	0.27
Arhgap8	0.57	1.20	0.40	0.28	0.45	0.61	0.09	-0.20
Cdc20	0.10	-0.49	-0.13	1.22	0.41	-0.04	0.11	0.39
Ccnb2	0.06	-0.80	-0.12	1.11	0.02	-0.18	0.08	0.79
Kif20a	0.07	-0.32	0.16	1.11	0.11	-0.11	0.24	-0.08
Wee1	0.88	0.16	0.35	0.19	0.19	0.00	1.08	0.67
Slc25a25	1.08	0.33	0.11	0.06	0.32	0.47	0.29	0.16
Bag3	1.66	1.16	0.81	0.57	0.20	0.07	0.01	0.06
Foxc2	1.22	0.36	0.53	0.43	0.46	-0.41	-0.27	0.06
Nr4a2	1.11	0.16	0.08	0.05	0.03	-0.11	-0.12	-0.08
Midn	1.01	0.13	0.07	0.05	-0.03	-0.07	-0.26	-0.25
Dlx2	1.44	0.20	0.07	-0.15	-0.25	-0.56	-0.07	-0.34
Ptgs2	1.55	-0.25	-0.24	-0.21	-0.25	-0.29	0.40	0.06
Ctgf	1.05	-0.24	-0.21	-0.21	-0.26	-0.28	0.36	-0.11
Phlda1	1.23	-0.41	-0.48	-0.46	-0.52	-0.13	0.04	-0.27
Btg2	1.44	-0.64	-0.70	-0.60	-0.68	-0.33	-0.15	0.06
Junb	1.10	-0.28	-0.02	-0.18	-0.47	-0.81	0.01	0.29
Ier3	2.16	-0.27	-0.57	-0.82	-1.11	-1.18	-0.22	0.12
Gsto1	0.42	1.22	0.39	-0.30	-0.64	-0.85	-0.34	0.47
Hmga2	0.23	0.99	0.29	-0.20	-0.89	-1.39	0.20	0.17
Pdpn	0.72	0.96	-0.06	-0.61	-1.06	-1.15	-0.59	-0.23
Irx3	-0.16	-0.29	-0.22	-0.15	-0.04	0.13	-1.51	-0.08
Ifitm3	0.10	-0.06	0.15	0.22	-0.35	-1.55	-0.15	0.19
Dnm1	0.05	-0.80	-0.25	-0.01	-0.43	-1.47	-0.06	-0.27
Prrx2	-0.05	-0.34	0.18	0.02	-0.09	-1.20	-0.34	-0.40
Fn1	0.10	0.04	0.00	-0.15	-0.24	-1.31	-0.03	-0.32
S100a4	0.13	-0.11	-0.06	-0.08	-0.28	-1.03	-0.28	-0.38
Emp1	0.01	0.36	-0.83	-0.73	-1.55	-1.95	-0.50	-0.44
Cd99	0.43	-0.11	-0.40	-0.38	-0.51	-1.18	-0.07	0.04
S100a6	0.14	-0.08	-0.18	-0.15	-0.69	-1.33	-0.21	0.11
Plp2	0.00	-0.37	-0.26	-0.24	-0.68	-1.33	-0.13	0.17
Ctsl	-0.12	-0.03	-0.06	-0.30	-0.77	-1.30	0.17	0.36
Lox	-0.44	-0.10	-0.32	-0.71	-1.28	-1.34	0.23	0.31
Mfsd1	-0.32	-0.60	-0.55	-0.76	-0.69	-1.19	0.01	-0.17
Zfp36l2	-0.18	-0.25	-0.33	-0.70	-0.66	-1.04	-0.14	0.28
App	-0.39	-0.19	-0.32	-0.55	-0.70	-1.33	-0.06	-0.05
Apbb1ip	-0.25	-1.12	-0.87	-0.71	0.03	-0.39	-0.31	0.53
Slc9a3r1	0.05	-0.68	-0.69	-0.68	-0.59	-0.54	-1.33	0.46
Zfp644	-0.91	-1.07	-0.49	-0.76	-0.56	-0.60	0.04	-0.34
Rab9	-0.71	-1.25	-0.82	-0.88	-0.67	-0.37	-0.20	-0.09
Mylk	-0.39	-1.08	-1.20	-1.32	-0.60	0.22	-0.12	-0.22
Sc4mol	-0.10	-1.27	-0.81	-0.97	-0.86	-0.10	-0.18	0.35
Rhoq	-0.23	-1.00	-0.83	-0.84	-1.13	-0.28	-0.52	0.08
Fdps	0.42	-1.73	-1.00	-1.08	-1.22	0.34	-0.12	-0.21
Fdft1	0.01	-1.46	-0.92	-0.93	-1.34	-0.04	-0.11	-0.35
Ogn	-0.52	-0.46	-0.89	-1.30	-1.17	-0.89	0.07	-0.54
Slc1a4	-0.09	-0.24	-0.87	-0.87	-1.00	-0.81	0.15	-0.19

Lgals3bp	-0.08	-0.37	-0.92	-1.06	-1.31	-0.55	-0.01	-0.50
Spp1	-0.47	-1.00	-1.57	-1.89	-2.28	-1.76	-0.39	0.48
Gstm2	0.36	-0.23	-1.12	-1.58	-1.33	-1.02	0.03	0.13
Herpud1	-0.05	-0.61	-0.93	-0.93	-1.08	-0.66	0.23	0.21
Gstm1	0.10	-0.41	-1.12	-1.07	-1.27	-0.41	0.07	0.11
Ier2	0.70	-1.20	-1.12	-1.32	-1.14	-1.42	-0.18	-0.03
Thbs2	-0.37	-1.10	-1.20	-1.50	-1.08	-0.66	-0.09	-0.58
D6Wsu116e	-0.36	-1.04	-0.91	-0.94	-0.81	-0.61	0.11	0.19
Klf6	-0.26	-1.70	-1.45	-1.19	-1.45	-1.15	0.17	0.39
Snx9	-0.45	-1.16	-1.03	-0.94	-0.98	-0.92	-0.15	0.09
Trib3	-0.30	-1.29	-1.35	-1.04	-1.45	-0.94	-0.11	-0.06
Ddit3	-0.74	-1.82	-1.77	-1.44	-1.73	-1.29	-0.35	-0.31
Ccl9	0.17	-0.75	-1.36	-1.31	-1.26	-1.08	-0.23	-0.51
Ifit3	-0.22	-1.67	-1.85	-1.83	-1.95	-1.63	-0.61	-0.79
Ifit1	-0.48	-1.75	-1.83	-1.80	-1.82	-1.64	-0.63	-0.86
Atf4	-0.14	-1.03	-1.02	-0.90	-1.19	-1.01	0.22	-0.23
Usp18	0.06	-1.54	-1.55	-1.44	-1.43	-1.16	-0.04	-0.44
Isgf3g	-0.25	-0.77	-0.82	-0.73	-1.06	-0.90	-0.15	-0.08
Isg15	-0.19	-1.35	-1.70	-1.72	-1.84	-1.73	-0.20	-0.37
Fhl2	0.00	-1.03	-1.07	-1.06	-1.27	-1.19	-0.05	0.00
Rasa4	0.03	-1.22	-1.54	-1.69	-1.61	-1.74	-0.15	0.01

Supplemmental Table 3.3. *Gene Ontology analysis of dex-regulated genes*

GOTERM_CC_ALL extracellular matrix
Wnt4 WINGLESS-RELATED MMTV INTEGRATION SITE 4
Col4a2 PROCOLLAGEN, TYPE IV, ALPHA 2
Col6a2 PROCOLLAGEN, TYPE VI, ALPHA 2
Lama2 LAMININ, ALPHA 2
Postn PERIOSTIN, OSTEOBLAST SPECIFIC FACTOR
Angptl4 ANGIOPOIETIN-LIKE 4
Tnc TENASCIN C
Fmod FIBROMODULIN
Lgals3 LECTIN, GALACTOSE BINDING, SOLUBLE 3
Col4a1 PROCOLLAGEN, TYPE IV, ALPHA 1
Lum LUMICAN
Ptn PLEIOTROPHIN
Adamts1 A DISINTEGRIN-LIKE AND METALLOPEPTIDSE (REPROLYSIN TYPE) WITH THROMBOSPONDIN TYPE 1 MOTIF, 1
Adam19 A DISINTEGRIN AND METALLOPEPTIDASE DOMAIN 19 (MELTRIN BETA)
Mmp3 MATRIX METALLOPEPTIDASE 3
Amelx AMELOGENIN X CHROMOSOME
Timp3 TISSUE INHIBITOR OF METALLOPROTEINASE 3
Col5a2 PROCOLLAGEN, TYPE V, ALPHA 2

GOTERM_BP_ALL immune response
Gadd45g GROWTH ARREST AND DNA-DAMAGE-INDUCIBLE 45 GAMMA
Samhd1 SAM DOMAIN AND HD DOMAIN, 1
Ccl2 CHEMOKINE (C-C MOTIF) LIGAND 2
Cxcl5 CHEMOKINE (C-X-C MOTIF) LIGAND 5

Irf1 INTERFERON REGULATORY FACTOR 1
C3 COMPLEMENT COMPONENT 3
Cd24a CD24A ANTIGEN
Ccl7 CHEMOKINE (C-C MOTIF) LIGAND 7
Ifi202b INTERFERON ACTIVATED GENE 202
Ifi203 INTERFERON ACTIVATED GENE 203
Cxcl1 CHEMOKINE (C-X-C MOTIF) LIGAND 1
H2-T18 HISTOCOMPATIBILITY 2, T REGION LOCUS 18

KEGG_PATHWAY TGF-BETA SIGNALING PATHWAY
Fst FOLLISTATIN
Acvrl1 ACTIVIN A RECEPTOR, TYPE II-LIKE 1
Myc MYELOCYTOMATOSIS ONCOGENE
Id2 INHIBITOR OF DNA BINDING 2
Id3 INHIBITOR OF DNA BINDING 3

GOTERM_CC_ALL intracellular membrane-bound organelle
Cebpb CCAAT/ENHANCER BINDING PROTEIN (C/EBP), BETA
Uqcrc1 UBIQUINOL-CYTOCHROME C REDUCTASE CORE PROTEIN 1
Gadd45a GROWTH ARREST AND DNA-DAMAGE-INDUCIBLE 45 ALPHA
Fgf7 FIBROBLAST GROWTH FACTOR 7
Preb PROLACTIN REGULATORY ELEMENT BINDING
Lpin1 LIPIN 1
Ptges PROSTAGLANDIN E SYNTHASE
Anxa1 ANNEXIN A1
Lgals3 LECTIN, GALACTOSE BINDING, SOLUBLE 3
Gadd45g GROWTH ARREST AND DNA-DAMAGE-INDUCIBLE 45 GAMMA
Prdx3 PEROXIREDOXIN 3
Idh2 ISOCITRATE DEHYDROGENASE 2 (NADP+), MITOCHONDRIAL
Fdx1 FERREDOXIN 1
Fh1 FUMARATE HYDRATASE 1
Tead4 TEA DOMAIN FAMILY MEMBER 4
Atp5a1 ATP SYNTHASE, H+ TRANSPORTING, MITOCHONDRIAL F1 COMPLEX, ALPHA SUBUNIT, ISOFORM 1
Bcl2l1 BCL2-LIKE 1
Pdk4 PYRUVATE DEHYDROGENASE KINASE, ISOENZYME 4
Nfil3 NUCLEAR FACTOR, INTERLEUKIN 3, REGULATED
Xdh XANTHINE DEHYDROGENASE
Nfkbia NUCLEAR FACTOR OF KAPPA LIGHT CHAIN GENE ENHANCER IN B-CELLS INHIBITOR, ALPHA
Arl4c ADP-RIBOSYLATION FACTOR-LIKE 4C
Pparg PEROXISOME PROLIFERATOR ACTIVATED RECEPTOR GAMMA
Samhd1 SAM DOMAIN AND HD DOMAIN, 1
Sfxn1 SIDEROFLEXIN 1
Clic4 CHLORIDE INTRACELLULAR CHANNEL 4 (MITOCHONDRIAL)
Rhob RAS HOMOLOG GENE FAMILY, MEMBER B
Bdnf BRAIN DERIVED NEUROTROPHIC FACTOR
Bnc1 BASONUCLIN 1
Sesn1 SESTRIN 1
Per1 PERIOD HOMOLOG 1 (DROSOPHILA)
Acaa2 ACETYL-COENZYME A ACYLTRANSFERASE 2 (MITOCHONDRIAL 3-OXOACYL-COENZYME A THIOLASE)
Snai2 SNAIL HOMOLOG 2 (DROSOPHILA)
Id3 INHIBITOR OF DNA BINDING 3
Top1 TOPOISOMERASE (DNA) I
Cd36 CD36 ANTIGEN

Nrip1 NUCLEAR RECEPTOR INTERACTING PROTEIN 1
Zfp385 ZINC FINGER PROTEIN 385
Vdr VITAMIN D RECEPTOR
Hic1 HYPERMETHYLATED IN CANCER 1
Klf5 KRUPPEL-LIKE FACTOR 5
Marcks MYRISTOYLATED ALANINE RICH PROTEIN KINASE C SUBSTRATE
Cav1 CAVEOLIN, CAVEOLAE PROTEIN 1
Sgk SERUM/GLUCOCORTICOID REGULATED KINASE
Ptn PLEIOTROPHIN
Mthfd2 METHYLENETETRAHYDROFOLATE DEHYDROGENASE (NAD+ DEPENDENT), METHENYLTETRAHYDROFOLATE CYCLOHYDROLASE
Ifi202b INTERFERON ACTIVATED GENE 202
Hmox1 HEME OXYGENASE (DECYCLING) 1
H2afx H2A HISTONE FAMILY, MEMBER X
Bhlhb2 BASIC HELIX-LOOP-HELIX DOMAIN CONTAINING, CLASS B2
Myc MYELOCYTOMATOSIS ONCOGENE
Tsc22d1 TSC22 DOMAIN FAMILY, MEMBER 1
1190002H23Rik RIKEN CDNA 1190002H23 GENE
Nr4a1 NUCLEAR RECEPTOR SUBFAMILY 4, GROUP A, MEMBER 1
Mt1 METALLOTHIONEIN 1
Dpep1 DIPEPTIDASE 1 (RENAL)
Hsp110 HEAT SHOCK PROTEIN 110
Ap1b1 ADAPTOR PROTEIN COMPLEX AP-1, BETA 1 SUBUNIT
Glul GLUTAMATE-AMMONIA LIGASE (GLUTAMINE SYNTHETASE)
Egr1 EARLY GROWTH RESPONSE 1
Stim1 STROMAL INTERACTION MOLECULE 1
Irf1 INTERFERON REGULATORY FACTOR 1
Mcl1 MYELOID CELL LEUKEMIA SEQUENCE 1
Rab3d RAB3D, MEMBER RAS ONCOGENE FAMILY
Etfdh ELECTRON TRANSFERRING FLAVOPROTEIN, DEHYDROGENASE
Klf9 KRUPPEL-LIKE FACTOR 9
Nusap1 EXPRESSED SEQUENCE AW547774
Cebpd CCAAT/ENHANCER BINDING PROTEIN (C/EBP), DELTA
Fkbp5 FK506 BINDING PROTEIN 5
Chst2 CARBOHYDRATE SULFOTRANSFERASE 2
Mcm7 MINICHROMOSOME MAINTENANCE DEFICIENT 7 (S. CEREVISIAE)
Furin FURIN (PAIRED BASIC AMINO ACID CLEAVING ENZYME)
Foxo3a FORKHEAD BOX O3A
Plat PLASMINOGEN ACTIVATOR, TISSUE
Zbtb16 ZINC FINGER AND BTB DOMAIN CONTAINING 16
Bcat2 BRANCHED CHAIN AMINOTRANSFERASE 2, MITOCHONDRIAL
Ifi203 INTERFERON ACTIVATED GENE 203
Cebpa CCAAT/ENHANCER BINDING PROTEIN (C/EBP), ALPHA
Copg COATOMER PROTEIN COMPLEX, SUBUNIT GAMMA
Terf2 TELOMERIC REPEAT BINDING FACTOR 2
Scp2 STEROL CARRIER PROTEIN 2, LIVER
Arfl4 ADP-RIBOSYLATION FACTOR 4-LIKE
Uqcrc2 UBIQUINOL CYTOCHROME C REDUCTASE CORE PROTEIN 2
Rgs2 REGULATOR OF G-PROTEIN SIGNALING 2
Cox5b CYTOCHROME C OXIDASE, SUBUNIT VB
Gata2 GATA BINDING PROTEIN 2
Glud1 GLUTAMATE DEHYDROGENASE 1
Mafb V-MAF MUSCULOAPONEUROTIC FIBROSARCOMA ONCOGENE FAMILY, PROTEIN B (AVIAN)
Amot ANGIOMOTIN
Id2 INHIBITOR OF DNA BINDING 2

Fosl1 FOS-LIKE ANTIGEN 1
Prdx6 PEROXIREDOXIN 6

GOTERM_CC_ALL mitochondrion
Uqcrc1 UBIQUINOL-CYTOCHROME C REDUCTASE CORE PROTEIN 1
Sfxn1 SIDEROFLEXIN 1
Clic4 CHLORIDE INTRACELLULAR CHANNEL 4 (MITOCHONDRIAL)
Bcat2 BRANCHED CHAIN AMINOTRANSFERASE 2, MITOCHONDRIAL
Acaa2 ACETYL-COENZYME A ACYLTRANSFERASE 2 (MITOCHONDRIAL 3-OXOACYL-COENZYME A THIOLASE)
Prdx3 PEROXIREDOXIN 3
Scp2 STEROL CARRIER PROTEIN 2, LIVER
Idh2 ISOCITRATE DEHYDROGENASE 2 (NADP+), MITOCHONDRIAL
Uqcrc2 UBIQUINOL CYTOCHROME C REDUCTASE CORE PROTEIN 2
Fdx1 FERREDOXIN 1
Cox5b CYTOCHROME C OXIDASE, SUBUNIT VB
Glul GLUTAMATE-AMMONIA LIGASE (GLUTAMINE SYNTHETASE)
Fh1 FUMARATE HYDRATASE 1
Glud1 GLUTAMATE DEHYDROGENASE 1
Mcl1 MYELOID CELL LEUKEMIA SEQUENCE 1
Atp5a1 ATP SYNTHASE, H+ TRANSPORTING, MITOCHONDRIAL F1 COMPLEX, ALPHA SUBUNIT, ISOFORM 1
Bcl2l1 BCL2-LIKE 1
Mthfd2 METHYLENETETRAHYDROFOLATE DEHYDROGENASE (NAD+ DEPENDENT), METHENYLTETRAHYDROFOLATE CYCLOHYDROLASE
Pdk4 PYRUVATE DEHYDROGENASE KINASE, ISOENZYME 4
Etfdh ELECTRON TRANSFERRING FLAVOPROTEIN, DEHYDROGENASE

SP_PIR_KEYWORDS lipid synthesis
none

SP_PIR_KEYWORDS nad
Fasn FATTY ACID SYNTHASE
Aldh1a1 ALDEHYDE DEHYDROGENASE FAMILY 1, SUBFAMILY A1
Mthfd2 METHYLENETETRAHYDROFOLATE DEHYDROGENASE (NAD+ DEPENDENT), METHENYLTETRAHYDROFOLATE CYCLOHYDROLASE
Impdh1 INOSINE 5'-PHOSPHATE DEHYDROGENASE 1
Xdh XANTHINE DEHYDROGENASE

GOTERM_BP_ALL glucose metabolic process
Aldoa ALDOLASE 1, A ISOFORM
G6pdx GLUCOSE-6-PHOSPHATE DEHYDROGENASE X-LINKED
G6pd2 GLUCOSE-6-PHOSPHATE DEHYDROGENASE 2
Pdk4 PYRUVATE DEHYDROGENASE KINASE, ISOENZYME 4

KEGG_PATHWAY OXIDATIVE PHOSPHORYLATION
Uqcrc1 UBIQUINOL-CYTOCHROME C REDUCTASE CORE PROTEIN 1
Uqcrc2 UBIQUINOL CYTOCHROME C REDUCTASE CORE PROTEIN 2
Cox5b CYTOCHROME C OXIDASE, SUBUNIT VB
Atp5a1 ATP SYNTHASE, H+ TRANSPORTING, MITOCHONDRIAL F1 COMPLEX, ALPHA SUBUNIT, ISOFORM 1

KEGG_PATHWAY CITRATE CYCLE (TCA CYCLE)
none

GOTERM_BP_ALL programmed cell death

Cebpb CCAAT/ENHANCER BINDING PROTEIN (C/EBP), BETA
Agt ANGIOTENSINOGEN (SERPIN PEPTIDASE INHIBITOR, CLADE A, MEMBER 8)
Rhob RAS HOMOLOG GENE FAMILY, MEMBER B
Aldh1a1 ALDEHYDE DEHYDROGENASE FAMILY 1, SUBFAMILY A1
Bdnf BRAIN DERIVED NEUROTROPHIC FACTOR
Foxo3a FORKHEAD BOX O3A
Zbtb16 ZINC FINGER AND BTB DOMAIN CONTAINING 16
Angptl4 ANGIOPOIETIN-LIKE 4
Snai2 SNAIL HOMOLOG 2 (DROSOPHILA)
Myc MYELOCYTOMATOSIS ONCOGENE
Nr4a1 NUCLEAR RECEPTOR SUBFAMILY 4, GROUP A, MEMBER 1
Gadd45g GROWTH ARREST AND DNA-DAMAGE-INDUCIBLE 45 GAMMA
Gas2 GROWTH ARREST SPECIFIC 2
Gas1 GROWTH ARREST SPECIFIC 1
Cd24a CD24A ANTIGEN
Sgk SERUM/GLUCOCORTICOID REGULATED KINASE
Mcl1 MYELOID CELL LEUKEMIA SEQUENCE 1
AI553587 EXPRESSED SEQUENCE AI553587
Bcl2l1 BCL2-LIKE 1

GOTERM_BP_ALL lipid metabolic process
Fasn FATTY ACID SYNTHASE
Agt ANGIOTENSINOGEN (SERPIN PEPTIDASE INHIBITOR, CLADE A, MEMBER 8)
Pnpla2 PATATIN-LIKE PHOSPHOLIPASE DOMAIN CONTAINING 2
Lpin1 LIPIN 1
Angptl4 ANGIOPOIETIN-LIKE 4
Acaa2 ACETYL-COENZYME A ACYLTRANSFERASE 2 (MITOCHONDRIAL 3-OXOACYL-COENZYME A THIOLASE)
Vldlr VERY LOW DENSITY LIPOPROTEIN RECEPTOR
Sult1a1 SULFOTRANSFERASE FAMILY 1A, PHENOL-PREFERRING, MEMBER 1
Ptges PROSTAGLANDIN E SYNTHASE
Nrip1 NUCLEAR RECEPTOR INTERACTING PROTEIN 1
Scarb1 SCAVENGER RECEPTOR CLASS B, MEMBER 1
Scp2 STEROL CARRIER PROTEIN 2, LIVER
Abhd5 ABHYDROLASE DOMAIN CONTAINING 5
Lpl LIPOPROTEIN LIPASE
Cav1 CAVEOLIN, CAVEOLAE PROTEIN 1
Prdx6 PEROXIREDOXIN 6

GOTERM_CC_ALL extracellular space
Fgf7 FIBROBLAST GROWTH FACTOR 7
Pltp PHOSPHOLIPID TRANSFER PROTEIN
Acvrl1 ACTIVIN A RECEPTOR, TYPE II-LIKE 1
Csf1 COLONY STIMULATING FACTOR 1 (MACROPHAGE)
Col4a2 PROCOLLAGEN, TYPE IV, ALPHA 2
Angptl4 ANGIOPOIETIN-LIKE 4
Vldlr VERY LOW DENSITY LIPOPROTEIN RECEPTOR
Ptges PROSTAGLANDIN E SYNTHASE
Dlk1 DELTA-LIKE 1 HOMOLOG (DROSOPHILA)
Ear1 EOSINOPHIL-ASSOCIATED, RIBONUCLEASE A FAMILY, MEMBER 1
Fjx1 FOUR JOINTED BOX 1 (DROSOPHILA)
Prdx3 PEROXIREDOXIN 3
Wisp1 WNT1 INDUCIBLE SIGNALING PATHWAY PROTEIN 1
Atp5a1 ATP SYNTHASE, H+ TRANSPORTING, MITOCHONDRIAL F1 COMPLEX, ALPHA SUBUNIT, ISOFORM 1
Lum LUMICAN

Itga5 INTEGRIN ALPHA 5 (FIBRONECTIN RECEPTOR ALPHA)
Col5a2 PROCOLLAGEN, TYPE V, ALPHA 2
Bdnf BRAIN DERIVED NEUROTROPHIC FACTOR
Gas6 GROWTH ARREST SPECIFIC 6
Thbd THROMBOMODULIN
Adm ADRENOMEDULLIN
Orm1 OROSOMUCOID 1
Serpine1 SERINE (OR CYSTEINE) PEPTIDASE INHIBITOR, CLADE E, MEMBER 1
Lpl LIPOPROTEIN LIPASE
Mertk C-MER PROTO-ONCOGENE TYROSINE KINASE
Ptn PLEIOTROPHIN
Ccl7 CHEMOKINE (C-C MOTIF) LIGAND 7
Mthfd2 METHYLENETETRAHYDROFOLATE DEHYDROGENASE (NAD+ DEPENDENT), METHENYLTETRAHYDROFOLATE CYCLOHYDROLASE
Amelx AMELOGENIN X CHROMOSOME
Wnt4 WINGLESS-RELATED MMTV INTEGRATION SITE 4
Hp HAPTOGLOBIN
Ccl2 CHEMOKINE (C-C MOTIF) LIGAND 2
Fst FOLLISTATIN
Cyr61 CYSTEINE RICH PROTEIN 61
Col6a2 PROCOLLAGEN, TYPE VI, ALPHA 2
Fmod FIBROMODULIN
Cxcl1 CHEMOKINE (C-X-C MOTIF) LIGAND 1
Dpep1 DIPEPTIDASE 1 (RENAL)
Fzd2 FRIZZLED HOMOLOG 2 (DROSOPHILA)
Stim1 STROMAL INTERACTION MOLECULE 1
Cp CERULOPLASMIN
Mmp3 MATRIX METALLOPEPTIDASE 3
Ly6f LYMPHOCYTE ANTIGEN 6 COMPLEX, LOCUS F
Agt ANGIOTENSINOGEN (SERPIN PEPTIDASE INHIBITOR, CLADE A, MEMBER 8)
Aqp2 AQUAPORIN 2
Chst2 CARBOHYDRATE SULFOTRANSFERASE 2
Furin FURIN (PAIRED BASIC AMINO ACID CLEAVING ENZYME)
Vcam1 VASCULAR CELL ADHESION MOLECULE 1
Plat PLASMINOGEN ACTIVATOR, TISSUE
C3 COMPLEMENT COMPONENT 3
Postn PERIOSTIN, OSTEOBLAST SPECIFIC FACTOR
Lama2 LAMININ, ALPHA 2
Bcat2 BRANCHED CHAIN AMINOTRANSFERASE 2, MITOCHONDRIAL
Tnc TENASCIN C
Col4a1 PROCOLLAGEN, TYPE IV, ALPHA 1
Cox5b CYTOCHROME C OXIDASE, SUBUNIT VB
Sema3c SEMA DOMAIN, IMMUNOGLOBULIN DOMAIN (IG), SHORT BASIC DOMAIN, SECRETED, (SEMAPHORIN) 3C
Cxcl5 CHEMOKINE (C-X-C MOTIF) LIGAND 5
Orm2 OROSOMUCOID 2

KEGG_PATHWAY MAPK Sgnaling Pathway
Map4k4 NCK INTERACTING KINASE
Gadd45g GROWTH ARREST AND DNA-DAMAGE-INDUCIBLE 45 GAMMA
Map3k6 MITOGEN-ACTIVATED PROTEIN KINASE KINASE KINASE 6
Gadd45a GROWTH ARREST AND DNA-DAMAGE-INDUCIBLE 45 ALPHA
Fgf7 FIBROBLAST GROWTH FACTOR 7
Map4k3 RIKEN CDNA 4833416M01 GENE
Bdnf BRAIN DERIVED NEUROTROPHIC FACTOR
Mras MUSCLE AND MICROSPIKES RAS

Mknk2 MAP KINASE-INTERACTING SERINE/THREONINE KINASE 2
Myc MYELOCYTOMATOSIS ONCOGENE
Dusp1 DUAL SPECIFICITY PHOSPHATASE 1
Nr4a1 NUCLEAR RECEPTOR SUBFAMILY 4, GROUP A, MEMBER 1

KEGG_PATHWAY WNT signaling pathway
Wnt4 WINGLESS-RELATED MMTV INTEGRATION SITE 4
Fzd1 FRIZZLED HOMOLOG 1 (DROSOPHILA)
Sfrp2 SECRETED FRIZZLED-RELATED SEQUENCE PROTEIN 2
Fzd2 FRIZZLED HOMOLOG 2 (DROSOPHILA)
Myc MYELOCYTOMATOSIS ONCOGENE
Fosl1 FOS-LIKE ANTIGEN 1

Supplemmental Table 3.4. *Gene Ontology analysis of DIM-regulated genes, not affected by dex treatment*

GOTERM_CC_ALL extracellular matrix
Lox LYSYL OXIDASE
Col15a1 PROCOLLAGEN, TYPE XV
Ctgf CONNECTIVE TISSUE GROWTH FACTOR
Spp1 SECRETED PHOSPHOPROTEIN 1
Fn1 FIBRONECTIN 1
Ogn OSTEOGLYCIN

GOTERM_BP_ALL immune response
Isgf3g INTERFERON DEPENDENT POSITIVE ACTING TRANSCRIPTION FACTOR 3 GAMMA
Ccl9 CHEMOKINE (C-C MOTIF) LIGAND 9
Spp1 SECRETED PHOSPHOPROTEIN 1
Il1rl1 INTERLEUKIN 1 RECEPTOR-LIKE 1
Ifit3 INTERFERON-INDUCED PROTEIN WITH TETRATRICOPEPTIDE REPEATS 3
Ifit1 INTERFERON-INDUCED PROTEIN WITH TETRATRICOPEPTIDE REPEATS 1
Bcap31 B-CELL RECEPTOR-ASSOCIATED PROTEIN 31
Cfd COMPLEMENT FACTOR D (ADIPSIN)

KEGG_PATHWAY TGF-BETA SIGNALING PATHWAY
none

GOTERM_CC_ALL intracellular membrane-bound organelle
1110020P15Rik RIKEN CDNA 1110020P15 GENE
Fhl2 FOUR AND A HALF LIM DOMAINS 2
Slc25a10 SOLUTE CARRIER FAMILY 25 (MITOCHONDRIAL CARRIER, DICARBOXYLATE TRANSPORTER), MEMBER 10
Foxc2 FORKHEAD BOX C2
Mtx2 METAXIN 2
Hsd11b1 HYDROXYSTEROID 11-BETA DEHYDROGENASE 1
Cdc2a CELL DIVISION CYCLE 2 HOMOLOG A (S. POMBE)
Srebf1 STEROL REGULATORY ELEMENT BINDING FACTOR 1
Dhcr7 7-DEHYDROCHOLESTEROL REDUCTASE
Mrpl12 MITOCHONDRIAL RIBOSOMAL PROTEIN L12
Alas1 AMINOLEVULINIC ACID SYNTHASE 1
Ormdl3 ORM1-LIKE 3 (S. CEREVISIAE)
Hspa5 HEAT SHOCK 70KD PROTEIN 5 (GLUCOSE-REGULATED PROTEIN)
Irx3 IROQUOIS RELATED HOMEOBOX 3 (DROSOPHILA)
Apoc1 APOLIPOPROTEIN C-I
Lipe LIPASE, HORMONE SENSITIVE
S100a6 S100 CALCIUM BINDING PROTEIN A6 (CALCYCLIN)

Kif20a KINESIN FAMILY MEMBER 20A
Mrpl51 MITOCHONDRIAL RIBOSOMAL PROTEIN L51
Isgf3g INTERFERON DEPENDENT POSITIVE ACTING TRANSCRIPTION FACTOR 3 GAMMA
Ogdh OXOGLUTARATE DEHYDROGENASE (LIPOAMIDE)
Acadm ACETYL-COENZYME A DEHYDROGENASE, MEDIUM CHAIN
Gnpat GLYCERONEPHOSPHATE O-ACYLTRANSFERASE
Dbi DIAZEPAM BINDING INHIBITOR
Cdc45l CELL DIVISION CYCLE 45 HOMOLOG (S. CEREVISIAE)-LIKE
Ndufc1 NADH DEHYDROGENASE (UBIQUINONE) 1, SUBCOMPLEX UNKNOWN, 1
Scd1 STEAROYL-COENZYME A DESATURASE 1
Txndc14 THIOREDOXIN DOMAIN CONTAINING 14
Uqcr UBIQUINOL-CYTOCHROME C REDUCTASE (6.4KD) SUBUNIT
Thrsp THYROID HORMONE RESPONSIVE SPOT14 HOMOLOG (RATTUS)
Nr4a2 NUCLEAR RECEPTOR SUBFAMILY 4, GROUP A, MEMBER 2
Bckdhb BRANCHED CHAIN KETOACID DEHYDROGENASE E1, BETA POLYPEPTIDE
Atp5o ATP SYNTHASE, H+ TRANSPORTING, MITOCHONDRIAL F1 COMPLEX, O SUBUNIT
Zfp36l2 ZINC FINGER PROTEIN 36, C3H TYPE-LIKE 2
Nr1h3 NUCLEAR RECEPTOR SUBFAMILY 1, GROUP H, MEMBER 3
Psma1 PROTEASOME (PROSOME, MACROPAIN) SUBUNIT, ALPHA TYPE 1
Sdhd SUCCINATE DEHYDROGENASE COMPLEX, SUBUNIT D, INTEGRAL MEMBRANE PROTEIN
BC054059 CDNA SEQUENCE BC054059
Ndufa9 NADH DEHYDROGENASE (UBIQUINONE) 1 ALPHA SUBCOMPLEX, 9
Hibadh 3-HYDROXYISOBUTYRATE DEHYDROGENASE
Ifitm3 INTERFERON INDUCED TRANSMEMBRANE PROTEIN 3
Chchd3 COILED-COIL-HELIX-COILED-COIL-HELIX DOMAIN CONTAINING 3
Pcna PROLIFERATING CELL NUCLEAR ANTIGEN
App AMYLOID BETA (A4) PRECURSOR PROTEIN
Dlx2 DISTAL-LESS HOMEOBOX 2
Ogn OSTEOGLYCIN
Gstz1 GLUTATHIONE TRANSFERASE ZETA 1 (MALEYLACETOACETATE ISOMERASE)
Cox6a1 CYTOCHROME C OXIDASE, SUBUNIT VI A, POLYPEPTIDE 1
Ddit3 DNA-DAMAGE INDUCIBLE TRANSCRIPT 3
Rab9 RAB9, MEMBER RAS ONCOGENE FAMILY
Wee1 WEE 1 HOMOLOG (S. POMBE)
Mdh2 MALATE DEHYDROGENASE 2, NAD (MITOCHONDRIAL)
Dgat1 DIACYLGLYCEROL O-ACYLTRANSFERASE 1
Ak2 ADENYLATE KINASE 2
Coq5 COENZYME Q5 HOMOLOG, METHYLTRANSFERASE (YEAST)
Nola3 NUCLEOLAR PROTEIN FAMILY A, MEMBER 3
Cox7a2 CYTOCHROME C OXIDASE, SUBUNIT VIIA 2
Klf6 KRUPPEL-LIKE FACTOR 6
Ptgs2 PROSTAGLANDIN-ENDOPEROXIDE SYNTHASE 2
Trib3 INDUCED IN FATTY LIVER DYSTROPHY 2
Mcm4 MINICHROMOSOME MAINTENANCE DEFICIENT 4 HOMOLOG (S. CEREVISIAE)
Mgst1 MICROSOMAL GLUTATHIONE S-TRANSFERASE 1
Midn MIDNOLIN
Aco2 ACONITASE 2, MITOCHONDRIAL
Cox7b CYTOCHROME C OXIDASE SUBUNIT VIIB
Hsd17b12 HYDROXYSTEROID (17-BETA) DEHYDROGENASE 12
Psen2 PRESENILIN 2
Herpud1 HOMOCYSTEINE-INDUCIBLE, ENDOPLASMIC RETICULUM STRESS-INDUCIBLE, UBIQUITIN-LIKE DOMAIN MEMBER 1
Mosc2 MOCO SULPHURASE C-TERMINAL DOMAIN CONTAINING 2
Pcx PYRUVATE CARBOXYLASE
Hmga2 HIGH MOBILITY GROUP AT-HOOK 2

Cs CITRATE SYNTHASE
Dld DIHYDROLIPOAMIDE DEHYDROGENASE
Xbp1 X-BOX BINDING PROTEIN 1
Tcf19 RIKEN CDNA 5730403J10 GENE
Ctsl CATHEPSIN L
Uqcrh UBIQUINOL-CYTOCHROME C REDUCTASE HINGE PROTEIN
Nol5a NUCLEOLAR PROTEIN 5A
Top2a TOPOISOMERASE (DNA) II ALPHA
Suclg1 SUCCINATE-COA LIGASE, GDP-FORMING, ALPHA SUBUNIT
Pcyox1 PRENYLCYSTEINE OXIDASE 1
Prrx2 PAIRED RELATED HOMEOBOX 2
Hipk2 HOMEODOMAIN INTERACTING PROTEIN KINASE 2
Adipoq ADIPONECTIN, C1Q AND COLLAGEN DOMAIN CONTAINING
Grpel1 GRPE-LIKE 1, MITOCHONDRIAL
Pttg1ip EXPRESSED SEQUENCE AI314311
Acsl1 ACYL-COA SYNTHETASE LONG-CHAIN FAMILY MEMBER 1
Slc25a25 SOLUTE CARRIER FAMILY 25 (MITOCHONDRIAL CARRIER, PHOSPHATE CARRIER), MEMBER 25
Timm23 TRANSLOCASE OF INNER MITOCHONDRIAL MEMBRANE 23 HOMOLOG (YEAST)
Pex11a PEROXISOMAL BIOGENESIS FACTOR 11A
Ndufb8 NADH DEHYDROGENASE (UBIQUINONE) 1 BETA SUBCOMPLEX 8
Sdhc SUCCINATE DEHYDROGENASE COMPLEX, SUBUNIT C, INTEGRAL MEMBRANE PROTEIN
Phlda1 PLECKSTRIN HOMOLOGY-LIKE DOMAIN, FAMILY A, MEMBER 1
Fdft1 FARNESYL DIPHOSPHATE FARNESYL TRANSFERASE 1
Sc4mol STEROL-C4-METHYL OXIDASE-LIKE
Bcap31 B-CELL RECEPTOR-ASSOCIATED PROTEIN 31
Uqcrq UBIQUINOL-CYTOCHROME C REDUCTASE, COMPLEX III SUBUNIT VII
Ndufb5 NADH DEHYDROGENASE (UBIQUINONE) 1 BETA SUBCOMPLEX, 5
Atf4 ACTIVATING TRANSCRIPTION FACTOR 4
Prnp PRION PROTEIN
Ccnb2 CYCLIN B2
2010100O12Rik RIKEN CDNA 2010100O12 GENE
Junb JUN-B ONCOGENE

GOTERM_CC_ALL mitochondrion
1110020P15Rik RIKEN CDNA 1110020P15 GENE
Ak2 ADENYLATE KINASE 2
Uqcrh UBIQUINOL-CYTOCHROME C REDUCTASE HINGE PROTEIN
Slc25a10 SOLUTE CARRIER FAMILY 25 (MITOCHONDRIAL CARRIER, DICARBOXYLATE TRANSPORTER), MEMBER 10
Suclg1 SUCCINATE-COA LIGASE, GDP-FORMING, ALPHA SUBUNIT
Coq5 COENZYME Q5 HOMOLOG, METHYLTRANSFERASE (YEAST)
Mtx2 METAXIN 2
Bckdhb BRANCHED CHAIN KETOACID DEHYDROGENASE E1, BETA POLYPEPTIDE
Atp5o ATP SYNTHASE, H+ TRANSPORTING, MITOCHONDRIAL F1 COMPLEX, O SUBUNIT
Sdhd SUCCINATE DEHYDROGENASE COMPLEX, SUBUNIT D, INTEGRAL MEMBRANE PROTEIN
Mrpl12 MITOCHONDRIAL RIBOSOMAL PROTEIN L12
Alas1 AMINOLEVULINIC ACID SYNTHASE 1
Grpel1 GRPE-LIKE 1, MITOCHONDRIAL
Cox7a2 CYTOCHROME C OXIDASE, SUBUNIT VIIA 2
Acsl1 ACYL-COA SYNTHETASE LONG-CHAIN FAMILY MEMBER 1
Ndufa9 NADH DEHYDROGENASE (UBIQUINONE) 1 ALPHA SUBCOMPLEX, 9
Slc25a25 SOLUTE CARRIER FAMILY 25 (MITOCHONDRIAL CARRIER, PHOSPHATE CARRIER), MEMBER 25

Hibadh 3-HYDROXYISOBUTYRATE DEHYDROGENASE
Mgst1 MICROSOMAL GLUTATHIONE S-TRANSFERASE 1
Ndufb8 NADH DEHYDROGENASE (UBIQUINONE) 1 BETA SUBCOMPLEX 8
Timm23 TRANSLOCASE OF INNER MITOCHONDRIAL MEMBRANE 23 HOMOLOG (YEAST)
Lipe LIPASE, HORMONE SENSITIVE
Chchd3 COILED-COIL-HELIX-COILED-COIL-HELIX DOMAIN CONTAINING 3
Mrpl51 MITOCHONDRIAL RIBOSOMAL PROTEIN L51
Ogdh OXOGLUTARATE DEHYDROGENASE (LIPOAMIDE)
Sdhc SUCCINATE DEHYDROGENASE COMPLEX, SUBUNIT C, INTEGRAL MEMBRANE PROTEIN
Acadm ACETYL-COENZYME A DEHYDROGENASE, MEDIUM CHAIN
Aco2 ACONITASE 2, MITOCHONDRIAL
Cox7b CYTOCHROME C OXIDASE SUBUNIT VIIB
Gstz1 GLUTATHIONE TRANSFERASE ZETA 1 (MALEYLACETOACETATE ISOMERASE)
Dbi DIAZEPAM BINDING INHIBITOR
Cox6a1 CYTOCHROME C OXIDASE, SUBUNIT VI A, POLYPEPTIDE 1
Mosc2 MOCO SULPHURASE C-TERMINAL DOMAIN CONTAINING 2
Pcx PYRUVATE CARBOXYLASE
Uqcrq UBIQUINOL-CYTOCHROME C REDUCTASE, COMPLEX III SUBUNIT VII
Ndufb5 NADH DEHYDROGENASE (UBIQUINONE) 1 BETA SUBCOMPLEX, 5
Ndufc1 NADH DEHYDROGENASE (UBIQUINONE) 1, SUBCOMPLEX UNKNOWN, 1
Cs CITRATE SYNTHASE
Mdh2 MALATE DEHYDROGENASE 2, NAD (MITOCHONDRIAL)
Dld DIHYDROLIPOAMIDE DEHYDROGENASE
2010100O12Rik RIKEN CDNA 2010100O12 GENE
Uqcr UBIQUINOL-CYTOCHROME C REDUCTASE (6.4KD) SUBUNIT

SP_PIR_KEYWORDS lipid synthesis
Pcx PYRUVATE CARBOXYLASE
Dhcr7 7-DEHYDROCHOLESTEROL REDUCTASE
Scd1 STEAROYL-COENZYME A DESATURASE 1
Ptgs2 PROSTAGLANDIN-ENDOPEROXIDE SYNTHASE 2
Fdft1 FARNESYL DIPHOSPHATE FARNESYL TRANSFERASE 1
Tpi1 TRIOSEPHOSPHATE ISOMERASE 1
Fdps FARNESYL DIPHOSPHATE SYNTHETASE
Sc4mol STEROL-C4-METHYL OXIDASE-LIKE

SP_PIR_KEYWORDS nad
Impdh2 INOSINE 5'-PHOSPHATE DEHYDROGENASE 2
Sc4mol STEROL-C4-METHYL OXIDASE-LIKE
Ndufb5 NADH DEHYDROGENASE (UBIQUINONE) 1 BETA SUBCOMPLEX, 5
Ndufc1 NADH DEHYDROGENASE (UBIQUINONE) 1, SUBCOMPLEX UNKNOWN, 1
Ldha LACTATE DEHYDROGENASE A
Mdh2 MALATE DEHYDROGENASE 2, NAD (MITOCHONDRIAL)
Ugdh UDP-GLUCOSE DEHYDROGENASE
Dld DIHYDROLIPOAMIDE DEHYDROGENASE
Dhrs7b DEHYDROGENASE/REDUCTASE (SDR FAMILY) MEMBER 7B
Ndufa9 NADH DEHYDROGENASE (UBIQUINONE) 1 ALPHA SUBCOMPLEX, 9
Hibadh 3-HYDROXYISOBUTYRATE DEHYDROGENASE
Gpd1 GLYCEROL-3-PHOSPHATE DEHYDROGENASE 1 (SOLUBLE)
Ndufb8 NADH DEHYDROGENASE (UBIQUINONE) 1 BETA SUBCOMPLEX 8

GOTERM_BP_ALL glucose metabolic process
Pcx PYRUVATE CARBOXYLASE
Adipoq ADIPONECTIN, C1Q AND COLLAGEN DOMAIN CONTAINING
Ogdh OXOGLUTARATE DEHYDROGENASE (LIPOAMIDE)

Atf4 ACTIVATING TRANSCRIPTION FACTOR 4
Fabp5 FATTY ACID BINDING PROTEIN 5, EPIDERMAL
Ldha LACTATE DEHYDROGENASE A
Mdh2 MALATE DEHYDROGENASE 2, NAD (MITOCHONDRIAL)
Hibadh 3-HYDROXYISOBUTYRATE DEHYDROGENASE
Gpd1 GLYCEROL-3-PHOSPHATE DEHYDROGENASE 1 (SOLUBLE)
Tpi1 TRIOSEPHOSPHATE ISOMERASE 1
Taldo1 TRANSALDOLASE 1
Pfkl PHOSPHOFRUCTOKINASE, LIVER, B-TYPE

KEGG_PATHWAY OXIDATIVE PHOSPHORYLATION
1110020P15Rik RIKEN CDNA 1110020P15 GENE
Uqcrh UBIQUINOL-CYTOCHROME C REDUCTASE HINGE PROTEIN
Sdhc SUCCINATE DEHYDROGENASE COMPLEX, SUBUNIT C, INTEGRAL MEMBRANE PROTEIN
Cox7b CYTOCHROME C OXIDASE SUBUNIT VIIB
Atp5o ATP SYNTHASE, H+ TRANSPORTING, MITOCHONDRIAL F1 COMPLEX, O SUBUNIT
Cox6a1 CYTOCHROME C OXIDASE, SUBUNIT VI A, POLYPEPTIDE 1
Ndufb5 NADH DEHYDROGENASE (UBIQUINONE) 1 BETA SUBCOMPLEX, 5
Uqcrq UBIQUINOL-CYTOCHROME C REDUCTASE, COMPLEX III SUBUNIT VII
Ndufc1 NADH DEHYDROGENASE (UBIQUINONE) 1, SUBCOMPLEX UNKNOWN, 1
Sdhd SUCCINATE DEHYDROGENASE COMPLEX, SUBUNIT D, INTEGRAL MEMBRANE PROTEIN
Cox7a2 CYTOCHROME C OXIDASE, SUBUNIT VIIA 2
Ndufa9 NADH DEHYDROGENASE (UBIQUINONE) 1 ALPHA SUBCOMPLEX, 9
Ndufb8 NADH DEHYDROGENASE (UBIQUINONE) 1 BETA SUBCOMPLEX 8
Uqcr UBIQUINOL-CYTOCHROME C REDUCTASE (6.4KD) SUBUNIT

KEGG_PATHWAY CITRATE CYCLE (TCA CYCLE)
Pcx PYRUVATE CARBOXYLASE
Ogdh OXOGLUTARATE DEHYDROGENASE (LIPOAMIDE)
Sdhd SUCCINATE DEHYDROGENASE COMPLEX, SUBUNIT D, INTEGRAL MEMBRANE PROTEIN
Cs CITRATE SYNTHASE
Sdhc SUCCINATE DEHYDROGENASE COMPLEX, SUBUNIT C, INTEGRAL MEMBRANE PROTEIN
Mdh2 MALATE DEHYDROGENASE 2, NAD (MITOCHONDRIAL)
Dld DIHYDROLIPOAMIDE DEHYDROGENASE
Aco2 ACONITASE 2, MITOCHONDRIAL
Suclg1 SUCCINATE-COA LIGASE, GDP-FORMING, ALPHA SUBUNIT

GOTERM_BP_ALL programmed cell death
App AMYLOID BETA (A4) PRECURSOR PROTEIN
Bag3 BCL2-ASSOCIATED ATHANOGENE 3
Phlda1 PLECKSTRIN HOMOLOGY-LIKE DOMAIN, FAMILY A, MEMBER 1
Btg2 B-CELL TRANSLOCATION GENE 2, ANTI-PROLIFERATIVE
Foxc2 FORKHEAD BOX C2
Bcap31 B-CELL RECEPTOR-ASSOCIATED PROTEIN 31
Ddit3 DNA-DAMAGE INDUCIBLE TRANSCRIPT 3
Cdc2a CELL DIVISION CYCLE 2 HOMOLOG A (S. POMBE)
Psen2 PRESENILIN 2
Hipk2 HOMEODOMAIN INTERACTING PROTEIN KINASE 2
Spp1 SECRETED PHOSPHOPROTEIN 1
Hspa5 HEAT SHOCK 70KD PROTEIN 5 (GLUCOSE-REGULATED PROTEIN)
Trib3 INDUCED IN FATTY LIVER DYSTROPHY 2
Cidec CELL DEATH-INDUCING DFFA-LIKE EFFECTOR C

GOTERM_BP_ALL lipid metabolic process
Pdpn PODOPLANIN
Acadm ACETYL-COENZYME A DEHYDROGENASE, MEDIUM CHAIN
Fdft1 FARNESYL DIPHOSPHATE FARNESYL TRANSFERASE 1
Gnpat GLYCERONEPHOSPHATE O-ACYLTRANSFERASE
Sc4mol STEROL-C4-METHYL OXIDASE-LIKE
Tpi1 TRIOSEPHOSPHATE ISOMERASE 1
Fdps FARNESYL DIPHOSPHATE SYNTHETASE
Hsd11b1 HYDROXYSTEROID 11-BETA DEHYDROGENASE 1
Hsd17b12 HYDROXYSTEROID (17-BETA) DEHYDROGENASE 12
Pcx PYRUVATE CARBOXYLASE
Srebf1 STEROL REGULATORY ELEMENT BINDING FACTOR 1
Nr1h3 NUCLEAR RECEPTOR SUBFAMILY 1, GROUP H, MEMBER 3
Adipoq ADIPONECTIN, C1Q AND COLLAGEN DOMAIN CONTAINING
Dhcr7 7-DEHYDROCHOLESTEROL REDUCTASE
Scd1 STEAROYL-COENZYME A DESATURASE 1
Fabp5 FATTY ACID BINDING PROTEIN 5, EPIDERMAL
Ptgs2 PROSTAGLANDIN-ENDOPEROXIDE SYNTHASE 2
Acsl1 ACYL-COA SYNTHETASE LONG-CHAIN FAMILY MEMBER 1
Lipe LIPASE, HORMONE SENSITIVE

GOTERM_CC_ALL extracellular space
Xbp1 X-BOX BINDING PROTEIN 1
Saa3 SERUM AMYLOID A 3
Ctgf CONNECTIVE TISSUE GROWTH FACTOR
Ctsl CATHEPSIN L
Ramp3 RECEPTOR (CALCITONIN) ACTIVITY MODIFYING PROTEIN 3
Coq5 COENZYME Q5 HOMOLOG, METHYLTRANSFERASE (YEAST)
Bckdhb BRANCHED CHAIN KETOACID DEHYDROGENASE E1, BETA POLYPEPTIDE
Pcyox1 PRENYLCYSTEINE OXIDASE 1
Osmr ONCOSTATIN M RECEPTOR
Adipoq ADIPONECTIN, C1Q AND COLLAGEN DOMAIN CONTAINING
Sdhd SUCCINATE DEHYDROGENASE COMPLEX, SUBUNIT D, INTEGRAL MEMBRANE PROTEIN
Grpel1 GRPE-LIKE 1, MITOCHONDRIAL
Aoc3 AMINE OXIDASE, COPPER CONTAINING 3
Ptgs2 PROSTAGLANDIN-ENDOPEROXIDE SYNTHASE 2
Ndufa9 NADH DEHYDROGENASE (UBIQUINONE) 1 ALPHA SUBCOMPLEX, 9
Ndufb8 NADH DEHYDROGENASE (UBIQUINONE) 1 BETA SUBCOMPLEX 8
Apoc1 APOLIPOPROTEIN C-I
Cd164 CD164 ANTIGEN
Cfd COMPLEMENT FACTOR D (ADIPSIN)
Mrpl51 MITOCHONDRIAL RIBOSOMAL PROTEIN L51
Lox LYSYL OXIDASE
Pdpn PODOPLANIN
Il1rl1 INTERLEUKIN 1 RECEPTOR-LIKE 1
Thbs2 THROMBOSPONDIN 2
Mosc2 MOCO SULPHURASE C-TERMINAL DOMAIN CONTAINING 2
Col15a1 PROCOLLAGEN, TYPE XV
Camp CATHELICIDIN ANTIMICROBIAL PEPTIDE
Ccl9 CHEMOKINE (C-C MOTIF) LIGAND 9
Spp1 SECRETED PHOSPHOPROTEIN 1
Retn RESISTIN
9130213B05Rik RIKEN CDNA 9130213B05 GENE

KEGG_PATHWAY MAPK Sgnaling Pathway
none

KEGG_PATHWAY WNT signaling pathway
none

Chapter 3 Discussion

The steps involved in adipocyte formation have remained unresolved for the past two decades. To gain insight into this process, we used a reductionist approach with two related aims: first, to test the hypothesis that individual components of the DIM cocktail regulate discrete commitment states in the progression from preadipocyte to adipocyte; second, to assess at the molecular level the contributions of the individual components to adipogenesis. Through this approach we determined conditions for differentiation of 3T3-L1 preadipocytes that are independent of insulin addition, as previously demonstrated[75,76], or of shifting to growth medium supplemented with FBS. Our approach yielded a simpler, more direct model for inducible adipogenesis. Differentiation can be divided into two distinct stages induced by two signaling pathways acting sequentially, but non-commutatively. The initial phase is driven by glucocorticoid signaling and is followed by a second phase driven by cAMP signaling. The significance of the relationship between dex and IBMX in 3T3-L1 cells was recapitulated in C3H10T1/2 cells and in primary MSCs.

The current models of fat ontogenesis do not seem to account for the diversity of adipocyte phenotypes observed *in vivo* and are simplistic compared to the much better understood hematopoietic system[59,75]. In our experiments, we isolated the actions of glucocorticoid signaling during adipogenesis and found that pretreatment with dex primes preadipocytes to respond to IBMX and induces a gene expression profile intermediary between that of preadipocytes and adipocytes. Thus, glucocorticoid signaling appears to define a novel commitment state, the dex-primed preadipocyte. Although the physiological relevance of these findings remains to be determined, it is interesting that

patients exposed to excess glucocorticoids present with expansion of a subset of fat depots. Conceivably, certain adipose niches (*e.g.,* visceral fat depot) may be permissive for differentiation of dex-primed preadipocytes, whereas other fat depots may be insensitive to glucocorticoid-induced adipogenesis because they lack the permissive signals that advance dex-primed preadipocytes through the adipogenic program.

In contrast to the outcomes of dex pretreatment of preadipocytes, the increased cAMP signaling resulting from IBMX pretreatment of those cells results in a failure to differentiate upon subsequent dex treatment; these cells are also partially resistant to differentiation induced by the DIM cocktail. Recently, Madsen *et al.* linked increased cAMP signaling in mouse liver and adipose tissues, induced by high-protein diet, to prevention of polyunsaturated fatty acid-induced adipogenesis and obesity[66]. These findings indicate that, in contrast to glucocorticoids, stimulation of cAMP signaling in preadipocytes fails to induce progression toward the adipocyte fate. On the contrary, it seems that IBMX drives preadipocytes toward a state that is off of the adipogenic pathway, but that does not represent a terminal differentiation fate. Accordingly, we found that IBMX-pretreated preadipocytes can differentiate into adipocytes if treated with dex for 48 h followed by IBMX for another 48 h (Supplemental Figure 3.1). Hence, dex signaling acts dominantly to cAMP signaling to return IBMX-treated preadipocytes to the adipogenesis pathway.

Thus, we suggest that glucocorticoids and cAMP appear to regulate adipogenesis independently by directing preadipocytes toward two cellular states. Dex-primed preadipocytes are on-pathway toward the adipocyte fate; IBMX-treated preadipocytes are off-pathway and differentiate efficiently only if brought back to the adipogenic pathway

by dex signaling. These two observations suggest a simple way by which adipogenesis can be spatially and temporally compartmentalized during development, normal adult life and in disease states. Specifically, preadipocytes may integrate order, intensity (e.g. dose of glucocorticoid) and duration of adipogenic signals to adopt distinct cellular states, along an adipogenesis axis, that differ in their sensitivity to further stimulation.

Adipocytes differentiated by treatment with dex followed by IBMX were less sensitive to induction of lipolysis by the b-adrenergic agonist isoproterenol when compared to DIM-differentiated adipocytes (Figures 3.4B). Interestingly, we found that this phenotype correlated with decreased levels of the lipid droplet protein perilipin A on dex-IBMX adipocytes when compared to DIM-differentiated adipocytes (Supplemental Figure 3.3B). Perilipin A is thought to influence adipocyte triglyceride storage through a mechanism that is dependent on its expression levels and phosphorylation state [19,20]. When unphosphorylated, perilipin A protects lipid droplets from the activity of cellular lipases and promotes triglyceride storage. Upon isoproterenol stimulation perilipin A is phosphorylated and promotes lipolysis through association with hormone-sensitive lipase on the surface of lipid droplets. Hence, the lower levels of perilipin A on dex-IBMX adipocytes may explain the lower sensitivity of these cells to isoproterenol-stimulated lipolysis.

In addition to being less responsive to the lipolytic effect of isoproterenol, dex-IBMX 3T3-L1 adipocytes stored less triglyceride and expressed lower leptin mRNA levels (Figure 3.4C and Supplemental Figure 3.3A). The triglyceride storage phenotype could reflect the absence of insulin-dependent activation of cyclic AMP response element binding protein (CREB), which in turn stimulates triglyceride accumulation in 3T3-L1

adipocytes. Additionally, it is consistent with clinical studies showing that excess circulating insulin levels are associated with larger subcutaneous adipocytes. The insulin sensitivity and basal rates of lipolysis of dex-IBMX adipocytes, however, were similar to DIM-differentiated adipocytes. These results indicate that selected aspects of adipocyte metabolic function can be tuned by the mode of differentiation to which preadipocytes are subjected. In an interesting parallel, the human visceral fat depot displays higher rates of catecholamine-induced lipolysis and expresses lower levels of leptin relative to the subcutaneous white fat depots[77,78]. The similarities between our cell culture results and the diversity of adipocytes in human subjects suggest a clear path for discerning the mechanisms that contribute to the final metabolic phenotype of adipose tissue. Importantly, the differences in expression of perilipin A suggest that its regulation might be part of the mechanism through which hormone-induced adipocyte metabolic diversity is generated.

We applied a candidate approach to infer the mechanism by which the order of exposure to dex and IBMX alters the adipogenesis signal. We found that relative to DIM treatment, IBMX-dex treated cells displayed delayed expression of C/EBPδ and did not substantially increase the protein levels of C/EBPα and PPARγ. Our findings suggest that early expression of C/EBPδ is required for efficient induction of C/EBPα and PPARγ. To explore additional mechanisms underlying the failure of IBMX-dex treatment to induce differentiation, we monitored Pref-1, whose repression by glucocorticoids is necessary for efficient adipogenesis of 3T3-L1 preadipocytes. We found that dex-IBMX treatment indeed represses Pref-1, whereas pretreatment with IBMX prevents stable repression of Pref-1 by dex. These results suggest a mechanism by which preadipocytes sense the order

of exposure to dex and IBMX and underscore a role of Pref-1 as a molecular gatekeeper of adipogenesis. In related studies, Feldman *et al.*[79] identified an adipogenesis role for a glucocorticoid receptor target gene, the TGFb family member myostatin (MSTN). Remarkably, C3H10T1/2 adipocytes differentiated by substitution of dex with MSTN and adipocytes of mice expressing MSTN in adipose tissue are smaller, more insulin sensitive and seem to be immature when compared to WT adipocytes. It will be interesting to determine the relationship of those "myostatin adipocytes" to the dex-primed preadipocytes described in our work.

In summary, by temporally uncoupling the signals that comprise the DIM cocktail, we discovered complex interactions of dex and IBMX during adipogenesis in cell culture that may enrich our understanding of the process and its regulation as played out in intact mammalian organisms. Our results, and those of Feldman *et al.,* imply that an array of intermediate cell types, perhaps reminiscent of those known in hematopoiesis, may punctuate cell fate pathways radiating from mesenchymal stem cells, and in particular proceeding toward mature adipocytes. The distinct metabolic capabilities of dex-IBMX adipocytes compared to DIM adipocytes may reflect a mechanism by which adipogenesis can be fine-tuned spatially, temporally and functionally to generate the diversity of adipocyte phenotypes described *in vivo*. In this context, it is intriguing that Pref-1 may, under certain circumstances, act as a sensor of glucocorticoid and cyclic AMP activities, ensuring that preadipocytes advance to differentiation only if a predetermined series of signaling events occurs in the correct order.

Acknowledgments

We thank the members of the Yamamoto lab for discussions and reagents, and Kaveh Ashrafi, Brian Black, Eric Bolton, Brian Feldman, Tony Gerber, Marlisa Pillsbury and Wally Wang for insightful comments on the manuscript. Primary mouse mesenchymal stem cells were generously provided by Brian Feldman. This work was supported by predoctoral fellowship 0515044Y and 0715058Y of the American Heart Association to C.P. and research grant CA020535 from NIH to K.R.Y..

Perspectives

Our work explored the question of how structurally simple steroid hormones coordinate complex and diverse physiological programs across multiple tissues. We propose that GR output diversity is directly related to the diversity of GR inputs. Inputs that modify GR, or the cellular state are integrated by GR to generate outputs that are variable and adaptable. Examples of inputs are: ligand, DNA, GR post-translational modifications, chromatin states, complement of transcriptional regulatory factors and co-modulators, expression of genes that affect a given GR output, etc. Typical outputs are: chromatin remodeling, modulation of target gene expression[12], gluconeogenesis and lipolysis induction[80,81], ECM remodeling[82], anti-inflammation, inhibition or promotion of cellular differentiation, cell cycle arrest[83,84], apoptosis[85], etc.

We characterized input-output relationships in cascades initiated by glucocorticoids in three contexts. First, we showed that the ligand itself is a regulatory input that impacts GR function and physiological output. Second, we determined that IL-13 and adipogenic signals modify GR responses to generate complex outputs. Finally, we studied the regulation of genes that act downstream of glucocorticoids and IL-13 to mediate physiological responses.

Our studies with non-steroidal arylpyrazole ligands revealed that changes in GR ligand structure affect GR transcriptional outputs. Ligand structure also affected GR outputs across cellular types. In fact, we found arylpyrazole ligands that induced adipogenesis, but failed to inhibit osteogenesis[83]. Studies parallel to ours have also characterized steroidal and non-steroidal selective GR modulators that display gene-specific effects and

might dissociate anti-inflammatory activities from adverse effects *in vivo*[86-90]. Miner et al.[91,92] characterized compound LGD5552. LGD5552 inhibits inflammation in an arthritis mouse model with efficacy comparable to prednisolone, but it does not induce a series of other adverse effects that include bone inhibition, adipose tissue formation, and hypertension. Our results and those of Miner et al. highlight the plasticity of GR as a signal transducer and hint at the possibility of undiscovered physiological ligands.

Cellular assays that are related to GR physiological outputs were crucial for the discovery of dissociating GR ligands. Ma et al.[93]applied this paradigm to the vitamin D receptor (VDR). These investigators identified nonsecosteroidal VDR ligands that were weaker agonists in intestinal cells when compared to epithelial cells. When tested *in vivo* these compounds dissociated the hypercalcemic activities of VDR from its effects in epithelial cell proliferation. Parallel studies have identified non-calcemic derivatives of the bile acid VDR ligand lithocholic acid that may be clinically useful[94-96]. Future investigation will be necessary to determine if additional members of the nuclear hormone receptor family have evolved the ability to display ligand-selective responses.

We found that the duration and magnitude of ligand stimulation also affect GR-dependent physiological outcomes. Dexamethasone treatment of 3T3-L1 cells for 2h induces significant transcriptional changes. However, this treatment does not induce adipogenesis. Dexamethasone must signal for 36h for preadipocytic populations to be fully primed to differentiate into adipocytes[84]. Similarly, Gruber et al. reported that dexamethasone-induced apoptosis of acute lymphocytic leukemia cells only reaches its peak after 72h of treatment[97]. Dexamethasone concentration and receptor levels also contributed to determine the percentage of cells that activated apoptotic programs.

Together these studies highlight the complex interaction between signals (GR levels, ligand concentration, and duration of treatment) that vary in a continuum, and phenotypes (differentiation and apoptosis) that exist as discrete states.

It has been suggested that the intrinsic noise, stochasticity and non-linear dynamics of gene regulatory networks contribute to transcriptional output determination and ultimately cell fate[98-100]. The dynamic and kinetic parameters of GR transcriptional networks have been determined for a single gene using single cell measurements[101,102], and genomewide for whole populations of cells[103]. Importantly, GR turnover during recruitment to an endogenous GRE is fast (half-life of 4s)[101]. Studies with endogenous glucocorticoids show that ligand binding also appears to occur cyclically, with a turnover of approximately 10 minutes[102]. It is still unknown how these different cycles are integrated by GR to generate transcriptional and physiological outputs that are accurate and robust. Future studies measuring whole gene networks in single cells will be necessary to generate quantitative models of how GR controls circuits that affect cellular decisions and ultimately tissue function.

The diversity of glucocorticoid-induced phenotypes is also dependent on interactions with non-glucocorticoid signaling pathways. We examined this mechanism of regulation of GR activity in 3T3-L1 preadipocytes and human bronchoepithelial cells. 3T3-L1 cells differentiate into adipocytes if treated simultaneously for 48h with dexamethasone, FBS, cAMP, and insulin[63]. We discovered that temporal uncoupling of dexamethasone and cAMP signals removes the need for insulin or FBS signaling, if dexamethasone signals first. Additionally, prior cAMP signaling in isolation inhibits adipogenesis induced by a differentiation cocktail that contains dexamethasone. Furthermore, adipocytes

differentiated by sequential treatment with dexamethasone and cAMP are metabolically different from those differentiated by simultaneous treatment with all four signals[84]. These results show that when glucocorticoids participate in adipogenesis induction at least two phenotypic outcomes are possible.

In parallel studies, we investigated the regulation of the human asthma marker genes POSTN, CLCA1 and SERPINB2 by glucocorticoids in human bronchoepithelial cells. We found that IL-13 induced POSTN, CLCA1 and SERPINB2 in primary human bronchoepithelial cells. Treatment with dexamethasone or budesonide inhibited the expression levels of asthma genes in these cells, consistent with their therapeutic activities in asthma control. Woodruff et al.[104] revisited these findings and found that asthmatic patients can be divided in two groups based on the levels of POSTN, CLCA1 and SERPINB2. High levels of POSTN, CLCA1 and SERPINB2 define asthmatic patients with a Th2-high gene signature that are glucocorticoid responsive. Conversely, asthmatic patients that present low POSTN, CLCA1 and SERPINB2 are Th2-low and do not respond to glucocorticoid therapy.

Our experiments in preadipocytes and bronchoepithelial cells highlight the fact that cellular type is not the sole determinant of outcome of glucocorticoid treatment in a particular tissue. Additional signals, and likely additional cell types in a tissue, interact with and may be required for glucocorticoid hormones to produce a complete repertoire of responses. Consequently, more specific glucocorticoid therapies might require modulation of non-glucocorticoid signaling pathways that selectively affect GR-controlled physiological outputs. Gerber et al.[105] recently applied this principle to identify

non-GR ligand, gene-selective GR modulators. These compounds do not bind the GR LBD, but still affect GR activity to generate gene- and tissue-specific responses.

The primary target genes and associated GREs that mediate the downstream effects of GR signaling remain for the most part unidentified. Currently, it is not known if the complex responses orchestrated by GR are effected by the thousands of genes normally affected by glucocorticoid treatment, or if more restricted gene networks are the core mediators of responses. Our work combined genomewide studies and functional assays to identify genes that mediate glucocorticoid responses in bronchoepithelial cells and preadipocytes.

Woodruff et al.[48] designed a genomewide clinical study that identified bronchoepithelial cell genes that were increased in asthmatic patients when compared to control subjects, and repressed by glucocorticoid therapy. Surprisingly, SERPINB2, CLCA1, and POSTN were the only genes that fit these criteria. CLCA1 and POSTN were previously implicated in asthma pathogenesis[55,106-108]. SERPINB2 was a novel asthma candidate gene. The pre-treatment levels of these asthma marker genes were positively correlated to the clinical response to inhaled glucocorticoid treatment. Likely, SERPINB2, CLCA1, and POSTN mediate the therapeutic responses of glucocorticoids and may themselves be relevant drug targets.

Our results studying the regulation of SERPINB2, CLCA1, and POSTN in primary human bronchoepithelial cells in cell culture suggest that the regulatory events that promote gene regulation in the asthmatic patients' lungs are similar to what we observed in cell culture. Interestingly, the kinetics of gene regulation of SERPINB2, CLCA1, and

POSTN was delayed when compared to typical primary targets of IL-13 and glucocorticoid signaling. Moreover, we could not detect GREs or STAT6 response elements proximal to the promoters of these genes. Possibly, secondary or tertiary target genes of GR and STAT6 regulate SERPINB2, CLCA1, and POSTN. If this hypothesis is correct the slower kinetics of SERPINB2, CLCA1, and POSTN gene activation and repression may be a consequence of gene network topology. Conceivably, the hierarchical level at which GR regulates gene networks may affect kinetic and dynamic parameters associated with disease development and therapeutic efficacy.

The preadipocyte-specific gene Pref-1 is an inhibitor of adipogenesis that is transcriptionally repressed by glucocorticoid treatment[74,109]. We found that sequential treatment of preadipocytes with dexamethasone followed by the cAMP activator IBMX led to efficient repression of Pref-1 transcription. However, pretreatment of preadipocytes with IBMX prevented the stable repression of Pref-1 by glucocorticoid treatment. These results indicate that Pref-1 is a GR target gene involved in adipogenesis and suggest a mechanism through which GR participates in the wiring of logic gates that control cell fate decisions. Specifically, preadipocytes may integrate order, intensity (e.g. dose of glucocorticoid) and duration of adipogenic signals to adopt cellular states, along an adipogenesis axis, that display various degrees of sensitivity to further stimulation.

Our studies have explored the mechanisms through which signaling specificity and diversity are generated and maintained in GR-controlled physiological programs. Collectively, our results suggest a model in which GR activity is modulated by several inputs that contribute to the fidelity, accuracy, and diversity of GR mediated responses. We discovered that GR induces a novel commitment state during adipogenesis and that

the GR regulated gene Pref-1 acts downstream of GR to control this decision. We also characterized the regulation of human asthma genes by GR and identified GR ligands that regulate these genes but do not inhibit osteogenesis. Importantly, our work suggests that the exploration of GR ligand chemical space and non-glucocorticoid signaling pathways are clear avenues for the development of more specific GR-based therapies.

Bibliography

1. Williams, R. *Williams textbook of endocrinology.* (Saunders: Philadelphia Pa., 2003).

2. Stewart, P. & Krozowski, Z. 11 beta-Hydroxysteroid dehydrogenase. *Vitam Horm* **57**, 249-324 (1999).

3. Seckl, J.R., Morton, N.M., Chapman, K.E. & Walker, B.R. Glucocorticoids and 11beta-hydroxysteroid dehydrogenase in adipose tissue. *Recent Prog. Horm. Res* **59**, 359-393 (2004).

4. Geerling, J.C. & Loewy, A.D. Aldosterone in the brain. *Am. J. Physiol. Renal Physiol* **297**, F559-576 (2009).

5. Morton, N.M. & Seckl, J.R. 11beta-hydroxysteroid dehydrogenase type 1 and obesity. *Front Horm Res* **36**, 146-164 (2008).

6. Beck, I.M.E. et al. Crosstalk in inflammation: the interplay of glucocorticoid receptor-based mechanisms and kinases and phosphatases. *Endocr. Rev* **30**, 830-882 (2009).

7. Suino-Powell, K. et al. Doubling the size of the glucocorticoid receptor ligand binding pocket by deacylcortivazol. *Mol. Cell. Biol* **28**, 1915-1923 (2008).

8. Madauss, K.P. et al. The first X-ray crystal structure of the glucocorticoid receptor bound to a non-steroidal agonist. *Bioorg. Med. Chem. Lett* **18**, 6097-6099 (2008).

9. Kauppi, B. et al. The three-dimensional structures of antagonistic and agonistic forms of the glucocorticoid receptor ligand-binding domain: RU-486 induces a transconformation that leads to active antagonism. *J. Biol. Chem* **278**, 22748-22754 (2003).

10. Bledsoe, R.K. et al. Crystal structure of the glucocorticoid receptor ligand binding domain reveals a novel mode of receptor dimerization and coactivator recognition. *Cell* **110**, 93-105 (2002).

11. Kian Tee, M. et al. Estradiol and selective estrogen receptor modulators differentially regulate target genes with estrogen receptors alpha and beta. *Mol Biol Cell* **15**, 1262-72 (2004).

12. So, A., Chaivorapol, C., Bolton, E., Li, H. & Yamamoto, K. Determinants of cell- and gene-specific transcriptional regulation by the glucocorticoid receptor. *PLoS Genet* **3**, e94 (2007).

13. Reddy, T.E. et al. Genomic determination of the glucocorticoid response reveals unexpected mechanisms of gene regulation. *Genome Res* (2009).doi:10.1101/gr.097022.109

14. Yamamoto, K. Multilayered control of intracellular receptor function. *Harvey Lect* **91**, 1-19 (1995).

15. Meijsing, S.H. et al. DNA binding site sequence directs glucocorticoid receptor structure and activity. *Science* **324**, 407-410 (2009).

16. Schäcke, H., Döcke, W.D. & Asadullah, K. Mechanisms involved in the side effects of glucocorticoids. *Pharmacol. Ther* **96**, 23-43 (2002).

17. Newton, R. & Holden, N.S. Separating transrepression and transactivation: a distressing divorce for the glucocorticoid receptor? *Mol. Pharmacol* **72**, 799-809 (2007).

18. Yamamoto, K. Steroid receptor regulated transcription of specific genes and gene networks. *Annu Rev Genet* **19**, 209-52 (1985).

19. Jordan, V. The secrets of selective estrogen receptor modulation: cell-specific coregulation. *Cancer Cell* **1**, 215-7 (2002).

20. Shang, Y. & Brown, M. Molecular determinants for the tissue specificity of SERMs. *Science* **295**, 2465-8 (2002).

21. Nicolaou, K.C. et al. Discovery and optimization of non-steroidal FXR agonists from natural product-like libraries. *Org. Biomol. Chem* **1**, 908-920 (2003).

22. Rosen, J. & Miner, J. The Search for Safer Glucocorticoid Receptor Ligands. *Endocr Rev* (2005).at <http://www.ncbi.nlm.nih.gov/entrez/query.fcgi?cmd=Retrieve&db=PubMed&dopt=Citation&list_uids=15814846>

23. Schafer, S.C. Dexamethasone suppresses eNOS and CAT-1 and induces oxidative stress in mouse resistance arterioles. *AJP: Heart and Circulatory Physiology* **288**, H436-H444 (2004).

24. Wallerath, T. et al. Down-regulation of the expression of endothelial NO synthase is likely to contribute to glucocorticoid-mediated hypertension. *Proc. Natl. Acad. Sci. U.S.A* **96**, 13357-13362 (1999).

25. Wallerath, T. et al. Dexamethasone lacks effect on blood pressure in mice with a disrupted endothelial NO synthase gene. *Nitric Oxide* **10**, 36-41 (2004).

26. Shah, N. & Scanlan, T. Design and evaluation of novel nonsteroidal dissociating glucocorticoid receptor ligands. *Bioorg Med Chem Lett* **14**, 5199-203 (2004).

27. Crouch, S.P., Kozlowski, R., Slater, K.J. & Fletcher, J. The use of ATP bioluminescence as a measure of cell proliferation and cytotoxicity. *J. Immunol. Methods* **160**, 81-88 (1993).

28. Luppen, C.A. et al. Brief bone morphogenetic protein 2 treatment of glucocorticoid-inhibited MC3T3-E1 osteoblasts rescues commitment-associated cell cycle and

mineralization without alteration of Runx2. *J. Biol. Chem* **278**, 44995-45003 (2003).

29. Leclerc, N. Gene expression profiling of glucocorticoid-inhibited osteoblasts. *Journal of Molecular Endocrinology* **33**, 175-193 (2004).

30. Wang, J. et al. Chromatin immunoprecipitation (ChIP) scanning identifies primary glucocorticoid receptor target genes. *Proc Natl Acad Sci U S A* **101**, 15603-8 (2004).

31. Ito, K., Barnes, P. & Adcock, I. Glucocorticoid receptor recruitment of histone deacetylase 2 inhibits interleukin-1beta-induced histone H4 acetylation on lysines 8 and 12. *Mol Cell Biol* **20**, 6891-903 (2000).

32. Luecke, H. & Yamamoto, K. The glucocorticoid receptor blocks P-TEFb recruitment by NFkappaB to effect promoter-specific transcriptional repression. *Genes Dev* **19**, 1116-27 (2005).

33. Chow, Y.H., Wang, Y., Plumb, J., O'Brodovich, H. & Hu, J. Hormonal regulation and genomic organization of the human amiloride-sensitive epithelial sodium channel alpha subunit gene. *Pediatr. Res* **46**, 208-214 (1999).

34. Nissen, R.M. The glucocorticoid receptor inhibits NFkappa B by interfering with serine-2 phosphorylation of the RNA polymerase II carboxy-terminal domain. *Genes & Development* **14**, 2314-2329 (2000).

35. Wang, H.C. et al. Oxidative stress disrupts glucocorticoid hormone-dependent transcription of the amiloride-sensitive epithelial sodium channel alpha-subunit in lung epithelial cells through ERK-dependent and thioredoxin-sensitive pathways. *J. Biol. Chem* **275**, 8600-8609 (2000).

36. Alheim, K. Identification of a functional glucocorticoid response element in the promoter of the cyclin-dependent kinase inhibitor p57Kip2. *Journal of Molecular Endocrinology* **30**, 359-368 (2003).

37. Jordan, V.C. Selective estrogen receptor modulation: concept and consequences in cancer. *Cancer Cell* **5**, 207-213 (2004).

38. Lefstin, J. & Yamamoto, K. Allosteric effects of DNA on transcriptional regulators. *Nature* **392**, 885-8 (1998).

39. Stafford, J., Wilkinson, J., Beechem, J. & Granner, D. Accessory factors facilitate the binding of glucocorticoid receptor to the phosphoenolpyruvate carboxykinase gene promoter. *J Biol Chem* **276**, 39885-91 (2001).

40. Diamond, M., Miner, J., Yoshinaga, S. & Yamamoto, K. Transcription factor interactions: selectors of positive or negative regulation from a single DNA element. *Science* **249**, 1266-1272 (1990).

41. Miner, J. & Yamamoto, K. Regulatory crosstalk at composite response elements. *Trends Biochem Sci* **16**, 423-6 (1991).

42. Leung, T., Hoffmann, A. & Baltimore, D. One nucleotide in a kappaB site can determine cofactor specificity for NF-kappaB dimers. *Cell* **118**, 453-64 (2004).

43. Rogatsky, I. et al. Target-specific utilization of transcriptional regulatory surfaces by the glucocorticoid receptor. *Proc Natl Acad Sci U S A* **100**, 13845-50 (2003).

44. Janderová, L., McNeil, M., Murrell, A.N., Mynatt, R.L. & Smith, S.R. Human mesenchymal stem cells as an in vitro model for human adipogenesis. *Obes. Res* **11**, 65-74 (2003).

45. Stanton, L., Sabari, S., Sampaio, A.V., Underhill, T.M. & Beier, F. p38 MAP kinase signalling is required for hypertrophic chondrocyte differentiation. *Biochem. J* **378**, 53-62 (2004).

46. Rayasam, G.V. et al. Ligand-Specific Dynamics of the Progesterone Receptor in Living Cells and during Chromatin Remodeling In Vitro. *Molecular and Cellular Biology* **25**, 2406-2418 (2005).

47. Lou, D.Y. Three Amino Acid Substitutions Selectively Disrupt the Activation but Not the Repression Function of the Glucocorticoid Receptor N Terminus. *Journal of Biological Chemistry* **272**, 4149-4156 (1997).

48. Woodruff, P.G. et al. From the Cover: Genome-wide profiling identifies epithelial cell genes associated with asthma and with treatment response to corticosteroids. *Proceedings of the National Academy of Sciences* **104**, 15858-15863 (2007).

49. Fulcher, M.L., Gabriel, S., Burns, K.A., Yankaskas, J.R. & Randell, S.H. Well-differentiated human airway epithelial cell cultures. *Methods Mol. Med* **107**, 183-206 (2005).

50. Dolganov, G.M. et al. A novel method of gene transcript profiling in airway biopsy homogenates reveals increased expression of a Na+-K+-Cl- cotransporter (NKCC1) in asthmatic subjects. *Genome Res* **11**, 1473-1483 (2001).

51. Vandesompele, J. et al. Accurate normalization of real-time quantitative RT-PCR data by geometric averaging of multiple internal control genes. *Genome Biol* **3**, RESEARCH0034 (2002).

52. Wagers, S.S. et al. Extravascular fibrin, plasminogen activator, plasminogen activator inhibitors, and airway hyperresponsiveness. *J. Clin. Invest* **114**, 104-111 (2004).

53. Evans, C.M., Kim, K., Tuvim, M.J. & Dickey, B.F. Mucus hypersecretion in asthma: causes and effects. *Curr Opin Pulm Med* **15**, 4-11 (2009).

54. Chen, Y., Nickola, T.J., DiFronzo, N.L., Colberg-Poley, A.M. & Rose, M.C. Dexamethasone-mediated repression of MUC5AC gene expression in human lung epithelial cells. *Am. J. Respir. Cell Mol. Biol* **34**, 338-347 (2006).

55. Takayama, G. et al. Periostin: A novel component of subepithelial fibrosis of

bronchial asthma downstream of IL-4 and IL-13 signals. *Journal of Allergy and Clinical Immunology* **118**, 98-104 (2006).

56. Ogden, C., Yanovski, S., Carroll, M. & Flegal, K. The epidemiology of obesity. *Gastroenterology* **132**, 2087-102 (2007).

57. Funahashi, T. & Matsuzawa, Y. Metabolic syndrome: clinical concept and molecular basis. *Ann Med* **39**, 482-94 (2007).

58. Farmer, S. Transcriptional control of adipocyte formation. *Cell Metab* **4**, 263-73 (2006).

59. Gesta, S., Tseng, Y. & Kahn, C. Developmental origin of fat: tracking obesity to its source. *Cell* **131**, 242-56 (2007).

60. Kondo, M. et al. Biology of hematopoietic stem cells and progenitors: implications for clinical application. *Annu Rev Immunol* **21**, 759-806 (2003).

61. Gesta, S. et al. Evidence for a role of developmental genes in the origin of obesity and body fat distribution. *Proc Natl Acad Sci U S A* **103**, 6676-81 (2006).

62. Tchkonia, T. et al. Identification of depot-specific human fat cell progenitors through distinct expression profiles and developmental gene patterns. *Am J Physiol Endocrinol Metab* **292**, E298-307 (2007).

63. Otto, T. & Lane, M. Adipose development: from stem cell to adipocyte. *Crit Rev Biochem Mol Biol* **40**, 229-42 (2005).

64. Fujikura, J. et al. Insulin-induced lipohypertrophy: report of a case with histopathology. *Endocr J* **52**, 623-8 (2005).

65. Rockall, A. et al. Computed tomography assessment of fat distribution in male and female patients with Cushing's syndrome. *Eur J Endocrinol* **149**, 561-7 (2003).

66. Madsen, L. et al. cAMP-dependent Signaling Regulates the Adipogenic Effect of n-6 Polyunsaturated Fatty Acids. *J Biol Chem* **283**, 7196-205 (2008).

67. Smyth, G. Linear models and empirical bayes methods for assessing differential expression in microarray experiments. *Stat Appl Genet Mol Biol* **3**, Article3 (2004).

68. Gentleman, R. et al. Bioconductor: open software development for computational biology and bioinformatics. *Genome Biol* **5**, R80 (2004).

69. Smyth, G. & Speed, T. Normalization of cDNA microarray data. *Methods* **31**, 265-73 (2003).

70. Burton, G., Nagarajan, R., Peterson, C. & McGehee, R. Microarray analysis of differentiation-specific gene expression during 3T3-L1 adipogenesis. *Gene* **329**, 167-85 (2004).

71. Bolstad, B., Irizarry, R., Astrand, M. & Speed, T. A comparison of normalization

methods for high density oligonucleotide array data based on variance and bias. *Bioinformatics* **19**, 185-93 (2003).

72. Dennis, G. et al. DAVID: Database for Annotation, Visualization, and Integrated Discovery. *Genome Biol* **4**, P3 (2003).

73. Wang, Y. & Sul, H. Ectodomain shedding of preadipocyte factor 1 (Pref-1) by tumor necrosis factor alpha converting enzyme (TACE) and inhibition of adipocyte differentiation. *Mol Cell Biol* **26**, 5421-35 (2006).

74. Smas, C., Chen, L., Zhao, L., Latasa, M. & Sul, H. Transcriptional repression of pref-1 by glucocorticoids promotes 3T3-L1 adipocyte differentiation. *J Biol Chem* **274**, 12632-41 (1999).

75. Schmidt, W., Poll-Jordan, G. & Loffler, G. Adipose conversion of 3T3-L1 cells in a serum-free culture system depends on epidermal growth factor, insulin-like growth factor I, corticosterone, and cyclic AMP. *J Biol Chem* **265**, 15489-95 (1990).

76. Liu, J. et al. Changes in integrin expression during adipocyte differentiation. *Cell Metab* **2**, 165-77 (2005).

77. Arner, P. Regional differences in protein production by human adipose tissue. *Biochem Soc Trans* **29**, 72-5 (2001).

78. Arner, P. Catecholamine-induced lipolysis in obesity. *Int J Obes Relat Metab Disord* **23 Suppl 1**, 10-3 (1999).

79. Feldman, B.J., Streeper, R.S., Farese, R.V. & Yamamoto, K.R. Myostatin modulates adipogenesis to generate adipocytes with favorable metabolic effects. *Proc. Natl. Acad. Sci. U.S.A* **103**, 15675-15680 (2006).

80. Dolinsky, V., Douglas, D., Lehner, R. & Vance, D. Regulation of the enzymes of hepatic microsomal triacylglycerol lipolysis and re-esterification by the glucocorticoid dexamethasone. *Biochem J* **378**, 967-74 (2004).

81. Kraus-Friedmann, N. Hormonal regulation of hepatic gluconeogenesis. *Physiol. Rev* **64**, 170-259 (1984).

82. Gebhardt, C. et al. Dermal Hyaluronan Is Rapidly Reduced by Topical Treatment with Glucocorticoids. *J. Invest. Dermatol* (2009).doi:10.1038/jid.2009.210

83. Wang, J. et al. Novel arylpyrazole compounds selectively modulate glucocorticoid receptor regulatory activity. *Genes Dev* **20**, 689-99 (2006).

84. Pantoja, C., Huff, J.T. & Yamamoto, K.R. Glucocorticoid signaling defines a novel commitment state during adipogenesis in vitro. *Mol. Biol. Cell* **19**, 4032-4041 (2008).

85. Frankfurt, O. & Rosen, S. Mechanisms of glucocorticoid-induced apoptosis in hematologic malignancies: updates. *Curr Opin Oncol* **16**, 553-63 (2004).

86. Roach, S.L. et al. Discovery of nonsteroidal glucocorticoid receptor ligands based on 6-indole-1,2,3,4-tetrahydroquinolines. *Bioorg. Med. Chem. Lett* **18**, 3504-3508 (2008).

87. Kuzmich, D. et al. Identification of dissociated non-steroidal glucocorticoid receptor agonists. *Bioorg. Med. Chem. Lett* **17**, 5025-5031 (2007).

88. De Bosscher, K. A fully dissociated compound of plant origin for inflammatory gene repression. *Proceedings of the National Academy of Sciences* **102**, 15827-15832 (2005).

89. Schacke, H. Dissociation of transactivation from transrepression by a selective glucocorticoid receptor agonist leads to separation of therapeutic effects from side effects. *Proceedings of the National Academy of Sciences* **101**, 227-232 (2003).

90. Cole, T.J. & Mollard, R. Selective glucocorticoid receptor ligands. *Med Chem* **3**, 494-506 (2007).

91. Miner, J.N. et al. Antiinflammatory glucocorticoid receptor ligand with reduced side effects exhibits an altered protein protein interaction profile. *Proceedings of the National Academy of Sciences* **104**, 19244-19249 (2007).

92. Lopez, F.J. et al. LGD-5552, an Antiinflammatory Glucocorticoid Receptor Ligand with Reduced Side Effects, in Vivo. *Endocrinology* **149**, 2080-2089 (2008).

93. Ma, Y. et al. Identification and characterization of noncalcemic, tissue-selective, nonsecosteroidal vitamin D receptor modulators. *J Clin Invest* **116**, 892-904 (2006).

94. Nehring, J.A., Zierold, C. & DeLuca, H.F. Lithocholic acid can carry out in vivo functions of vitamin D. *Proc. Natl. Acad. Sci. U.S.A* **104**, 10006-10009 (2007).

95. Ishizawa, M. et al. Lithocholic acid derivatives act as selective vitamin D receptor modulators without inducing hypercalcemia. *J. Lipid Res* **49**, 763-772 (2008).

96. Makishima, M. et al. Vitamin D receptor as an intestinal bile acid sensor. *Science* **296**, 1313-1316 (2002).

97. Gruber, G. et al. Levels of glucocorticoid receptor and its ligand determine sensitivity and kinetics of glucocorticoid-induced leukemia apoptosis. *Leukemia* **23**, 820-823 (2009).

98. Zhou, G., Xin, L., Liu, D. & Liang, C. Remembering the cell fate during cellular differentiation. *J. Cell. Biochem.* **96**, 962-970 (2005).

99. Kim, H.D., Shay, T., O'Shea, E.K. & Regev, A. Transcriptional regulatory circuits: predicting numbers from alphabets. *Science* **325**, 429-432 (2009).

100. Hager, G.L., McNally, J.G. & Misteli, T. Transcription dynamics. *Mol. Cell* **35**, 741-753 (2009).

101. Voss, T.C., John, S. & Hager, G.L. Single-cell analysis of glucocorticoid receptor

action reveals that stochastic post-chromatin association mechanisms regulate ligand-specific transcription. *Mol. Endocrinol* **20**, 2641-2655 (2006).

102. Stavreva, D.A. et al. Ultradian hormone stimulation induces glucocorticoid receptor-mediated pulses of gene transcription. *Nat. Cell Biol* **11**, 1093-1102 (2009).

103. John, S. et al. Kinetic complexity of the global response to glucocorticoid receptor action. *Endocrinology* **150**, 1766-1774 (2009).

104. Woodruff, P.G. et al. T-helper type 2-driven inflammation defines major subphenotypes of asthma. *Am. J. Respir. Crit. Care Med* **180**, 388-395 (2009).

105. Gerber, A.N., Masuno, K. & Diamond, M.I. Discovery of selective glucocorticoid receptor modulators by multiplexed reporter screening. *Proc. Natl. Acad. Sci. U.S.A* **106**, 4929-4934 (2009).

106. Nakanishi, A. et al. Role of gob-5 in mucus overproduction and airway hyperresponsiveness in asthma. *Proc. Natl. Acad. Sci. U.S.A* **98**, 5175-5180 (2001).

107. Kamada, F. et al. Association of the hCLCA1 gene with childhood and adult asthma. *Genes Immun* **5**, 540-547 (2004).

108. Toda, M., Tulic, M.K., Levitt, R.C. & Hamid, Q. A calcium-activated chloride channel (HCLCA1) is strongly related to IL-9 expression and mucus production in bronchial epithelium of patients with asthma. *J. Allergy Clin. Immunol* **109**, 246-250 (2002).

109. Wang, Y., Kim, K., Kim, J. & Sul, H. Pref-1, a preadipocyte secreted factor that inhibits adipogenesis. *J Nutr* **136**, 2953-6 (2006).

It is the policy of the University to encourage the distribution of all theses, dissertations, and manuscripts. Copies of all UCSF theses, dissertations, and manuscripts will be routed to the library via the Graduate Division. The library will make all theses, dissertations, and manuscripts accessible to the public and will preserve these to the best of their abilities, in perpetuity.

I hereby grant permission to the Graduate Division of the University of California, San Francisco to release copies of my thesis, dissertation, or manuscript to the Campus Library to provide access and preservation, in whole or in part, in perpetuity.

Carlos Joel A. B. Bantug — 12/22/09

Author Signature — Date